DURABILITY DESIGN OF CONCRETE ELEMEMTS AGAINST DETERIORATION OF BOND DUE TO CORROSION

By Vipin Kumar Bansal

Department of Civil Engineering and Applied Mechanics McGill University
Montreal, Canada
May, 2005

THESIS SUBMITTED TO THE FACULTY OF GRADUATE STUDIES AND RESEARCH IN PARTIAL FULFILMENT OF THE REQUIREMENTS FOR THE DEGREE OF MASTER ENGINEERING

Your file Votre référence
ISBN: 0-494-12580-2
Our file Notre référence
ISBN: 0-494-12580-2

Acknowledgements

I would like to express my sincere appreciation to all those who contributed to the preparation, development and publication of this work. In particular, I acknowledge the following people.

I express my sincere gratitude to my supervisor, Professor M.S. Mirza, Department of Civil Engineering and Applied Mechanics, McGill University, for his help and able guidance throughout this research program. The constant encouragement, support and inspiration he offered, were important to the completion of the research program.

I am extremely grateful to all my friends, in particular, Beena John, Jai, Masum and Saif for their encouragement and help during the course of this program.

I would like to sincerely thank Nabil Saliba for the translation of the abstract to French.

Lastly, and foremost, I express my deepest love and warmest appreciation to all my family members. I would like to express my deep gratitude to my parents, brother and sisters in India, my wife Pooja and my little child Sahil, for their encouragement, advice and assistance at each and every step of this program.

Abstract

Corrosion of steel reinforcement embedded in concrete is a world-wide problem that has caused extensive damage to various types of structures and is responsible for damage worth billion of dollars, requiring extensive repairs and rehabilitation. The relationship between the rebar mass loss, deteriorating bond characteristics at the steel rebar-concrete interface and cracking of reinforced concrete need to be studied urgently, for assessment of concrete structures deteriorating due to corrosion of the reinforcing steel. This will help in developing procedures for design of new concrete structures for safety, serviceability and service life against corrosion of reinforcement.

The main objective of this research program is to formulate a framework for durability design of concrete elements against deterioration of bond at the steel rebar-concrete interface due to corrosion of reinforcing bars. Mass loss of the reinforcement is an important parameter in defining the corrosion level. Therefore, it can be used to develop a correlation between corrosion, cracking and bond strength at the steel rebar-concrete interface. A preliminary design equation for prediction of bond strength at different corrosion levels is presented. Secondly, the existing state of the art of design of concrete elements for durability against deterioration of bond due to corrosion is established.

The results indicate that initially the bond strength increases with corrosion, which lead to the formation of a firm layer of corrosion products on the steel rebar-concrete interface, thereby improving the bond strength characteristics slightly. However, at higher levels of corrosion, a firm layer of corrosion products transforms into a flaky layer

resulting in the deterioration of bond. Following this stage, the bond strength decreases almost linearly with the increase in mass loss. A preliminary design method for durability against deterioration of bond due to corrosion is proposed, which will help the practicing engineers with the evaluation and amelioration of the existing infrastructure and with the design of new concrete infrastructure for durability against corrosion of reinforcing steel.

Résumé

La corrosion des armatures en acier enrobées de béton est un problème universel qui cause de gros dommages à plusieurs types de structures. Ces dommages remontent à plusieurs milliards de dollars et exigent des réparations et des réhabilitations assez élaborées. La relation entre la perte de masse des armatures, la dégradation des critères d'adhésion entre l'acier et le béton, et la fissuration du béton armé doit être étudiée en priorité afin d'évaluer la performance des structures en béton armé détériorées par la corrosion de l'acier des armatures. Une étude pareille aidera au développement des méthodes de conception de nouvelles structures en béton armé en termes de sécurité, aptitude au fonctionnement, et durée de résistance à la corrosion des armatures.

L'objectif principal de ce projet de recherche est la formulation d'un cadre de directives pour la conception et l'étude de la durabilité des membres en béton armé contre la détérioration des efforts d'adhésion entre les armatures en acier et le béton, causée par la corrosion de ces armatures. La perte en masse des armatures est un paramètre important dans l'établissement de l'étendu de la rouille. Alors, elle peut être utilisée pour élaborer une corrélation entre la corrosion, la fissuration, et l'effort d'adhésion au niveau de l'interface armature-béton. Cette thèse propose une équation de préconception qui prédit les efforts d'adhésion correspondent à plusieurs degrés de corrosion. En second lieu, une revue de la littérature la plus récente relative à la conception de la durabilité du béton armé et à sa résistance à la détérioration des efforts d'adhésion résultant de la corrosion est aussi présentée.

Les résultats de la recherche montrent que les forces d'adhésion entre les armatures et le béton augmentent avec l'élargissement de l'étendue de la rouille. Cette augmentation résulte de la formation d'une couche rigide de résidus de rouille à l'interface entre les armatures en acier et le béton. En outre, la rigidité de cette couche se dégrade avec la progression de la rouille entraînant l'affaiblissement des forces d'adhésion acier-béton. Une fois cette étape franchie, les efforts d'adhésion diminueront en proportion linéaire avec la perte en masse. Une méthode de préconception de durabilité contre la détérioration des efforts d'adhésion est proposée dans ce projet de recherche. Elle aidera les ingénieurs pratiquants dans l'évaluation et l'amélioration des infrastructures existantes, et dans l'étude de nouvelles infrastructures en béton pour une meilleure durabilité vis-à-vis de la corrosion des armatures en acier.

Table of Contents

List of Figures

List of Tables

List of Symbols

A	free increase in radius
C	cover thickness of the concrete
C_S	concentration of chloride at the concrete surface
C_{th}	critical chloride threshold
C_x	concentration of chloride ions at distance x from the surface
c_{env}	the environmental coefficient
c_{air}	the air content coefficient
f_{ck}	characteristic compressive strength of concrete in MPa
c_T	the temperature coefficient
d_b	rebar diameter
d	depth of carbonation
d	slip in inches
D_{min}	the minimum diameter of the steel bar
erf	compressive strength
K_c	carbonation coefficient
ML	mass loss of reinforcement
p_f	probability of error function
f'_c	specified failure of the structure within the target service life
$p_{f\max}$	maximum allowable failure probability
p_{target}	target probability of failure of the structure

r_0	the rate of corrosion at + 20° C
R	resistance of the structure
ΔR_{max}	the maximum loss of radius of the steel bar
$R(t_d)$	resistance at the end of the design service life
$R(t_g)$	resistance at the end of target service life
r	rate of corrosion
S	the load effects
$S(t_d)$	load effects at the end of the design service life
$S(t_g)$	load effects at the end of target service life
S_{max}	the maximum allowable depth of corrosion
t_0	time to initiation of corrosion
t_1	the propagation time for corrosion at cracking
t	time of exposure
t_d	design service life
t_g	target service life
t_L	service life
u	bond strength
X	carbonation depth,
x	depth of corrosion penetration
ϕ	Resistance factor for resistance R
ψ	Partial safety factors for resistance degradation (ΔR)
λ	Partial safety factors for load effect S

ψ	Partial safety factors for resistance degradation (ΔR)
λ	Partial safety factors for load effect S
γ_t	Lifetime safety factor
v	the volume of the rust relative to the volume of the uncorroded steel
u_p	Percentage bond strength

Chapter 1

Introduction

1.1 Background Information

Steel reinforced concrete constitutes a major versatile and economic construction material, used in all kinds of infrastructure facilities around the world. Corrosion of steel reinforcement embedded in concrete is a world-wide problem that has caused extensive damage to various types of structures and is responsible for damage worth billion of dollars, requiring extensive repairs and rehabilitation. As a result of the inherent protective characteristics of the concrete, reinforcement corrosion would not normally occur, provided that the surrounding concrete is of suitable quality and is designed properly for the intended environmental exposure. Nevertheless, corrosion can result if the above criteria are not fulfilled, or if other factors are not as anticipated, or have changed during the life of the structure. Design of concrete structures based on material strength rather than on durability, the excessive use of de-icing salts, and construction in increasingly aggressive environments are some of the factors that have led to a very large number of concrete structures experiencing reinforcement corrosion in recent decades. The damage is initiated and sustained in part by the chemical action of chlorides that are routinely used to keeps roads ice-free and provide traction during the winters, or it results from exposure to marine environments. Chlorides penetrate the cover of the reinforced concrete member by a combination of diffusion and capillary suction, and gradually propagate to the steel surface. When the chloride concentration at the steel surface exceeds a threshold limit and provided that oxygen is available for the oxidation process, corrosion (rusting) begins. The ensuing degradation of steel causes a loss of the effective steel cross-section, thereby impacting the flexural capacity and deformability of the member. The load-carrying capacity of the structural member can decrease gradually due to the on-going reduction of the cross-sectional area of the steel rebars, and cracking and spalling of concrete cover, along with the gradual deterioration of bond at the steel-concrete interface. This deterioration of bond at the steel rebar-concrete interface is far more serious than the loss of flexural capacity due to any reduction in cross-sectional area. Recent McGill research (Amleh, 2000) has shown that a cross-section loss of about 15% can result in a loss of about 85% in the bond at the steel-concrete interface, which has far more serious consequences for safety of the structure.

Structural collapses of reinforced concrete structures due to corrosion are rare. Corrosion of reinforced concrete has caused failures of two multi-storey parking structures in North America (Jacob & Carper, 1997). A post tensioned concrete bridge collapsed in Wales due to de-icing salt induced corrosion in the strands; another bridge collapsed for the same reasons in Belgium (Woodward and Williams, 1989). Concrete damage has to be well advanced before a reinforced concrete structure is at risk. The most common problem caused by the corrosion of reinforcing steel is the spalling of the concrete cover along with the deterioration of bond at the steel concrete interface.

1.2 Importance of corrosion to society

Infrastructure must be properly planned, constructed, operated and maintained. Unless all of these engineering and management functions are fulfilled adequately, either the systems will not fully meet the intended requirements, or they will become too costly. It has been estimated that around 50% of the national wealth is invested in the infrastructure around the world (Grigg, 1988). Also, 50 % of the expenditure in construction industry is incurred on repair, maintenance and remediation. Therefore, it is evident even marginal measures can result in substantial savings. Deterioration of infrastructure is occurring at a continually increasing rate all around the world, principally due to corrosion of the reinforcing steel.

In Canada, with the large-scale use of de-icing salts dictated by the cold climate, the situation is alarming. The cost of Canada's infrastructure is estimated between three and five trillion dollars (Mirza, 1998). Canada's concrete infrastructure, a significant portion of which is near the end or past its design life, has a replacement value of over half a trillion dollars (Concrete Canada, 1993). Because of lack of funding, and the related political decisions leading to deferred maintenance and lack of consideration of durability and performance in the initial design, the current infrastructure rehabilitation is estimated at well over $200 billion. The cost of rehabilitation due to corrosion of reinforcing steel alone is $ 30 billion per year in Canada (Concrete Canada, 1993). The cost of repairing existing Canadian concrete parking structures has been estimated to be between $6-8 billion. The condition of infrastructure has a direct impact on productivity, international competitiveness, social-economic developments and above all the quality of the life of all its citizens. Canadian engineers must assume a responsible leadership role in successfully mitigating the crisis to ensure that Canada continues to remain among the world leaders in terms of quality of life. It should be noted that if no corrective measures are taken now, the infrastructure will continue to deteriorate at an accelerated rate and it may cost a few hundred billion dollars compared to the current required expenditure, and in some cases, it might have to be replaced at a much higher cost.

The deterioration of concrete bridges in the United States is a monumental problem. The Federal Highway Administration (FHWA) recognized the financial consequences of the problem associated with the corrosion of the reinforcing steel in concrete bridges in the early 1970's. The cost of bridge deck repairs estimated at $70 million per year in 1973 by the Federal Highway Administration (FHWA) was increased to $200 million per year by 1975. In 1981, the US General Accounting Office published a report covering 91% of the nation's bridges, estimated the rehabilitation/replacement costs at about $33.2 billion. Nearly 32% of the 581,000 bridges existing in the national highway structure system were listed as being structurally deficient, or functionally obsolete. The cost of repairing and replacing these bridges was estimated at about $100 million, and approximately 20 percent of the total estimated cost was due to the corrosion deterioration of these bridges.

The situation is almost same for Europe, the Asian Pacific countries and Australia. In the United Kingdom alone, repair costs of damaged concrete are estimated at over 1 trillion Canadian dollars per year (Page, 1996). Hence, corrosion of the reinforcing steel embedded in concrete is a major problem facing civil engineers today as they maintain an ageing infrastructure. In summary, premature deterioration of concrete structures is a multibillion-dollar problem around the world. Presently, more concrete structures are suffering from durability problems than was the case fifty years ago. Consequently, the inherited problems of corrosion in existing concrete structures are likely to increase considerably in the future. Hence, the ability to assess the severity of corrosion in existing structures for maintenance and inspection scheduling and the use of corrosion data for predicting the remaining service life are becoming increasingly important.

1.3 Loss of Performance with Time

Concrete structures are designed to provide satisfactory performance over a long period of time. The life of any structure depends on the preservation of the physical integrity of its components. According to the Canadian Highway Bridge Design Code CHBDC S6-2000, the bridges are generally required to have a design life of 75 years, but a number of them are suffering from durability problems at a fraction of this age. The performance of a structure is determined by the safety, serviceability and the appearance of a structure. In practice, the primary concern is to ensure a satisfactory performance over a sufficiently long period of time. The performance over time, whether due to initial good quality, or repeated repair of "not-so-good structure", is termed the service life of the structure (CEB, 1992).

Somerville (1984) has described graphically the relationship between concrete performance and time as shown in Fig.1.1.

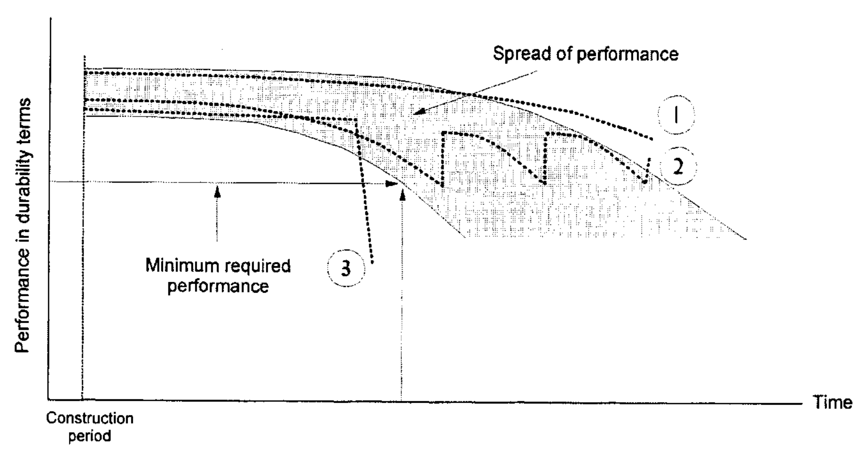

Fig. 1.1: Loss of performance with time (Somerville, 1984)

Negligible deterioration, indicated by curve 1, may not be achievable and requires high initial expenditure. The performance depicted in curve 3 follows a high rate of deterioration and failure occurs suddenly and catastrophically. Most concrete follows a pattern similar to curve 2, showing significant deterioration with time, but intermittent maintenance or rehabilitation changes the performance level, or alters the rate of deterioration. Hence, continuous monitoring of the condition of structures on site is necessary to determine the state of health of a structure upon completion and regularly during its life by further routine tests and monitoring techniques.

1.4 Impact of Corrosion

The design of new concrete structures and the repair of existing deteriorated concrete structures require an understanding of the various causes and mechanisms of corrosion of reinforcing and prestressing steel. The concrete cover acts as a physical barrier to the access of aggressive agents because of its hardness and resistance to wear and tear, and to permeation of fluids containing aggressive compounds. The high alkalinity of concrete normally provides excellent protection to the reinforcing steel. The seawater spray in marine structures and carbonation of concrete in industrial environments also lead to the depassivation of the protective oxide layer on the reinforcing steel in concrete structures. Errors and lack of quality control in mixing, placing, consolidating and curing of concrete making it more permeable are also responsible for the occurrence of these distresses. In addition, the incorrect use of different types of cements, supplementary cementitious materials, superplasticizers and other additives available commercially and used without a full understanding of their properties has also resulted in deterioration of concrete structures because of steel corrosion.

Steel in concrete is normally immune from corrosion because of the high alkalinity of concrete; the pH of the pore water can be greater than 12.5, which protects the embedded steel against corrosion. The passivation of the embedded steel reinforcing bars is caused by this alkalinity of concrete. Due to the high pH, a microscopic oxide layer is formed on the surface of the steel bar preventing the dissolution of iron. However, low permeability concretes, made using low water-cement ratios and good construction practices minimize the penetration of corrosion inducing agents and increase the electric resistivity of the concrete to some degree, which reduces the rate the corrosion by retarding the flow of electric current within the concrete. The steel reinforcement in a majority of concrete structures does not corrode because of these inherent protective characteristics, provided that there is a suitable quality of concrete and proper design of the structure for the intended environmental exposure, which does not change during the life of the structure. The corrosion of steel in concrete may result when the above conditions are not fulfilled.

Corrosion of the reinforcing steel causes a decrease in the bar diameter which affects adversely the mechanical properties of the steel bar in terms of its ultimate strength, yield strength, ductility, etc. When reinforcement corrodes, the corrosion products on the bar surface occupy a larger volume than the original iron in steel in the uncorroded condition, thereby causing large internal pressures, leading to cracking and spalling of the concrete cover. Also, the loss of cover causes loss of confinement and a reduction in the bond strength at the interfacial zone between the two materials. In addition, the surface of the bar becomes covered with corrosion products, leading to a considerable decrease in bond at the steel-concrete interface, eventually all of the concrete around the steel bar is forced off by the pressure from growing corrosion products, and the reinforcement loses not only any remaining protection against corrosion, but also loses a significant part of the bond resistance to transfer the force from the reinforcing steel to the surrounding concrete and vice-versa. Corrosion is very serious in post-tensioned prestressed concrete structures due to the fact that the reinforcement is deliberately stressed in tension prior to any loading of the structure. In addition, the post-tensioning tendons are free to move within the concrete over the beam length as they may be anchored only at the ends; such movements are prevented in grouted tendons. Therefore, rusting of tendons may take place without any visible sign on the concrete surface causing a sudden structural failure without any advance warning.

In summary, reinforcing steel is used in reinforced concrete to resist the tensile forces, and to control its cracking. However, corrosion not only deteriorates the steel bar and its function of transferring the tensile forces from the concrete and steel and vice-versa, but it also deteriorates the concrete by spalling of the cover. Therefore, corrosion has a strong influence on the bond behaviour at the concrete-steel rebar interface. As corrosion of the reinforcing steel progresses, the bond strength between the reinforcing steel and the concrete diminishes progressively, and thus major repair or replacement is needed. Numerous reports are available which discuss how to control the corrosion, but very limited data is available about its influence on the bond behaviour at the concrete-steel rebar interface.

The relationships between rebar corrosion, deteriorating bond characteristics at the steel-concrete interface and cracking of concrete need to be studied urgently, to enable assessment of the concrete structures deteriorated due to corrosion of the reinforcing steel. This will also help in developing procedures for design of new concrete structures for safety, serviceability and the required service life against corrosion of the reinforcement, and for repair and rehabilitation of existing structures, which have deteriorated due to corrosion of reinforcing steel. Research centres all over the world have started addressing the issue of durability of reinforced concrete structures in codes with increased emphasis on the protection provided to the reinforcing steel.

1.5 Objectives and Scope of Thesis

The main objective of this thesis is to formulate a framework for durability design of concrete elements against deterioration of bond due to corrosion of the embedded steel reinforcing bars. The principal factors influencing the durability of structural concrete are the anticipated environmental loads (macroclimate and microclimate), function of the structure, established performance criteria, material characteristics and their performance, member geometry and structural detailing, workmanship and quality control, protective measures and timely maintenance during the intended service life. It is quite important to describe the microclimate (the environment in the immediate vicinity of the structural element), details of geometry and material characteristics and factors influencing corrosion of the reinforcing bars. The importance of concrete with low water-cement (w/c) ratio and an appropriate concrete cover thickness (C) to rebar diameter d_b, reflected in the C/d_b ratio, is stressed in this research program. Mass loss of the reinforcement is an important parameter in a given situation; definition of the corrosion level can be used to develop a correlation between corrosion, cracking, bond strength at the concrete-steel rebar interface, and the ultimate strength of the reinforced concrete element. The first objective is to establish the existing state of the art of design of concrete elements for durability against deterioration of bond due to corrosion. Secondly, a correlation is developed between corrosion cracking, bond strength at the steel-concrete interface. Thirdly, a durability design model for design of concrete elements against deterioration of bond due to corrosion is developed. Finally, a preliminary design method for durability against deterioration of bond at the steel-concrete interface due to corrosion of rebars is proposed. The design method will help the practicing engineers with the evaluation and amelioration of the existing infrastructure and with the design of new concrete infrastructure for durability against corrosion of the reinforcing steel.

Chapter 2

Corrosion of Reinforcing Steel Embedded in Concrete

2.1 Introduction

Corrosion of reinforced concrete recognized early in the twentieth century has become worse in recent years with the widespread use of de-icing salt on highways and bridge decks. It is one of the main causes, which induces an early deterioration of concrete structures, reducing their service life and consequently their residual life. Good quality concrete provides excellent protection for the reinforcing steel. Steel does not corrode immediately after embedment. Physical protection is itself provided by the concrete acting as a barrier to the aggressive elements, while chemical protection is afforded by the concrete's high alkalinity. In spite of these inherent protective qualities, corrosion of reinforcing steel has become the most common cause of deterioration in concrete structures.

The service life of concrete structure is defined from the time when the structure is put into operation until a maximum tolerated extent of deterioration occurs in the structure. Tuutti (1982) proposed a model to describe the corrosion process and approximate overall picture of the service life of the structure, as illustrated in the Fig. 2.1.

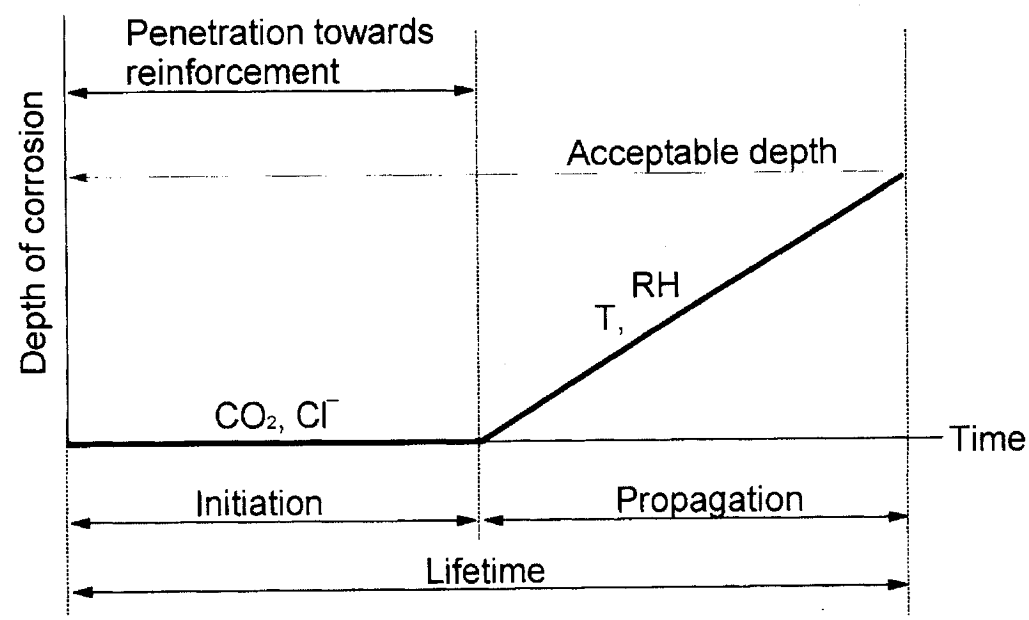

Fig. 2.1: Schematic sketch of steel corrosion sequence in concrete (Tuutti, 1982)

Tuutti (1982) divided the service life of a concrete structure with respect to reinforcement corrosion into two stages – initiation stage and a propagation stage. The initiation stage involves depassivation of the reinforcing steel by penetration of chloride ions, while during the propagation stage, corrosion reaction occurs and its rate can be controlled by the availability of oxygen (O_2), and the environmental controlling parameters: temperature (T) and relative humidity (RH). The model provides the probability of approximating the effects of various parameters values and of predicting an approximate service life and the remaining service of the structure.

2.2 Initiation stage

The initiation period of the corrosion process consists of the time from the erection of the structure until the steel depassivates due to the external aggressive agents reaching the reinforcement surface. The pore solution, surrounding the reinforcing steel, is highly alkaline with a pH value between 13 and 14. An environment of this type causes the steel to be passivated, thereby allowing the formation and maintenance of a stable thin passive film on the steel surface. The corrosion rate is depressed to an insignificantly low level by the formation of the iron oxides on the steel surface. This state of passivation is maintained until the concrete in contact with the reinforcement becomes carbonated, or until a sufficient concentration of aggressive ions (normally chloride ions) reaches the steel surface. The ions either move through the concrete pores, or through the cracks.

Corrosion of steel initiates if the concrete is not of adequate quality, that is the structure was not properly designed for the service environments, or the environment was not anticipated or it changed during the service life of concrete structure. The factors influencing the initiation period, namely the environmental conditions, the material properties and the design of the structure will be discussed, but first the transport mechanisms by which aggressive substances enter the concrete are reviewed.

2.2.1 Transport mechanisms in concrete

For the ingress of external agents, the continuous pore network, cracks and other defects provide the path along which transport occurs into the cover concrete (covercrete). The process of fluid flux is generally described in terms of absorption, diffusion and permeability.

2.2.1.1 Absorption (Capillary suction)

Absorption is the process whereby the concrete takes in a liquid by capillary suction to fill the pore space available within the material. Capillary suction results in the ingress of chloride-contaminating solutions can penetrate into the concrete through the pore system.

2.2.1.2 Diffusion

Diffusion is the process by which a liquid, gas or ion migrates through the concrete under the action of a concentration gradient. It is defined by a diffusion coefficient, or a diffusivity value. In other words, the difference between the concentration outside and inside the pore system is the driving force for diffusion in concrete.

2.2.1.3 Permeation

Permeability is a flow property and is defined as that property of a porous medium, which characterizes the ease with which a fluid will pass through it, under the action of a differential pressure. It is strictly related to the flow that occurs under an applied pressure differential. The terms permeability and porosity are often misinterpreted. Porosity is a measure of the total volume occupied by pores. It is possible for a material to be porous, but impermeable, if it contains a series of interconnected air voids. Permeability is the degree of ease with which water, air and chloride ions can move through the concrete pore system.

2.2.1.4 Cracks in concrete

All of the above transport mechanisms rely heavily on the continuous pore network within the concrete. However, cracks and other defects can also provide a path along which transport can occur. It is understood during design that reinforced concrete structures will crack to a certain extent under loading. However, other phenomenon such as freezing and thawing, alkali-aggregate reactivity, sulphate attack and rebar corrosion also lead to cracking. Cracks in concrete facilitate the corrosion process by providing easy access for the penetration of dissolved chloride ions, carbon dioxide, oxygen and moisture.

2.2.1.5 Defects in concrete

Poorly compacted concrete can develop cavities, excessive bleeding of concrete, and can result in water pockets. In addition, honeycombing around the steel rebar can occur if the maximum aggregate size is too large, or if there is an insufficient content of fine aggregates. All of these defects can provide paths for transport.

2.2.2 Influence of environmental conditions

Concrete is a strong, durable and long lasting building material even in aggressive environments. However, concrete structures such as bridge decks are exposed to very severe environments, which promote the penetration of chlorides. The bridge deck environment constitutes a very severe exposure condition for the concrete where it is subjected to alternate wetting and drying, freezing and thawing and application of de-icing salts.

2.2.2.1 Ingress of chlorides

Chlorides may be present in the concrete during its manufacture, or they may have penetrated from some source during its service. Chloride ion contamination has been identified as the main culprit in the breakdown of the protection afforded by the passive film. Chloride ions from seawater or de-icing salts may penetrate via the pores to the interior of the concrete. Main factors influencing chloride ingress are chloride concentration, environmental conditions, such as humidity and temperature, permeation properties and chloride binding capacity of the pore walls, and the chemical reactions (Bob, 1996). For reinforced concrete exposed to chlorides in service, the maximum permissible water-soluble chloride ion content in concrete is 0.15% by mass of cement according to both the ACI 318 Committee Building Code Requirements for Reinforced Concrete (1990) and the CSA Standard A23.1 (1994).

Mechanism of chloride attack

The ability of the pore structures in the hydrated cement paste to bind the chloride ions provides resistance to the transport mechanisms. There are three forms of chlorides in concrete. Some of the chlorides are physically bound being adsorbed on the surface of gel pore wall, while other are chemically bound to the cement hydrates. The remaining chlorides are the free chloride ions dissolved in the pore solution. (Fig. 2.2)

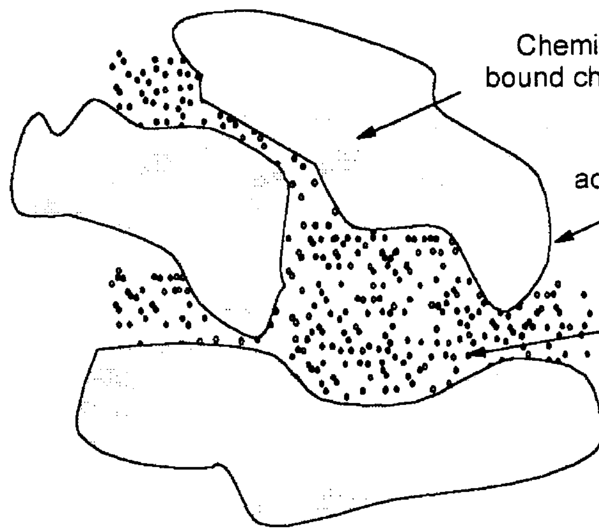

Fig. 2.2: Three different forms of chloride in concrete (Tuutti, 1982)

There exists dissolution equilibrium between bound chlorides and free chloride ions in the pore water, and only the free chloride ions in the pore water cause the most damage due to the corrosion of reinforcement. Although the high alkalinity (pH>13) of the concrete cover provides both chemical and physical barriers to corrosion, the presence of chloride ions in the concrete can lead to corrosion of the reinforcing steel, provided that the corrosion reaction can be sustained by an adequate supply of oxygen and moisture. For corrosion to be initiated, there has to be a certain minimum concentration of chloride ions at the surface of the steel, which is termed the threshold value. The threshold can be presented as a total chloride content, a free chloride content, or as the ratio of the free chloride ions to hydroxyl ions (Cl^- : OH^-). In the presence of chloride ions, depending on the Cl^-/OH^- ratio, the passive film can be destroyed at pH values considerably above 11.5. When the Cl^-/OH^- ratio are higher than 0.6, steel is no longer protected against corrosion as the iron-oxide film either becomes permeable or unstable under these conditions. When the concentration of chloride ions exceeds the threshold value, depassivation of the steel can take place and corrosion can commence. Different codes recommend the maximum chloride contents values, which are not the true threshold values for the onset of corrosion (Table 2.1).

Table 2.1: Threshold chloride content values in various codes

Threshold chloride (percent by weight of cement)		
Source	Free (water-soluble)	Total (acid-soluble)
ACI 201	0.10 to 0.15*	-
ACI 222	-	0.20
BS 8110	-	0.40
ACI 318	0.15	-
CSA 23.1	0.15	-

*0.10% for moist environment exposed to chlorides; 0.15% for moist environment not exposed to chloride environments

2.2.2.2 Carbonation

Carbonation of concrete results in reduction of its alkalinity, thereby permitting corrosion of reinforcing steel. It is a slow process, however, carbonation-induced corrosion is not as common as the corrosion induced by the chlorides. Carbonation of concrete involves a chemical reaction between atmospheric carbon dioxide and the products of the cement hydration.

Carbon dioxide from the air penetrates air filled pores of the concrete and it reacts with the hydration products from the hydration cement paste (hcp), especially with $Ca(OH)_2$ to form $CaCO_3$.

$$Ca(OH)_2 + CO_2 \rightarrow CaCO_3. + H_2O \qquad (2.1)$$

The process is schematically represented in Fig. 2.3. The reaction gives rise to neutralization of the pore solution to pH values below 9. Due to carbonation, the value of pH changes very suddenly and it appears as a narrow zone or carbonation front separating the zones – one into the concrete pore with pH values greater than 12 and the other towards the concrete surface with pH values less than 8.

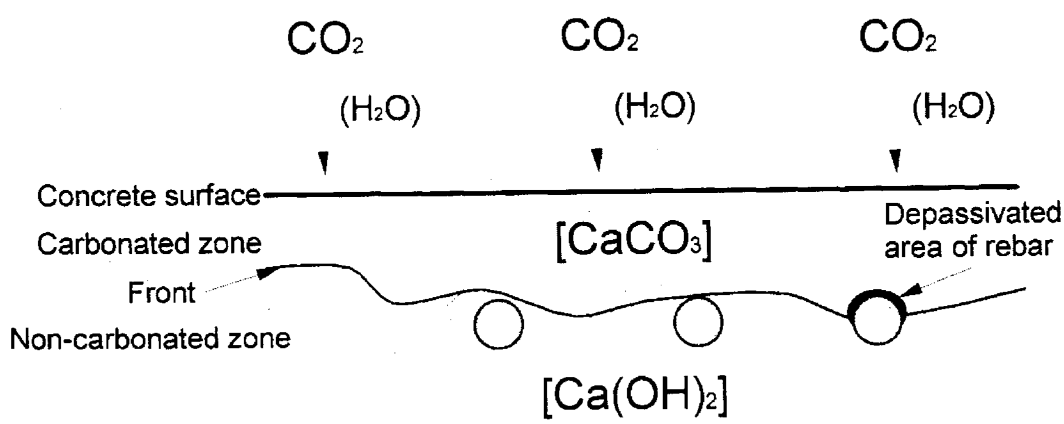

Fig. 2.3: Schematic representation of the carbonation process (Richardson, 1991)

The outer zone of the concrete is affected first, but with the passage of time, carbonation proceeds deeper into the mass, as carbon dioxide diffuses inwards from the surface.

The rate of carbonation is dependent on factors such as the w/c ratio, cement type, cement proportion in the concrete mix, concrete cover thickness and its permeability. The rate of carbonation can be predicted as as a model describing the depth of carbonation expected over a period of time:

$$X = k\sqrt{t} \tag{2.2}$$

where X = carbonation depth,

t = time of exposure, and

k = constant which is a function of material properties and environmental conditions

It must be emphasized that conditions under which carbonation, or corrosion may occur are not always similar. The highest rate of carbonation occurs at a relative humidity between 50 to 70 percent. Whereas the rate of corrosion will be significant only where the relative humidity values in the pores adjacent to the steel are higher than about 75%.

2.2.2.3 Freezing and Thawing Cycles

The resistance to various forms of deterioration associated with cycles of freezing and thawing is one of the most important aspects of concrete durability in Canada and in the United States. The cyclic freezing and thawing process is commonly encountered in cold climate conditions. These cyclic actions occur due to the formation of ice crystals within the matrix of the concrete. The pores in the cement paste are differentiated as gel pores, capillary pores compaction pores and air pores, more generally as micropores, capillary pores and macropores depending on their sizes (Fig. 2.4). The capillary pores and the macropores are particularly relevant with regard to durability. It is estimated that water in gel pores does not freeze above -78°C. Therefore, when the saturated cement paste is subjected to freezing conditions, while the water in large cavities turns into ice, the gel pore water continues to exist as liquid water. This creates a thermodynamic disequilibrium between the frozen water in capillaries and the super cooled water in the

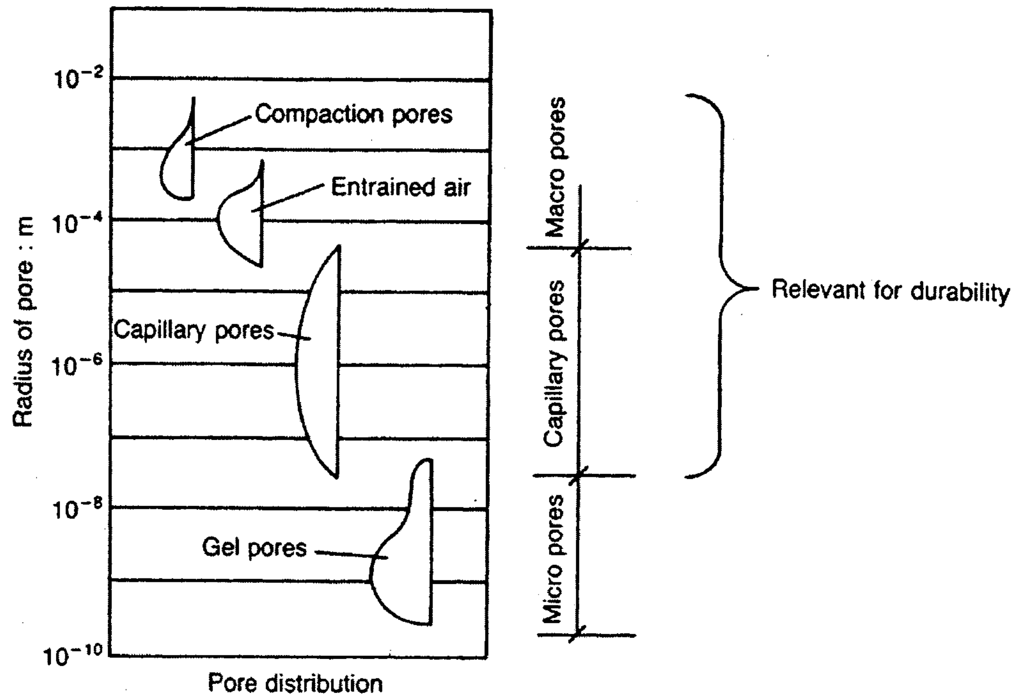

Fig. 2.4: Pore size distribution (CEB Design Guide, 1989)

gel pores. This forces the water in gel pores to migrate to the large cavities where it can freeze. This supply of water increases the volume of ice in the capillary pores steadily until there is no more room to accommodate. On freezing, there is an increase in volume of approximately nine percent and this leads to the generation of internal stresses, unless the expanded product can move easily to some air voids deliberately provided in the vicinity. The effect becomes progressively more severe as the matrix of the material gets fissured: the opening of the structure permits the formation of a greater number of sites at which the effect can take place. The damage takes the form of cracking and spalling. Most of the highly industrialized nations located in the very cold regions of northern hemisphere, are very dependent on sophisticated highway networks, which are kept clear by applying de-icing salts during the winter. The combined action of freeze-thaw cycles and the use of de-icing salts has a more severe effect than the former alone. The de-icing salts lower the freezing point and thus prevent the formation of ice. Their application causes a substantial drop in temperature at the concrete surface (temperature shock) during thawing of ice. The de-icing salts also result in a significant change in the freezing behaviour of the pore water in the concrete (Fig. 2.5). Due to the temperature shock and the change in the freezing behaviour of the pore water, in the regions of larger pores, as well as at greater depths, water freezes within a smaller temperature range. Also, certain concrete layers suffer freezing at different times, which results in scaling.

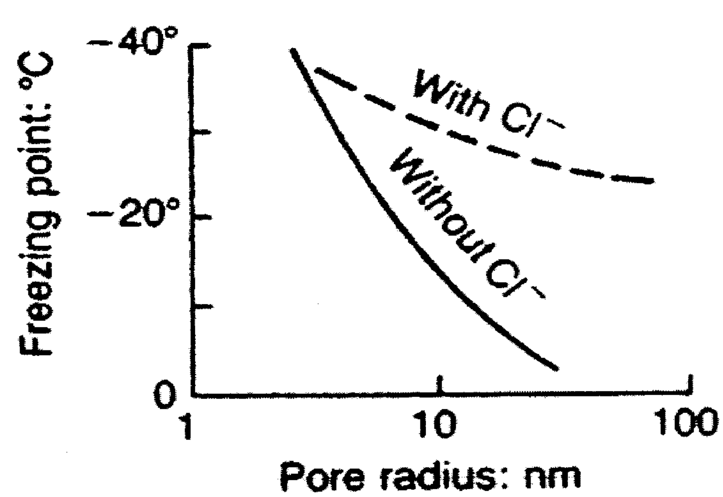

Fig. 2.5: Effect of chlorides on the freezing properties of pore water (CEB Design Guide, 1989)

When the salts are used for de-icing roads and bridge surfaces, some of the salts become absorbed by the upper part of the concrete. This produces a high osmotic pressure, with a consequent movement of water toward the coldest zone where freezing takes place and hydraulic pressure is developed. The ice removal agents contribute to the deterioration of concrete causing delamination of the surface layer, but most importantly it is an important source of chlorides, significantly increasing the possibility of a faster rate of corrosion of the reinforcement.

2.2.3 Factors influencing corrosion mechanism

Corrosion protection of the reinforcing steel is dependent on the concrete properties, and the factors that affect the protective quality of concrete are:

- Cement content
- Water/cement ratio
- Aggregates
- Cement
- Supplementary cementing materials
- Admixtures
- Adequate placement, compaction and curing of concrete

These factors affecting concrete quality are directly or indirectly linked with the corrosion mechanism. The permeability of concrete is one of the fundamental properties that influence the ingress of aggressive elements leading to the initiation of corrosion and the extent of the concrete damage. The permeability of concrete is a function of the pore size and distribution, the degree of interconnection of the pores and the moisture content of the permeable pore structure (Richardson, 2002). Basheer *et al.* (1994) developed a corrosion-permeability interaction model, which shows the relation of corrosion with the permeability of concrete (Fig.2.6).

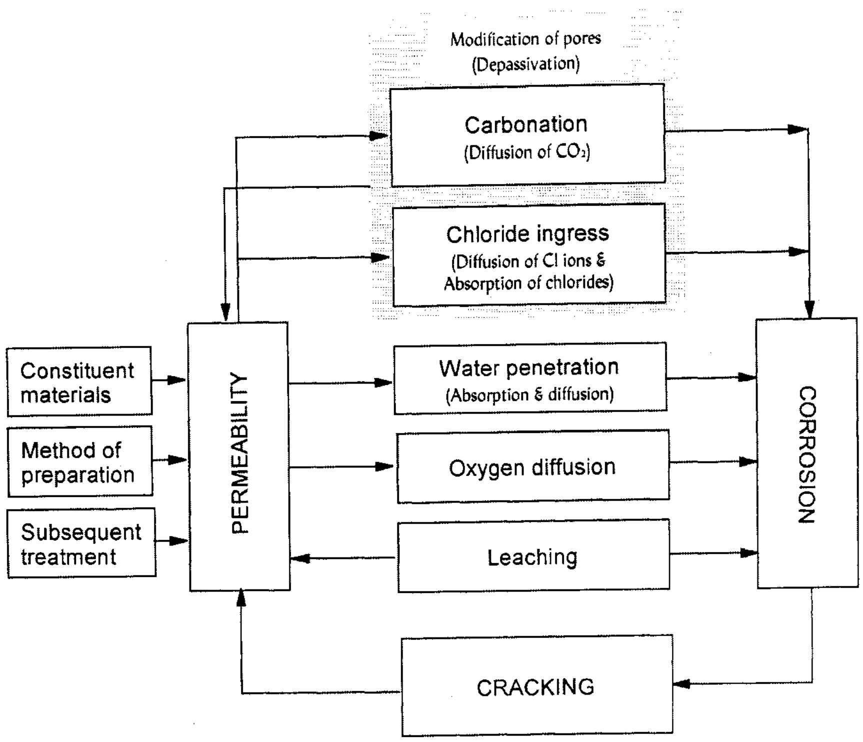

Fig. 2.6: Corrosion-permeability interaction model (Basheer *et al.*, 1994)

It is understood that the permeability of concrete is the key to control the various processes involved in the corrosion phenomenon. The composition of concrete must guarantee a passive state of steel reinforcement from the time of fabrication of the structure until the end of its design service life.

Water /cement ratio

The water/cement ratio influences the permeability and strength of concrete. The permeability of concrete will increase with an increase in the water/cement ratio. An increase in permeability results ultimately in an increase in chloride diffusivity, easier ingress of oxygen and low resistance to corrosion. With an increase in the chloride diffusivity, depassivation of steel reinforcement will occur initiating corrosion, and with an increase in oxygen and a decrease in the corrosion resistance, the corrosion rate will increase. The permeability of concrete increases significantly with water/cement ratios larger than 0.6 (CEB Design Guide, 1989), however, the ACI Building Code 318 specifies a maximum w/c ratio of 0.4 for reinforced normal weight concrete exposed to de-icing chemicals.

Cement type and cement content

The cement type and content are the most important factors influencing the permeability of concrete. Tricalcium aluminate [C_3A] and tetra calcium alumino ferrite [C_4AF] are important constituents of the cement with regard to the steel corrosion. The main form of binding of the chloride ions is by reaction with C_3A to form an insoluble calcium chloroaluminate hydrate (Friedel's salt). Chlorides also react with C_4AF to form choloroferrite. Corrosion initiation time and threshold values were found to increase systematically, whereas the initial mass loss of the reinforcement decreased, as the C_3A content of the cement increase. The cements blended with natural pozzolans, blast furnace slag or fly ash have the properties of slow hardening at an early age and a more rapid hardening at later ages, which help to develop a concrete with lower permeability. An increase in the cement content can increase the binding capacity of the concrete for chlorides and carbon dioxide, which helps to lower their penetration rate due to decreased permeability of concrete. The CEB Design Guide (1989) recommends cement content in the range of 300 kg/m^3 to achieve a low permeability and sufficient durability. However, research has shown that increasing the cement factor with no reduction in the water/cement ratio causes no noticeable reduction in the reinforcement corrosion.

Aggregates

The aggregates play a major role in influencing the permeability of the concrete and their effect on the resistivity of the concrete against environmental aggressors. They occupy approximately 70 percent of the volume of concrete. The selection of aggregate size and its grading is an important step in durability design. If the aggregates are too absorbent (high water absorptivity) during the wetting and drying cycle, they can retain more water, which helps the corrosion process. Some quantities of minerals contaminate the aggregates by becoming reactive. The most common example is alkali-silica reactivity, which generates disruptive forces initiating the formation of cracks, which provide an easier access for water and other environmental aggressors to reach the steel reinforcement. Selection of more rounded and well graded aggregates helps in reducing the permeability of concrete.

Compaction and curing

The permeability of the surface layer of the concrete may be increased by a factor of five to ten if the concrete is insufficiently cured. Curing measures must begin immediately after concreting and they must not be interrupted. Poor compaction tends to increase the permeability of the concrete to such an extent that the protection of steel reinforcement no longer exists. Inadequate curing can result in weak, porous and permeable material near the surface of the concrete that is vulnerable to the ingress of various harmful substances from the environment. Prolonged curing substantially increases the time to initiation of corrosion.

Supplementary cementitious materials and admixtures

The use of supplementary cementitious materials, such as fly ash, silica fume, ground granulated blast furnace slag, and natural pozzolans, in concrete structures has become a widely accepted practice in many countries, primarily due to their favourable effects on concrete durability. They have been found to be beneficial in retarding the reinforcement corrosion.

2.2.4 Structural design

During the design phase of the structure, consideration of proper design, adequate cover and drainage are the best possible ways to avoid long-term problems. The structure provides high resistance against environmental aggressors by providing adequate cover and drainage, and by maintaining a simple layout of the steel reinforcement.

Thickness of concrete cover

By rough approximation, the rate of carbonation (increase of carbonation depth with time) and the rate of penetration of chlorides into the concrete with time follow a square-root law. This means that if the concrete cover is halved, the critical state for incipient danger of corrosion will be reached in less than a quarter of the time. (Fig. 2.7)

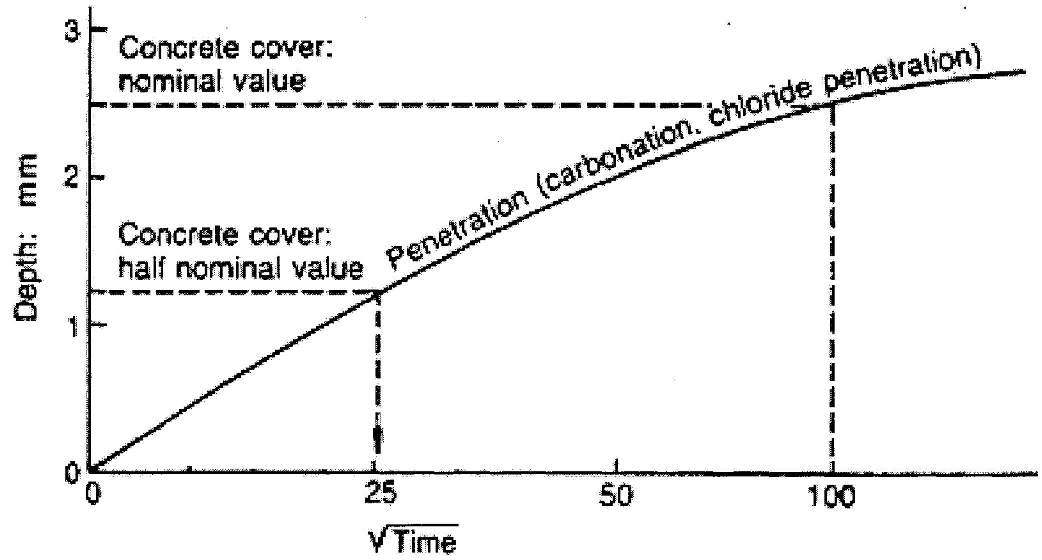

Fig. 2.7: Example of the effect of the thickness of concrete cover (CEB Design Guide, 1989)

It shows that for the normal concrete cover, the carbonation reaches the surface of the reinforcement after 100 years, if the cover is reduced to half of the nominal thickness, the penetration occurs in only 25 years.

Thick and dense concrete cover over the embedded steel provides a permanent protection against corrosion and contributes to an improved bond response at the steel-concrete interface. A thick, good quality cover helps to delay carbonation and ingress of chloride ions, thereby preserving the passivity of the reinforcement and consequently delaying the initiation of corrosion.

Drainage

Poor drainage often increases the degree of saturation of the concrete and aggravates the consequences of frost action. Provision of falls and drainage systems on slabs and on horizontal members will reduce the time during which the surface of the concrete is in contact with water and the dissolved aggressive substances, and results in a delay in the initiation of corrosion. However, the drainage systems are installed occasionally at the wrong location, or they are not well maintained. Therefore, they cannot serve their purpose and play their role in serving the service life of the structure.

2.3 Propagation stage

The presence of chloride ions either in the concrete mix or due to ingress from the immediate environment, and a decrease of the hydrated cement paste pore solution pH because of the concrete carbonation are two known major causes of the breakdown of the passive layer on the surface of the steel bar embedded in concrete. The propagation period is defined as the period from the moment of depassivation at the face of the reinforcing steel and it includes corrosion at a perceptible rate until the limiting stage is attained when the structure loses its bearing capacity, operational properties, or external form.

According to RILEM Report of TC-60 CSC (1988), this stage can be divided into three parts and is schematically represented in Fig. 2.6. The expansive corrosion products formed around the steel bar usually propagate to the concrete surface causing cracks. At this point, the supply of deleterious substances increases due to the presence of longitudinal cracks and thereby accelerates the rate of corrosion. Rust stains and spalling follows, resulting in the loss of serviceability of the concrete structure. At the end of the functional service, the deterioration process continues with a decrease in the load bearing capacity of the member, which is related to corrosion via a reduction in the cross section of the reinforcing steel and the deterioration of bond at the steel-concrete interface, causing failure as shown in the Fig. 2.8.

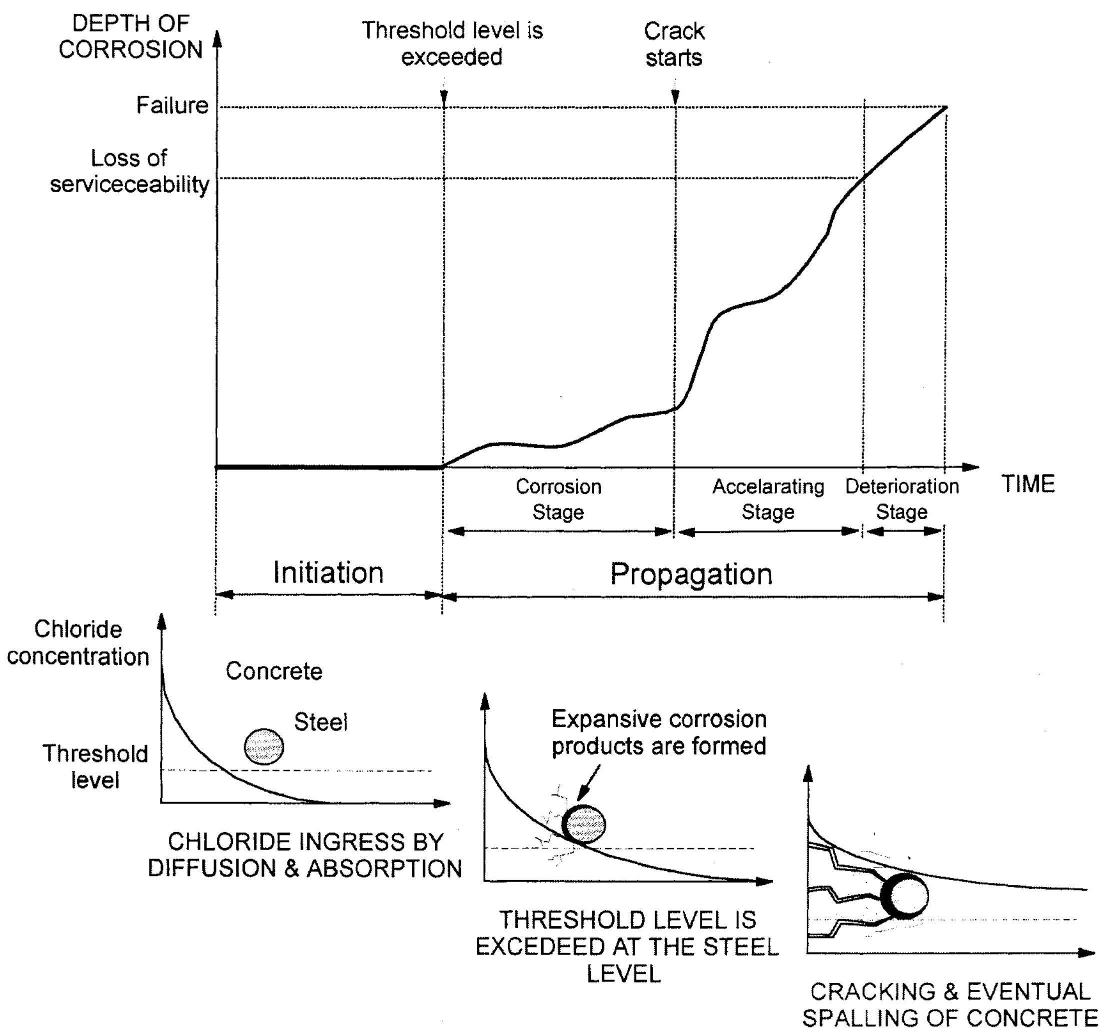

Fig. 2.8: Corrosion stages (RILEM, 1988)

2.3.1 Corrosion

Corrosion is the process of the transformation of a metal to its 'native' form, which is the natural ore state, often as oxides, chlorides or sulphates. This transformation occurs because the compounds such as the oxides "involve" less energy than pure metals, and hence, they are more stable thermodynamically. The corrosion process does not take place directly, but rather as a series of electrochemical reactions with the passage of electric current. Corrosion also depends on the nature and type of the metal, the immediate environment, temperature and other related factors. Corrosion may be defined as the destructive attack of a metal by chemical or electrochemical reactions with its environment. Therefore, corrosion is an electrochemical process, which must be understood to produce a durable concrete.

It must be emphasized that corrosion is possible only if sufficient moisture and oxygen are available. This electrochemical process causing corrosion of the reinforcing steel in the concrete is similar to the action that takes place in a flashlight battery which involves an anodic reaction, consisting of oxidation of iron, and a cathodic reaction where this reaction consumes any electrons produced during oxidation of iron, an electrical conductor, and an electrolyte. The dissolution of the metal in the concrete occurs at the anodic sections where ions are generated in the solution in the form of hydrated anions (the negative pole) by the half-cell reaction where the iron is oxidized to ferrous ions.

Corrosion occurs at the anode and results in a loss of metal from the section, which adheres loosely to the metal section as an oxide. This oxide product is lost eventually from the section under continued corrosion. The Fe^{2+} is transformed into oxides of iron by a different number of complex reactions, and the volume of reaction products can be several times the volume of iron. The electrons released at the anode where the reduction takes place move towards the cathodic regions of the surface where they are assimilated by the atoms of the dissolved oxygen or hydrogen ions consumed by the cathodic half - cell reaction. When the pore solution is alkaline and has ready access to the air, the reduction of dissolved oxygen takes place.

The electrical circuit is completed through the electrolyte solution in which the hydrated ions move through the hydrated cement paste (hcp) pore solution in the concrete as mentioned above. Figure 2.9 is a schematic representation of the corrosion of steel in concrete.

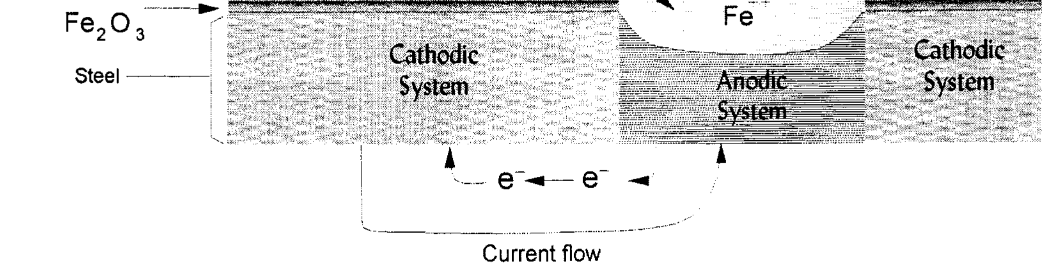

Fig. 2.9: Corrosion process (Mehta and Montiero, 1993)

Once the hydroxyl ions are produced, they migrate to the anode and react with the hydrated anions (Fe^{2+}) to yield ferrous hydroxide. In the presence of oxygen, the ferrous hydroxide oxidizes and is converted to a more stable form to produce hydrated oxide of iron [$2Fe(OH)_3$] which is commonly known as rust. The final product, the rust, is an admixture of $Fe(OH)_2$, $Fe(OH)_3$, FeO, Fe_2O_3, Fe_3O_4, and other ferric and ferrous oxides, hydroxides, chloride, and hydrates. Their composition depends on the availability of the pore water, its pH and composition, and the oxygen supply. The corrosion process can be summarized as follows:

<u>OXIDATION (Anodic reaction)</u>

$$Fe \rightarrow Fe^{2+} + 2e^{-} \tag{2.3}$$

<u>REDUCTION (Cathodic reaction)</u>

$$O_2 + 2H_2O + 4e^{-} \rightarrow 4(OH)^{-} \tag{2.4}$$

The intermediate reactions can be obtained by adding the partial anodic and cathodic reactions as:

$$2Fe + 2H_2O + O_2 \rightarrow 2Fe^{2+} + 4OH^{-} \rightarrow 2Fe(OH)_2 \tag{2.5}$$

Ferrous hydroxide [$Fe(OH)_2$] precipitates from the solution, however, this compound is unstable in an oxygenated solution and oxidizes to the ferric form as:

$$2Fe(OH)_2 + H_2O + \tfrac{1}{2} O_2 \rightarrow 2Fe(OH)_3 \text{ (Rust)} \tag{2.6}$$

2.4 Forms of corrosion and their protection

Corrosion will not occur either in dry concrete where the electrolytic process is impeded, or in water-saturated concrete where oxygen cannot penetrate, even if the passive layer is destroyed. The highest corrosion rate will occur in the concrete surface layers subjected to highly changing wetting and drying conditions. Corrosion of reinforcement can take different forms, ranging from widespread general uniform corrosion to very localized attack. The prevailing environment and the rate of the corrosion, by the degree of polarization of anodic or cathodic processes and their potential differences, or the electrical resistances of the cement matrix, determine the type of corrosion. Fontana (1986) presented eight kinds of corrosion, which are included here in a summary form for completeness:

- Pitting corrosion- The breakdown of passive film occurs locally which results in the breakdown of macro-galvanic cells. The anodic and cathodic reactions are separated with larger cathodic areas supporting small concentrated anodic areas. Such a microcell is usually associated with high levels of moisture giving low electrical resistance in the concrete and easy transport of the ions so that the anodes and cathodes are separated. In the chloride-induced corrosion, the passive layer will be dissolved only over small surface areas, so that small anodic and huge cathodic areas will exist on the surface, which causes substantial local reductions in the cross-sections of the reinforcement. In addition, the chloride ions will act as a catalyst in the pit and accelerate the dissolution of iron in the anodically acting pit. (Fig. 2.10)

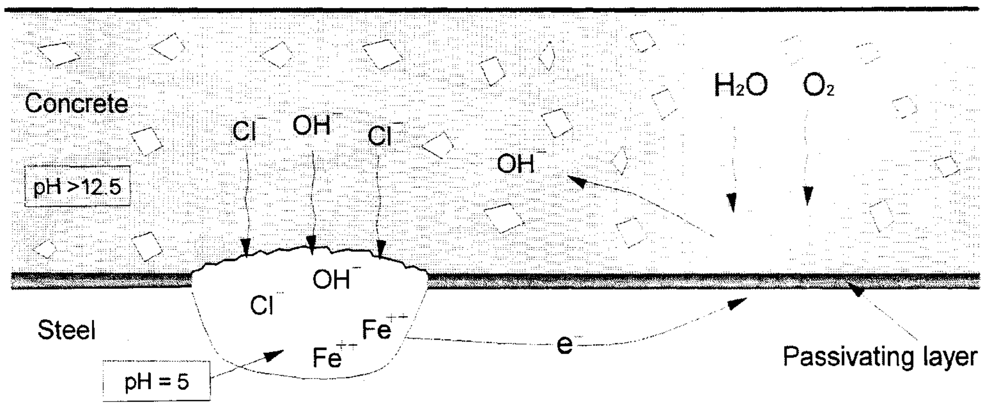

Fig. 2.10: Schematic representation of pitting corrosion in the presence of chlorides (Schiessl, 1987)

Pitting can be reduced by additions of alloys such as 2% molybdenum in stainless steels.

- Galvanic corrosion- This form depends on the contact between two different metals in an electrolyte, such as seawater. Of the two metals, the less noble one becomes the anode and undergoes corrosion. Galvanic corrosion can be reduced by cathodic protection.
- Uniform attack- This form of corrosion is easier to control because the average rate of corrosion can be determined and a corrective step can be taken. All parts of the metal surface are in equal contact with the corrosive environment, and the metal itself is uniform in metallurgical properties and composition. Atmospheric corrosion is a form of uniform corrosion. The common methods of prevention include painting, enamelling and metallic coatings.
- Intergranular corrosion- This results from grain boundaries acting as anodic areas. The granular structure of most metal or alloys can be viewed under a microscope.

This structure consists of quantities of individual grains, and each of these tiny grains has a distinct boundary that differs chemically from the metal within the grain center. A specific example is 'sensitization' of austenitic stainless steels due to formation of chromium carbides near the grain boundaries. This occurs when the steels are heated in the range of 500-800°C in service or during welding. This can be avoided by choosing stainless steels with titanium, or niobium additions, called stabilized stainless steels or stainless steels with low carbon content.

- Selective leaching- This is due to the dissolution of one of the alloying elements from the alloy, leaving the material spongy and weak. For example, in dezincification of brass, zinc leaves the material, resulting in failure of brass components.
- Erosion corrosion- This occurs mainly due to the mechanical action or impingement attack particularly in rotating parts in liquids. For example, pump impellers are subjected to erosion corrosion due to solid particles or formation of bubbles and cavitation. Proper design and selection of alloys, filtering of liquids, deaeration can reduce erosion corrosion.
- Crevice corrosion- This form of corrosion results in oxygen starved areas undergoing dissolution. This may occur under crevices (bolts or rivets attached to plates). Protection can be offered by improved design and by deaeration of water.
- General corrosion- This form of corrosion is normally characterized by a reaction which proceeds uniformly over the entire surface of the metal. All points on the surface corrode at a similar rate because corrosion occurs on a microcell level.

This occurs when the concrete is generally drier not allowing the separation of the anode and cathode, as ions cannot move large distance as shown in Fig. 2.11.

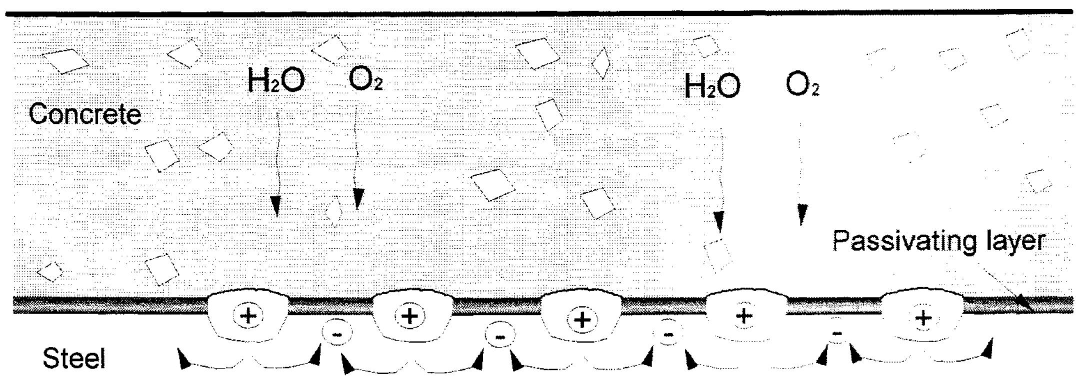

Fig. 2.11: General corrosion (Broomfield, 1997)

General corrosion results in cracking, rust staining and spalling of the concrete. There is usually sufficient warning, hence this form of corrosion is not as dangerous as pitting corrosion.

2.5 Protective strategies for corrosion of reinforcing steel

2.5.1 Design stage

- Proper concrete design
  - High quality concrete with low w/c ratio (w/c ratio≤0.5, and 0.4 if severe chloride attack is expected)
  - Thicker concrete cover thickness
  - Use of concretes blended with slag, natural pozzolans, fly ash, silica fume
  - Good curing plan

    - Reinforcement of concretes made by addition of stainless steel, glass and polypropylene fibre-reinforced bars
- Provision of adequate drainage facilities to avoid any possible saturation with water
- Careful structural detailing including concrete cover thickness, and reinforcement size and spacing
- Limit crack widths for steel reinforcement and prestressing steel
- Consider replaceability of structural elements

2.5.2 Execution stage

- Proper curing and compaction of concrete
- Set curing time depending on the aggressivity of the environment and the curing sensitivity of the concrete mix
- Use of stable spacers to meet specified minimum cover thickness tolerance values
- Use of improved formwork (permeable lining)
- Use of temporary coatings and impregnations in curing
- Better quality control

2.5.3 Other protective measures

Other protective measures to prevent corrosion of reinforcing steel are:

- Coatings, such as oils, grease, tar, bitumen, paints and electro-deposited platings
- Membranes

- Treatment of medium by addition of inhibitors, such as potassium dichromate for aluminium alloys, deaeration of water/cement ratio
- Use of sacrificial anodes –galvanizing
- Penetrating sealers
- Fibre-reinforced concrete
- Epoxy-coated bars
- Nickel-clad bars
- Use of normal steel, or high strength steel
- Cathodic protection

Chapter 3

Durability design of concrete structures

3.1 Introduction

Traditionally, durability design of concrete structures is based on implicit prescriptive rules for materials, material compositions, working conditions, structural dimensions, etc. Examples of such rules are requirement for minimum concrete cover, maximum water/cement ratio, minimum cement content, crack width limitation, air content, cement types and coatings on the concrete. These rules are sometimes related to the type of environmental exposure such as indoor climate, wet exposure, presence of de-icing salts, seawater, etc. The purpose of all of these rules is to secure robustness in concrete structures, although no clear definition for service life has been presented. The explicit relationships between the performance and the service life of structures need to be developed as design tools. Clients and owners of buildings have shown keen interest in setting service life requirements for structures especially in 1990's. Also, durability and service life concepts have been stressed in the various contract briefs. New methods for more scientific durability design of structures are needed. The vast research from 1970s to 1990s on concrete durability has produced reliable information and knowledge on deterioration processes. Because of this knowledge, it is now possible to incorporate durability in the mechanical design of concrete structures. The durability models help the designers to make decisions on the required dimensions and material specifications for structures with a service life requirement.

3.2 Durability design

The term "durability" is defined as the capability of a building, assembly, component, structure or product to maintain minimum performance over at least a specified time period under the influence of the various degradation factors. Durability design of concrete structures can be considered as a comprehensive design procedure that could guarantee satisfactory performance of the structure over the required service life without wasting the earth's resources. A comprehensive design should integrate safety, serviceability and durability considerations based on a clear and accurate understanding of the entire time-dependent behaviour of the structure over the design service life.

3.3 Importance of durability design

During its construction and its subsequent lifetime, a structure must perform many functions with regard to strength and serviceability. The conditions under which it fulfills this will change in the course of time, and the properties of the structure itself are time-dependent. If the structure ceases to perform after the passage of time, rehabilitation or replacement will become necessary. Otherwise, the structure would have reached its technical service life. To assess durability of a structure is not simple. The conditions under which the structure needs to function are comparatively uncertain. Because of these uncertainties, the service lives of essentially similar structures under similar conditions may vary considerably. The concept of service life is, therefore, difficult to apply in a meaningful way. For this reason, the first step is to develop a durability philosophy. Traditional strength-based design for new concrete structures has failed to provide reliable long-term performance of structures exposed to aggressive environments. Most national building codes have aimed at ensuring that the structure being designed, constructed and operated would perform satisfactorily at the ultimate and the serviceability limit states. Therefore, a capacity reduction factor is used in the calculation of the resistance of the concrete structures for consideration of the variation of the material properties, member geometry and details, deficiencies in construction practice and quality control, and the normal variation in the applied loads. However, these considerations do not include the time-dependent behaviour of the loads and the resistances of the concrete structures. The load may change as the highway loading has increased significantly over the past several years. The resistance of a concrete structure will decrease due to ageing of the material and deterioration because of the various environmental influences. Therefore, the long-term performance of the concrete structure over the design service life is not adequately reliable to guarantee safety of the concrete structure. A typical example is the abandoned Dickson Bridge in Montreal, which was constructed in 1959 and it was decommissioned in 1993 (Mirza *et. al.*, 1998). The "supposed" design service life of the bridge was about 70 years, however the bridge had to be decommissioned after only 35 years. Amleh (2000) noted that the influence of the service environmental conditions, poor quality control in construction practices and materials contributed to the early failure of the bridge. This example shows that in order to obtain a satisfactory performance over the design service life, a comprehensive durability design must be undertaken during the design phase; also adequate quality control is needed during the construction phase, along with regular maintenance throughout the service life.

3.4 Durability design concept

3.4.1 Service life

The service life of a structural system is the period of time after completion of construction, or installation during which all essential properties meet, or exceed minimum acceptable values, when routinely maintained. In other words, it is period of time after the completion of the structure during which the structure maintains a satisfactory performance without any unacceptable expenditure on maintenance and repair. The exact definition of service life is obscured by the fact that maintenance routines are performed during the service life of the structure. Maintenance can influence the length of the service life. The problem of service life of a structure can be approached from at least three different aspects (Sarja and Vesikari, 1996):

- Technical aspects
    - Mechanical and other structural performance
    - Serviceability and convenience in use
    - Aesthetics
- Economic aspects
- Functional aspects

Different aspects give rise to different requirements. Technical aspects require a satisfactory technical performance of the structure, which includes the structural integrity of the structure, adequate load-bearing capacity of the structure and adequate serviceability performance of the structure, such as acceptable deflection, cracking and vibration requirements and/or strength of materials. Most of the technical requirements are normally included in the various codes and standards. Structures must be designed so that the minimum safety level is attained during the intended service life despite degradation and ageing of materials. Defects in materials can also lead to poor serviceability, or inconvenience in the use of the structure. For example, the disintegration of concrete pavement can cause inconvenient vibrations and impact on vehicles. Functional requirements are related to the normal use of the structures, for example, the width and height of a bridge must fulfill the traffic requirements both on and under the bridge. The length of service life is not only dependent on the technical condition, but also on the societal change such as the traffic volume development. Economic consideration is based on the investment and the costs of operating the structure; the owner always wants to minimize their expenditures by ensuring durable structures and minimizing their life cycle costs.

Richardson (2002) noted that the design service life of a building or a structure should be determined based on the expectation of the client. The client needs to indicate the category of structure as " temporary", "normal", or "major infrastructural". Then, the designer must determine the expected service life for the different structures according to the information in the standards and codes, which provides the clients with multiple options to balance between the first cost and the life-cycle cost.

3.4.2 Theory of failure probability and service life

The simplest mathematical model for describing the event 'failure' comprises a load effect variable S and a resistance variable R. In principle, S and R can be any quantities relating a cause and an effect and can be expressed in any units.

If R and S are independent of time, the event can be expressed as (Richardson, 2002):

$$p\{\text{failure}\} = p\{R < S\} \tag{3.1}$$

It means that failure occurs if the resistance is smaller than the load effects.

Either the load effect S, or the resistance variable R can be time-dependent quantities, thus making the failure probability also a time-dependent quantity. Considering $R(\tau)$ and $S(\tau)$ as instant physical values of the resistance and the load at moment, τ, the failure probability in a lifetime t could be defined as

$$p(t) = p\{ R(\tau) < S(\tau) \} \quad \text{for all } \tau \leq t \qquad 3.2(a)$$

The determination of quantity p(t) given by equation 3.2(a) is mathematically difficult. Considering R and S as stochastic quantities with time-dependent or constant density distributions, the equation 3.2(a) becomes:

$$p(t) = p\{ R(t) < S(t) \} \qquad 3.2(b)$$

According to equation 3.2(b), the failure probability increases continuously with time (Fig. 3.1)

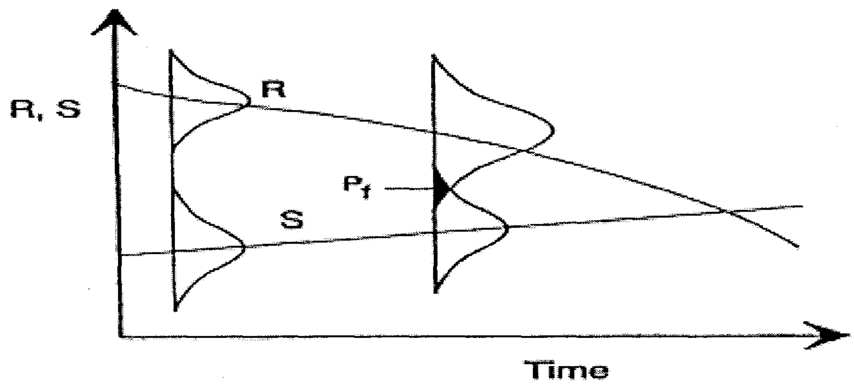

Fig. 3.1: The increase of failure probability (Sarja and Vesikari, 1996)

At the time t=0, the density distributions of the load and the resistance are far apart and the failure probability is relatively small at first, when the structure is just put into operation. The distributions approach each other with increase in time forming an increased overlapping area, which is an indication of the failure probability, although it does not represent the probability of failure directly.

3.4.3 Principles of durability design

According to the RILEM Report of TC 130-CSL (Sarja and Vesikari, 1996), the basic equations of durability design can be developed according to two principles:

- Performance principle
- Service life principle

While using the performance principle, the basic design formula is given by setting a relationship between the load effect variable, S, and the performance variable, R. The performance, evaluated by a performance model must be greater than the effects resulting from the applied load. In the case of service life principle, the service life evaluated by a service life model must be greater than the required target service life. Normally, both principles yield the same results. The selection of an appropriate principle depends upon the set up of the design problem.

3.4.4 Methods of durability design

Based on the RILEM Report of TC 130-CSL (Sarja and Vesikari, 1996), three methods that could be used for durability design are the deterministic method, stochastic method and lifetime safety factor method. The methods for traditional static or dynamic design can be used for durability design in the same way. These methods are presented here for completeness.

3.4.4.1 Deterministic design method

In deterministic durability design, the load, resistance, service life and other parameters can be used as deterministic entities without any consideration for their statistical distributions.

Assuming that the load effect S and the resistance R are time-related functions, the load S and resistance R can be $S(t_g)$ and $R(t_g)$ at the end of target service life, t_g.

According to the performance principle, the design equation can be written as:

$$R(t_g) - S(t_g) > 0 \tag{3.3}$$

where $R(t_g)$ = the resistance at the end of design service life, t_g, and

$S(t_g)$ = the load effects at the end of the design service life

According to the service life principle, the corresponding design equation is given by:

$$t_L - t_g > 0 \tag{3.4}$$

where t_L is the design service life.

3.4.4.2 Stochastic design method

In stochastic design, the statistical distributions of the various parameters such as the load effects, response of the structure, service life, resistance, and a maximum allowable failure probability are required.

The design process must ensure that

$$p_f = p\{(R-S) < 0\}_{tg} < p_{f\max} \tag{3.5}$$

where p_f = the probability of failure of the structure within the target service life t_g

$p_{f\max}$ = the maximum allowable failure probability

Uncertainty exists in the resistance of the concrete structure because the actual resistance of the concrete structure will depend on the material selection, the quality of construction, including concrete compaction and curing. The resistance will decrease with time due to ageing, deterioration and other factors; therefore a considerable uncertainty will be involved. The load effects also have uncertainty; its daily fluctuation and the rare possibility of an unexpected extraordinary load should also be considered in design.

Richardson's (2002) probabilistic concepts are shown in Fig. 3.2, which shows the deterioration process at an increasing rate with the age of the structure. The variation of the maximum level of deterioration is showed at the acceptable level of damage at the right end of the service life axis.

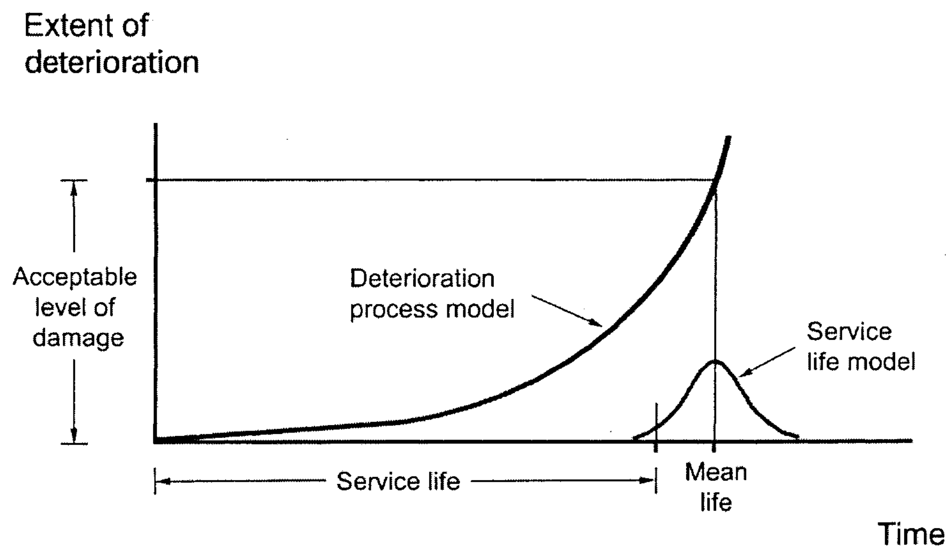

Fig. 3.2: Concept of service life prediction based on durability considerations (Richardson, 2002)

3.4.4.3 Semi-probabilistic design method

Multiple variables and their distributions exist in the durability design problem, which result in complex mathematical solutions (Richardson, 2002). Therefore, semi-probabilistic approach, which is similar to the existing design methods for conventional design methods, is needed for practical durability design.

Lounis and Mirza (1996) proposed a semi-probabilistic approach for durability design, where partial safety factors for the resistance, resistance deterioration and load effects have been derived using the first order, second moment reliability theory. The design equation is

$$\phi R - \psi \Delta R \geq \lambda S \tag{3.6}$$

where ϕ, ψ and λ are partial safety factors for resistance R, resistance degradation (ΔR) and load effects (S).

When the equations for load effects, resistance and service life are complex and many degradation factors affect the performance of structure, application of stochastic design methods may be difficult. In such cases, it is reasonable to apply the lifetime safety factor method proposed by Sarja and Vesikari (1996). For practical application of the stochastic method, they introduced a lifetime safety factor to obtain the design service life, as:

$$t_d = \gamma_t t_g \tag{3.7}$$

where t_d = the design service life,

γ_t = the lifetime safety factor, and

t_g = target service life.

The design process must ensure that

$$R(t_d) - S(t_d) \geq 0 \tag{3.8}$$

$$\text{or, } t_L - t_g > 0 \tag{3.9}$$

where $R(t_d)$ = resistance at the end of the design service life,

$S(t_d)$ = load effects at the end of the design service life, and

t_L = service life.

3.4.5 Durability design model for safety

Sarja and Vesikari (1996) stated that durability design of concrete structures could be treated using the same basic methodology as the traditional static, or dynamic design. The conventional performance-based structural design assumes for simplicity that the resistance and load effects are constant throughout the service life of the structure. The basic design equation is:

$$p_f = p\{R < S\} < p_{target} \tag{3.10}$$

where R = the resistance at the beginning of the service life,

S = the load at the beginning of the service life,

p_f = the probability of failure of the structure within the target service life, t_g

p_{target} = the target probability of failure of the structure.

However, this assumption is not correct because the resistance will decrease due to ageing of the material and deterioration resulting from the various environmental attacks. Also, the load effects may change, for example, the highway loading may increase significantly over time. Therefore, the resistance and load effects are functions of time, as *R(t)* and *S(t)*. The model for performance-based durability design can be expressed as

$$p_f = p\{R(t) < S(t)\} < p_{target} \qquad 0<t<t_L \tag{3.11}$$

where p_{target} = the acceptable maximum value of the probability of failure,

R(t) = the resistance at time *t* during the service life,

S (t) = the load effect at time *t* during the service life, and

p_f = the probability of failure of the structure within the target service life, t_g

3.4.6 Durability design model for serviceability

3.4.6.1 Durability design model based on service life

Based on the stochastic theory, Sarja and Vesikari (1996) set durability design requirement as follows: the probability of the service life of a structure being shorter than the target life must be smaller than a certain allowable probability. The design equation is:

$$p_f = p\{t_L < t_g\} < p_{f\max} \tag{3.12}$$

where p_f = the probability of failure of the structure within the target service life, t_g

$p_{f\max}$ = the maximum allowable failure probability,

t_L = service life, and

t_g = target service life.

Sarja and Vesikari (1996) also proposed a durability design model based on service life using the lifetime safety factor method. The condition is written as

$$t_L - \gamma_t t_g > 0 \tag{3.13}$$

where t_L = the service life,

t_g = the target service life, and

γ_t = the lifetime safety factor.

3.4.6.2 Durability design model for chloride-induced corrosion

The chlorides are mainly responsible for the depassivation of steel reinforcement, which leads to corrosion. The chloride transport in concrete may take place through three different ways. (i) permeation of salt solution (ii) capillary absorption and (iii) diffusion of chloride ions. Common parameter for all these three transport mechanism is that they require a certain level of moisture in the pore system of concrete.

The model available for evaluation of finding the chloride content at any depth (RILEM Report of TC-130 CSL, 1996) is:

$$C_x = C_s[1 - erf[\frac{x}{2\sqrt{(Dt)}}]\ ] \tag{3.14}$$

where C_x = the chloride content at depth x,

C_s = the chloride concentration at the concrete surface,

x = depth from the surface of the structure,

D = diffusion coefficient,

t = time, and

erf = error function.

The initiation time for corrosion is given by the equation

$$C_{th} = C_s \left[1 - erf\left[\frac{c}{2\sqrt{(Dt_0)}}\right]\right] \tag{3.15}$$

C_{th} = the critical chloride content (the generally accepted threshold value for the reinforced concrete is 0.4 % by the weight of cement and 0.2 % by the weight of cement for prestressed concrete, and this corresponds to approximately 0.05 to 0.07 by weight of concrete, 0.025- 0.035 for prestressed concrete)

c = the concrete cover thickness,

D = diffusion coefficient for the concrete, and

t_0 = initiation time of corrosion

This equation can be simplified by using a parabolic function

$$C_x = C_s \left[1 - \left[\frac{x}{2\sqrt{(3Dt)}}\right]\right]^2 \tag{3.16}$$

The value of t_0 (initiation time of corrosion) can be written as:

$$t_0 = \frac{1}{12D}\left[\frac{c}{1 - \sqrt{(C_{th}/C_s)}}\right]^2 \tag{3.17}$$

The propagation time at cracking can be calculated as:

$$t_1 = S_{max} / r$$

or $$t_1 = (D - D_{min}) / 2r \qquad (3.18)$$

where t_1 = the propagation time for corrosion at cracking,

r = the rate of corrosion at cracking,

S_{max} = the maximum allowable depth of corrosion, and

D_{min} = the minimum diameter of the steel bar.

3.4.6.3 Durability design model for carbonation-induced corrosion

Carbon dioxide in the air penetrates the concrete, neutralizing its alkaline components and producing a carbonation front, which advances towards the interior. When this carbonation front reaches the reinforcement, the passive film on the steel becomes unstable and it dissolves, enabling generalized corrosion to occur. As mentioned earlier, the rate of carbonation is related to the square root of time:

$$d = K_c t^{0.5} \qquad (3.19)$$

where d = the depth of carbonation at time t,

K_c= the carbonation coefficient for the concrete and is dependent on the strength of concrete, binding agents, cement content, environmental factors such as temperature and humidity, and

t = time or age.

The value of K_c (RILEM Report of TC-130 CSL, 1996):

$$K_c = c_{env} c_{air} a (f_{ck}+8)^b \qquad (3.20)$$

where c_{env} = the environmental coefficient,

c_{air} = the air content coefficient,

f_{ck} = characteristic compressive strength of concrete in MPa, and

a,b are the parameters depending upon the binding agent.

Steel depassivation

The depassivation of steel can occur due to chloride ingress or carbonation of concrete. When corrosion develops, three main phenomena are involved:

- A decrease in the steel cross-section
- A decrease in the bond characteristics at the steel rebar-concrete interface
- Cracking in the concrete cover and therefore decrease in the concrete load bearing cross-section

The propagation time of corrosion can be calculated using the equation (RILEM Report of TC-130 CSL, 1996):

$$t_l = \Delta R_{max}/r \tag{3.21}$$

where t_l = the propagation time of corrosion (in years),

ΔR_{max} = the maximum loss of radius of the steel bar, and

r = the rate of corrosion.

Cracking time of concrete cover

The propagation time can also be calculated as (RILEM Report of TC-130 CSL, 1996):

$$t_l = 80(C/D\mathrm{r}) \tag{3.22}$$

where C = the thickness of the concrete cover, and

D = diameter of rebar

The rate of corrosion strongly depends on the ambient conditions and can be approximated by using the following equation (RILEM Report of TC-130 CSL, 1996):

$$r = c_T \, r_0 \tag{3.23}$$

where c_T = the temperature coefficient, and

r_0 = the rate of corrosion at + 20° C.

3.4.7 Durability design through an "all-encompassing" prescriptive approach.

The durability design method depends on a complete understanding of each relevant deterioration mechanism and the expected service life of the structure in a quantitative manner (Richardson, 2002). Although research around the world has identified the key deterioration mechanisms and their controlling parameters, further research is needed to refine the mathematical models for the various modes of deterioration. Therefore, the "all-encompassing" prescriptive design approach can be used before the scientific durability design method is developed and accepted by the practising engineers. This involves consideration of design details and deemed-to-satisfy rules, such as the control of minimum cement content, maximum water/cement ratio, and minimum cover thickness, compaction and curing.

3.5Practical examples of durability design

3.5.1 The Great Belt Link

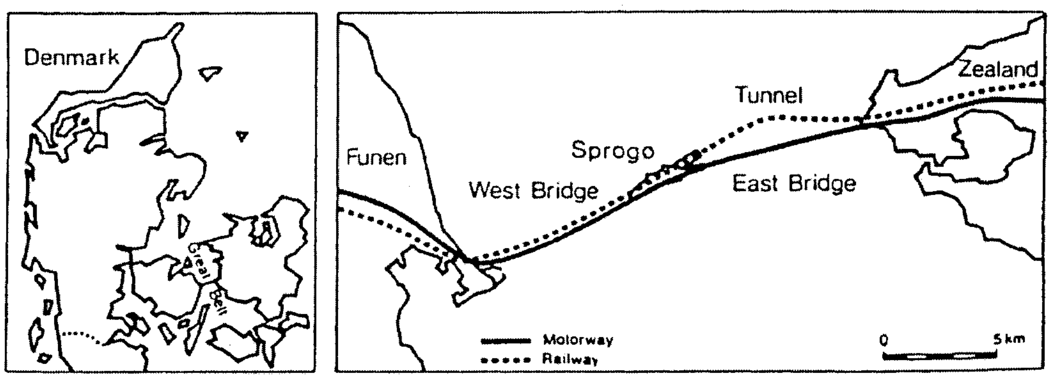

Fig. 3.3: The Great Belt Link (Rostam, 1994)

Rostam (1994) reported a detailed example of durability design - the design of the concrete structures for Denmark's Great belt Link, which used "Multi-Stage Protection Strategy" to achieve a design service life of 100 years. The Great Belt fixed link in Denmark, a US$ 4 billion project, was constructed to improve the northern European transportation network and will be later completed with fixed links to Sweden and Germany for full interconnection of Scandinavia with Central Europe. The project included a 1624 m-span suspension bridge, which is the longest bridge span in the world; it integrated a major bridge with elements weighing up to 7300 tonnes placed by a floating crane, and a tunnel driven through the tough ground conditions. There were three major structures in the link: a railway tunnel, a high-level motorway bridge and low-level dual mode bridge for railway and motorway. Danish consultants with COWI Consult acting as the lead design partnered with three major consultants to establish a joint venture which comprised Mott MacDonald, Carl Bro Group and Leonharft, Andrä und Partner in the West Bridge Project, and RambØll, Hannemann & Højlund.

To obtain a 100 years design service life, the multi-stage protection strategy was adopted from design and construction to maintenance. The environmental aggressivity was defined and strict requirements were set from the design and the construction phases to operation processes when the structure is exposed to aggressive environment.

The environmental aggressivity was defined according to the chloride and the sulphate concentrations in the soil and the seawater. The chloride concentration in soil of the east tunnel and in seawater was 19,000 ppm and the sulphate concentration in soil of the East tunnel was 2,500 ppm. This exposure could become serious for structures expected to reach 100 years service life and subjected to evaporative effects.

Based on the aggressivity of the different environments, the concrete cover is specified for different locations. For example, the fully submerged caissons and parts of the pier shafts under sea level are considered to be exposed to an environment with limited aggressivity and the cover thickness for this part of structure is 50 mm + 5 mm tolerance. The splash zone of the pier shafts is considered to be the most exposed parts of the bridges and the cover thickness for this part of structure is 70 mm + 5 mm tolerance. Because of the risks of corrosion from deicing salts, the cover thickness of the concrete edge beams of the West bridge was specified as 70 mm + 5 mm tolerance.

The concrete mix proportions for the main structures of the Great Belt Link were carefully specified to obtain high quality concretes, however, the existing technology was uncertain whether it was enough to guarantee an expected service life of 100 years. Table 3.1 shows the concrete mix design for the Great Belt Link.

Table 3.1: Comparison of actual concrete mix proportions for the different main structures of the Great Belt Link: Rostam (1994)

	Great Belt Link		
	East Bridge	**East Tunnel**	**West Bridge**
Concrete Type	**A**	**A1**	**B**
Cement (kg/m^3)	315	335	320
Fly ash (kg/m^3)	40	40	38
Microsilica (kg/m^3)	20	20	16
Water (kg/m^3)	130	128	138
Sand (kg/m^3)	575	585	245
Aggregate 2/8 mm (kg/m^3)	450	-	575
Aggregate 8/16 mm	478	1360	392
Aggregate 16/32 mm	347	-	586
Air entrainment (%)	0.6	-	1.9
Plastisizer (kg/m^3)	1.5	0.8	1.7
Superplastisizer (kg/m^3)	5.0	3.0	6.5
W/c ratio	0.34	0.32	0.37
Air, fresh (%)	5.5	1.7	6.0
Slump (mm)	120	10	140

The curing time is specified for the different types of concrete to get the highest possible integrity and low penetrability. Type A concrete was cured for 240 maturity hours and type B for 96 maturity hours. In addition, differential temperatures were also controlled curing during hardening of the concrete. Detailed 2D and 3D finite element calculations were performed to ascertain the concrete properties at an early age based on the actual concrete mix, which would be successful in minimizing or avoiding the cracks. The additional multi-stage protection strategies used in East Tunnel included:

- Using an annular grout with high binding capacity for chlorides and sulphates
- Using high strength concrete in some segments with fully gasketed joint seals to ensure a water tight lining
- Using epoxy coating for the welded reinforcement cages
- Preparing for future cathodic protection of welded reinforcement cages.

The multi-stage protection strategies used in the West Bridge and East Bridge included:

- Using temporary cathodic protection for submerged caissons using sacrificial anodes located in the sea.
- Impregnating silane in the splash zone of pier shafts and edge beams
- Using permeable formwork liner for most road and railway edge beams and critical parts of the pier shafts.

Moreover, durability design of the Great Belt Link also considered the service life maintenance such as routine inspection and the replacement of the elements whose design service life is less than 100 years. The design service life of bridge elements are clearly defined, the primary structural elements were designed with a service life over 100 years, the secondary structural elements for 40-60 years and the bridge equipment such as the pavement is expected to be replaced at 20-30 year intervals. Durability monitoring through equipping the critical zones with advanced corrosion monitoring equipment was part of the preplanned operation and maintenance procedures in the Great Belt Link project.

3.5.2 Confederation Bridge

The design and the construction of the **Confederation Bridge** from Borden (Prince Edward Island) to Cape Tormentine (New Brunswick) is one of the engineering marvels of this century. The design engineers had to achieve a 100-year design standard in all aspects, including the bridge resistance to the combined effects of wind, waves and ice. In addition, the construction engineers faced their own challenges. They were required to build a 13 km long bridge in about three and a half years (with the construction season lasting only six months each year) to new and exacting standards. The construction engineers met this challenge by precasting the massive elements on land, then assembling the 185 main components in the strait with the fleet of giant marine equipments. The high engineering standards, creative thinking and a condensed construction time frame are only part of the story. The team of Canadian Engineers was full aware of the historical, constitutional and cultural significance of a permanent link between Prince Edward Island and mainland Canada. For these reasons, the **Confederation Bridge** is truly one of the greatest engineering achievements of the 20th century. The approach taken to ensure the 'durability' of the bridge for 100 years while designing and constructing was a safety index β = 4.00 for the ultimate limit states and the use of High Performance Concrete (HPC).

Bridge Description:

The 12.9 km long Confederation Bridge crosses the Northumberland Strait between New Brunswick and Prince Edward Island. It consists of 20 approach spans of segmentally erected precast concrete and 44 main spans, each of which is 250 m in length and is made up of four massive precast elements.

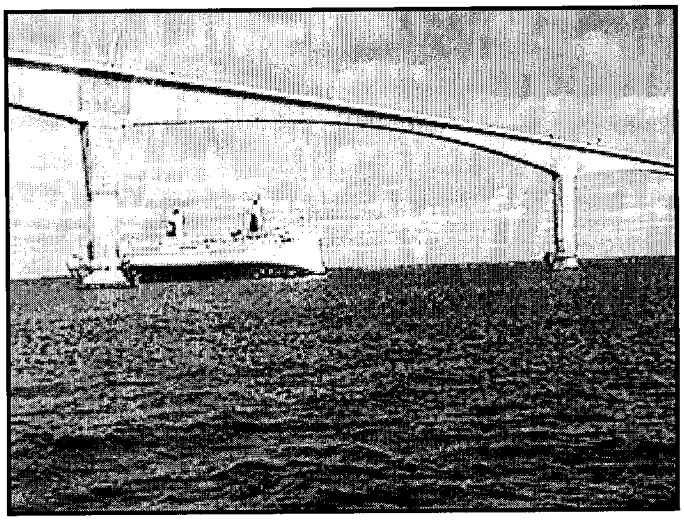

Fig. 3.4: The Confederation Bridge (www.confederationbridge.com)

The total crossing is divided into three major sections: the 1320 m (4330 ft) New Brunswick Approach, the 10,990 m (36,050 ft) main bridge, and the 570 m (1870 ft) Prince Edward Island Approach. The main bridge spans are 250 m (820 ft) long and have a depth varying from 4.5 to 14.5 m (15 to 48 ft); both approach structures have typical spans of 93 m (305 ft) and a depth varying from 3.0 to 5.1 m (10 to 17 ft). Water depths in the Strait vary along the alignment, with a maximum depth of about 35 m (115 ft) in the navigation channel. The salient features of the Confederation Bridge are summarized in Table 3.2.

Table 3.2: Salient features of Confederation Bridge

Basic Structure:	Shore to shore bridge; no causeway component
Structural Materials:	Reinforced, post-tensioned concrete
Length:	12.9 km (8 miles), crossing the Strait at its narrowest point
Width:	11 m. (36 feet) from barrier wall to barrier wall, including one lane and one emergency shoulder in each direction.
Typical Elevation:	40 m. (131 feet) off the water.
Typical Clearance:	23 m. (75 feet) off the water by 220 m. (722 feet) wide
Navigation Span Elevation:	60 m. (197 feet)
Depth of Strait:	Up to 35 m. (115 feet)
Main Bridge Footings:	Gravity foundation on bedrock
Main Bridge Piers:	Octagonal shafts
Main Bridge Girders:	Precast concrete box girders ranging from 4.5 m. (15 feet) to 14 m. (46 feet) deep, 190 m. (623 feet) length.
Main Bridge Spans:	44 piers, 11,000m. (6.8 miles) total; typical span length 250m. (820 feet)
Main Bridge Drop-In Span:	Precast concrete box girder, 60 m. (197 feet) length
PEI Approach Bridge:	7 piers, 580 m. (1/3 mile) total
NB Approach Bridge:	14 piers, 1.29 km (8/10 mile) in total
Approach Bridge Footings:	Spread footing with drilled shear keys
Approach Span Piers:	Rectangular shafts
Approach Bridge spans:	93 m

Structural Design:

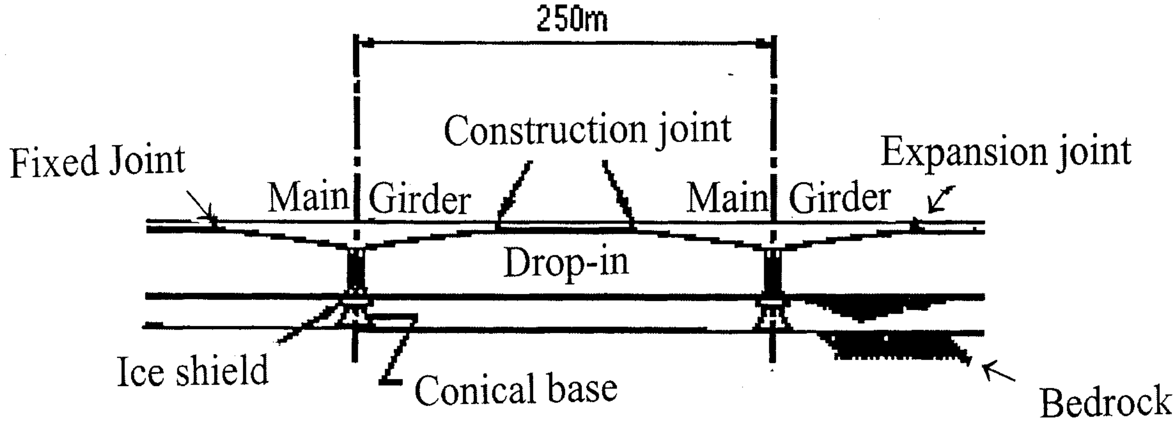

Fig. 3.5: Typical frame in design of Confederation Bridge (www.confederationbridge.com)

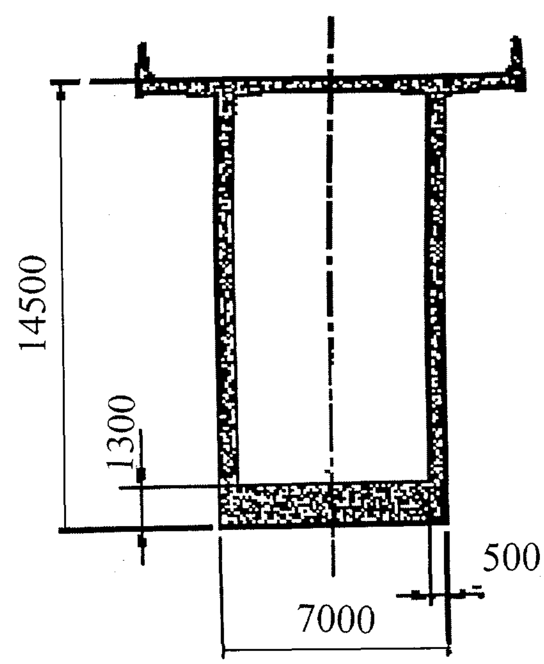

Fig. 3.6: Section at pier of Confederation Bridge (www.confederationbridge.com)

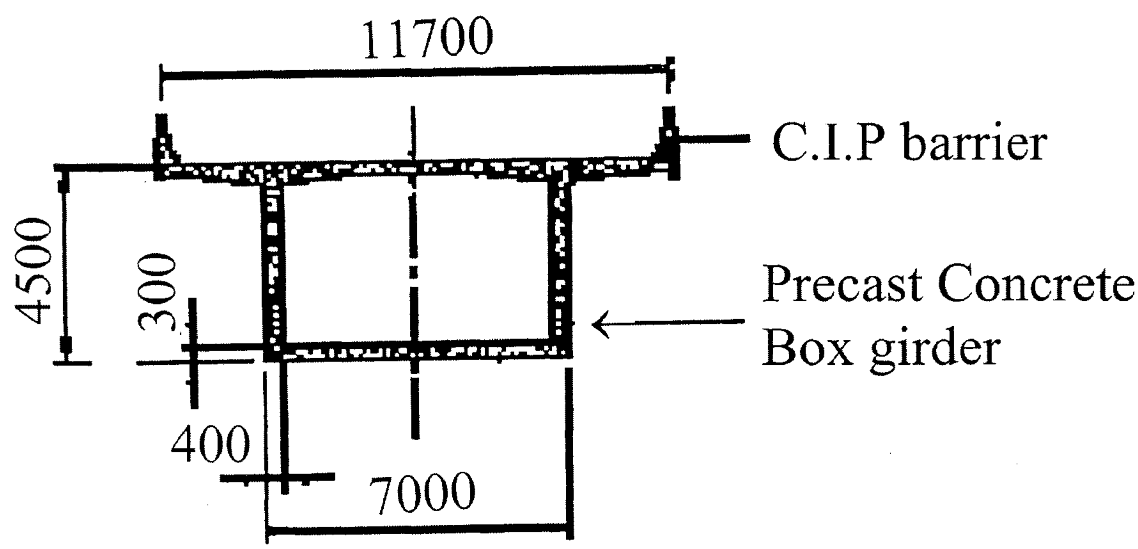

Fig. 3.7: Section near midspan of Confederation Bridge

The design concept for the bridge is a gravity-based precast concrete structure consisting of approach spans at each end, in conjunction with typical marine span frames (Fig. 3.5) crossing the Northumberland Strait. Each frame consists of a pair of 190 m double cantilever main girders fixed to 8m octagonal piers supported on conical pier supported on conical pier bases founded on bedrock. Drop-in girders 60 m in length complete the frame.

The approach spans are designed using a segmental balanced cantilever system with typical spans of 93m.

Main Bridge Components:

The bridge superstructure is a single cell, precast, prestressed trapezoidal box girder; the substructure is precast, or cast-in-place concrete. The roadway width is constant at 11.0 m from barrier to barrier; total bridge width is 12m. The profile grade of the main bridge is 40.80m above the project datum, increasing to 59m at the midpoint of the navigation span. The structural scheme of the main bridge consists of a series of 21 two-column portal frames connected by 22 drop-in spans. These frames and drop-in expansion spans form 43 main bridge spans, each 250m long.

Precast, prestressed concrete was selected for the construction of these components. Precasting satisfied the following major constraints: total project construction schedule of three years with completion by a fixed date, environmental limitations imposed by ice and weather on the time available for marine work in the Strait, and durability requirements dictated by design for a 100-year service life.

To achieve a 100-year service life, specific project criteria were developed for design, material selection, workmanship, and quality control. Special load combinations and load and resistance factors for ultimate and serviceability limit states were derived for the bridge design. For this a full calibration process using probabilistic reliability techniques was performed.

The design target safety index, β, which is a measure of the probability of failure of a structural member, is 4.0 for multi-load-path components and 4.25 for single-load-path components. For serviceability limit states, crack control and concrete cover for corrosion protection of reinforcing steel and prestressing tendons were evaluated for the different structural elements.

Table 3.3 represents the specified concrete properties for different classes of concrete used for the construction of Confederation Bridge:

Table 3.3: Different classes of concrete used for the construction of Confederation Bridge (www.lafargenorthamerica.com)

	Concrete Class		
	Class A	**Class B**	**Class C**
Strength: MPa			
18 hours	30		
28 days	55	30	
91 days	60	40	
28 days cast in air			35
28 days cast in water			28
10SF cement: min kg/m^3	450	300	400
Fly ash: max kg/m^3		130	
W/cm: max	0.34		0.4
Chloride Permeability: max coulombs	1000	1000	
Water permeability: max m/s	14^{-10}		
Air content (%)	5 to 8	5 to 8	4 to 7
Spacing factor: µm			
Mean	230	230	-
Individual max	260	260	-
Slump: mm	180+/-40	180+/-40	
Slump flow: mm	-		500 to 600
Chloride content: max % of cement	0.06	0.06	

Other Protective measures

The maintenance and inspection plan undertaken by the SCDI (Strait Crossing Development Inc.) is according to the latest technology and standards available. A multi-year monitoring and research project has been established to study the performance of the bridge. A state-of-the-art distribution data logger system measures ice load, thermally induced stresses and bridge dynamics such as tilt and bridge vibration on the instrumented bridge pier.

Few highlights of the program are mentioned below:

- *Use of sensors for monitoring the bridge*

  The engineers have included more than 750 sensors into the bridge design to measure the various forces. The sensors monitor everything from deformations in the bridge concrete to changes in temperature in the bridge and vibrations caused by traffic, as well as earthquakes.

- *Weather Monitoring Systems*

  The weathering systems are provided for constantly monitoring the weather conditions, wind speed, direction, air temperature, road temperature, humidity, dew point and rate of precipitation.

- *Ice monitoring program*

  The main objectives of the ice-monitoring program are as under:

  1. To observe the behaviour of ice against the conical ice breaking cones.
  2. To observe the geometric characteristics of the ice interacting with the piers.
  3. To observe the velocity of the interacting ice.
  4. To measure the pressures and local load distribution resulting from the ice interaction.
  5. To measure the global response of the pier under the action of ice and to derive the total ice force from this response.

  To measure the ice forces on the instrumented bridge pier, twenty-eight ice load panels are installed on the pier's ice shield. Each ice panel is divided into eight impact zones which function as load cells. Each zone produces a signal from a Wheatstone bridge comprised of strain gauges. To convert the 224 differential signals to single ended signals, four FDI 5016 multi-channel signal-conditioning racks are used. The single ended signals are band limited to approximately 5 Hz using Frequency Devices DP74 Series low-pass 4-pole Bessel filters which are located on 5016-4FF/DP74 quad cards. The amplified and filtered ice load panel signals are then sent to two high-speed data loggers.

- *Wind monitoring systems.*

  To measure dynamic response of the bridge under high wind conditions, seismic activity or from vehicular traffic on the bridge, a suite of 75 accelerometer signals is distributed throughout a 1 km section (Pier 30 to Pier 34) of the bridge. The accelerometer signals are sent to Frequency Devices 8044-3, eight channel filter mounting assemblies populated with D68L8L-50.0 Hz and D64L4L-5.00 Hz low-pass 8- and 4-pole Bessel filters which serve as anti-aliasing filter boards for the accelerometer signals before they are sent to high-speed data loggers that are distributed along the same 1 km length of bridge. The 8044-3 boards were chosen because they could be mounted in the NEMA4X junction boxes that house the data loggers.

- *Cathodic protection of reinforcement steel*

  Vetek Systems Corporation, Austria by using their product VETEK V2000, constantly monitors the corrosion of steel reinforcement. V2000 is a monitoring cable, which is used to signal the start and cessation of corrosion, and the intensity of the corrosion. The monitoring system is provided in the Deck & Piers.

- There are 7300 drain ports to allow for the runoff of rainwater, melting of snow and ice.
- The bridge surface is a long lasting bituminous mixture that minimizes vehicle spray during wet weather and allows for effective drainage of rainwater.
- A new process called Siemens-Martin Open Hearth Process manufactured all the steel for the bridge. This was a new way founded by the English and French companies to fabricate higher quality corrosion resistant steel.
- Lafarge Canada Inc., a wholly –owned subsidiary of Lafarge Corporation, manufactured three classes of **concrete** for the bridge components (High performance concrete **HPC**) (Table 3.3). Class **A**, a structural concrete for the main girders, drop-in spans, pier shafts, bases and abutments, makes up the majority of concrete. Type **C,** was used for mass concrete and approach pier foundations. Type **F** is tremie (underwater) concrete used for structural purposes. Cement specifications for this bridge called for an interground Type 10SF blended hydraulic cement. Type 10SF is a blend of Type 10 Portland cement and up to 10 percent silica fume.
- 52-degree conical ice shield is located on the pier shaft to break-up the ice. The ice shield actually lifts up the ice, which breaks under its own weight.

Chapter 4

Bond Behaviour

Corrosion of reinforcing steel embedded in concrete affects structural performance in two different ways: by loss of steel section, and through deterioration of bond at the steel-concrete interface. Bond between the steel reinforcement and concrete is necessary to ensure composite interaction of the two materials. This chapter deals with some basic information about bond, its mechanisms, and factors affecting bond strength, failure modes and other parameters related to bond.

4.1 Introduction

In the case of structural concrete, " bond stress is regarded as the shear stress at the steel bar-concrete interface which, by transferring load between the bar and the surrounding concrete, modifies the steel stress", (Park and Paulay, 1975). Bond stress is the name assigned to the unit shearing force parallel to the bar axis on the steel-concrete interface. These bond forces transfer the force from the steel bar to the surrounding concrete and vice-versa. The external load is very seldom applied directly to the reinforcing steel, which receives its share of the load through the surrounding concrete. Thus, an effective concrete must have a positive interaction between the steel bar and the surrounding concrete to obtain a force transfer between the two materials. This is a fundamental phenomenon, as it influences many aspects of the behaviour of the reinforced concrete, such as cracking, deformability, instability, and others. The transfer of load between the steel and concrete is affected by the phenomena of bonding at the steel-concrete interface, which ensures secure gripping of the reinforcement and the working of the reinforcing steel in conjunction with the concrete, to form a reliable structural element capable of withstanding both tensile and compressive forces.

The bond is affected by many factors such as change in temperature, variation in the loading of the member, creep in the concrete, corrosion etc. However, bond must be capable of adjusting to any alteration of the above influencing phenomena. Little research work has been undertaken to study the effect of corrosion on bond behaviour, whereas considerable research has been undertaken on bond, tension stiffening and crack width control. Corrosion of steel in reinforced concrete reduces the durability of concrete structures. The corrosion is probably the most serious concern for the deterioration of bond between the steel and the concrete than the reduction in load carrying capacity of the steel bars due to a decrease in the cross sectional area. Since concrete is weak in tension, cracking is expected when the tensile stress induced in a reinforced concrete member exceeds the tensile strength of the concrete. The load carried by the concrete prior to cracking is transferred by bond to the concrete on each side of the crack. Thus, the original specimen transforms into blocks of varying lengths separated by tension cracks and linked by the reinforcement

4.2 Bond Mechanisms

Bonding between a deformed steel reinforcing bar and concrete consists of adhesion, friction and mechanical bond. Friction bond is based on the friction and shear resistance caused by the roughness at the steel rebar surface and the concrete. In case of deformed steel bars, adhesion and friction play a minor role which is limited to low load levels and small slip values. Mechanical bond is based on the geometry of the ribs of the reinforcing bars, which is quantified by the rib area and by the angle of the sloping face of the ribs.

4.2.1 Adhesion

Adhesion results from the chemical bond, which is created at steel-concrete interface. Failure of adhesion bond occurs at very small relative displacements and therefore adhesion plays only a minor role in practice. It has been assumed that adhesion can break down due to the action of the service loads or due to the shrinkage of concrete. The ACI Committee 408 (1991) suggested that the bond strength due to adhesion is between 0.48-1.03 MPa. After breakage of the adhesion bond, force transfer is provided by friction.

4.2.2 Friction

Friction is the resistance against a displacement between two surfaces that are kept in contact by a compressive force perpendicular to the contact plane. Baltay and Gjelsvik (1990) explained the different coefficient of friction between concrete and mild steel, with or without mill scale. Some concrete particles are harder than a machined surface of mild steel, resulting in plastic deformation of the steel surface. On the contrary, the steel surface with mill scale is not penetrated by the concrete particles, and as a consequence, the coefficient of friction is lower. At a higher level of normal stress, the concrete starts to crush and concrete particles are not pressed into the steel surface anymore. Then the steel start to plough through the concrete and the difference in the coefficient of friction for both steel and concrete disappears. Based on the work of Treece and Jirsa (1989), the ACI Committee 408 (1991) suggested that friction could contribute up to 35% of the ultimate strength governed by the splitting of the concrete cover.

4.2.3 Mechanical Interlocking

Mechanical bond is based on the geometry of the ribs of the reinforcing bars, which is quantified by the rib area and by the angle of the sloping face of the ribs. The surface profile of the steel bar usually dictates the amount of mechanical interlocking that be generated between the steel bar and the concrete. For deformed steel bars, bearing against the lugs is considered to be the most significant transfer mechanism at higher load levels. The force transfer mechanism is due to the mechanical interlocking between the ribs and the concrete keys. The slip of the deformed bar occur in two ways either through pushing the concrete away from the bar by the ribs (wedging action), or through crushing of the concrete by the ribs.

4.3 Bond Failure modes

There are two basic modes of failure in transfer of forces from the deformed steel bar surface to the concrete and vice-versa. In the first mode, the concrete crushes locally at the bearing surface of the lug, and with adequate concrete cover and rebar anchorage length, there is no pull out failure of the rebar (with the applied tensile force being less than the potential total resistance available along the rebar length), and with an increase in the applied force, the bar will finally yield, continue to deform until it fractures. This mode of failure may be associated with some cracking at the concrete surface near the loaded end (Fig. 4.1). However, with an inadequate concrete cover thickness and/or inadequate anchorage length, the same rebar gets pulled out of concrete, stripping the concrete between the lugs (Fig. 4.2). These failure mechanisms are dependent on the geometry of the rebar lugs - their height and spacing along the rebar length. A lug with a larger height will tend to strip the concrete within the lugs, while that with a shorter height and sloping sides would also have some tendency to slip. The second mode of failure is more dominant in conventional structural concrete as the rebar lugs bear on a conical surface around the lug, which results in a 'herring bone' type of force transfer (Fig. 4.3). Figure 4.4 shows the free body diagram of the concrete showing actions at the bore left by the steel bar. The accumulated longitudinal, or tangential components of these interface forces equilibrate the longitudinal rebar force, while the normal components act radially on the concrete barrel (created by the steel rebar), causing a bursting pressure similar to that in water pipes (Fig. 4.5). This would lead to longitudinal and/or transverse cracking at the weaker concrete cover sections, where the concrete tensile strength is exceeded. These splitting cracks cause a decrease in the hold of the "surrounding concrete" on the steel rebar, which results in reduction of the bond resistance at the steel-concrete interface.

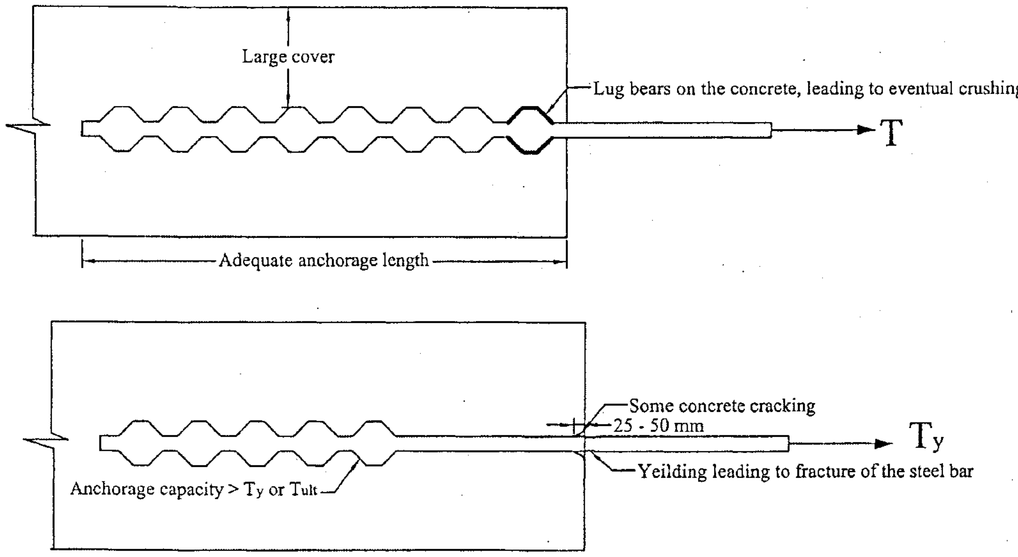

Fig. 4.1: Bond failure mechanism due to crushing and fracture of reinforcing steel in concrete (adequate cover and anchorage length)

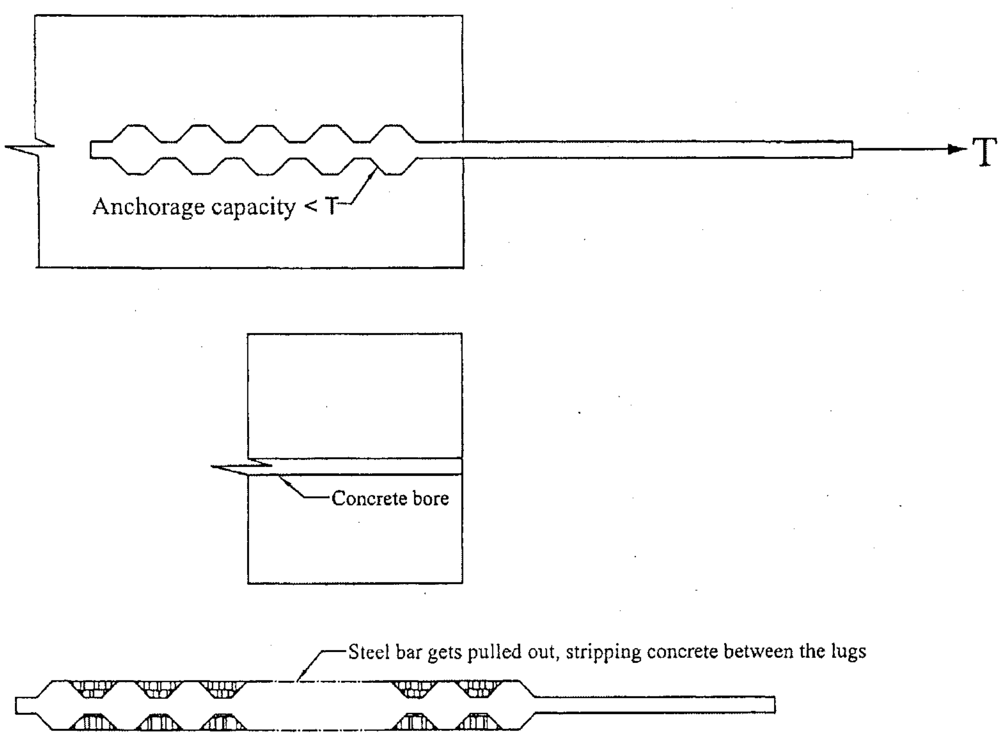

Fig. 4.2: Bond failure mechanism due to stripping of concrete (inadequate cover and anchorage length)

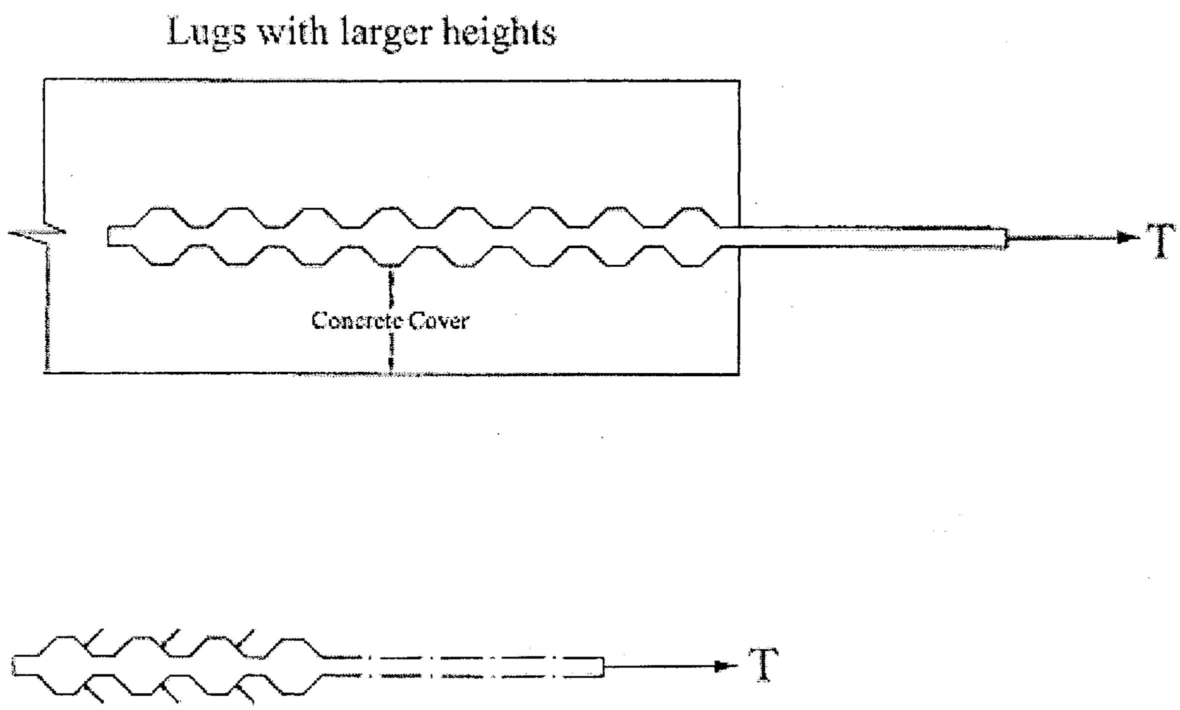

Fig. 4.3: Free body diagram of a steel bar (Herring bone type of conical forces)

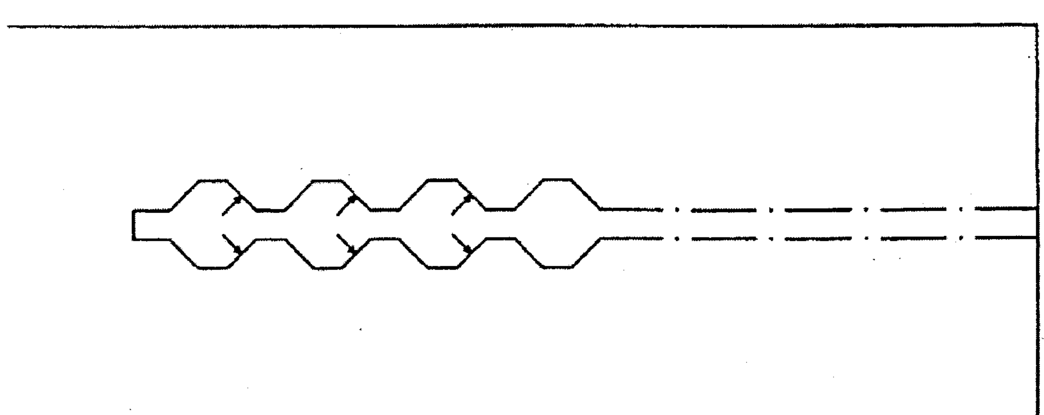

Fig. 4.4: Free body diagram of the concrete showing actions at the bore left by the steel bar

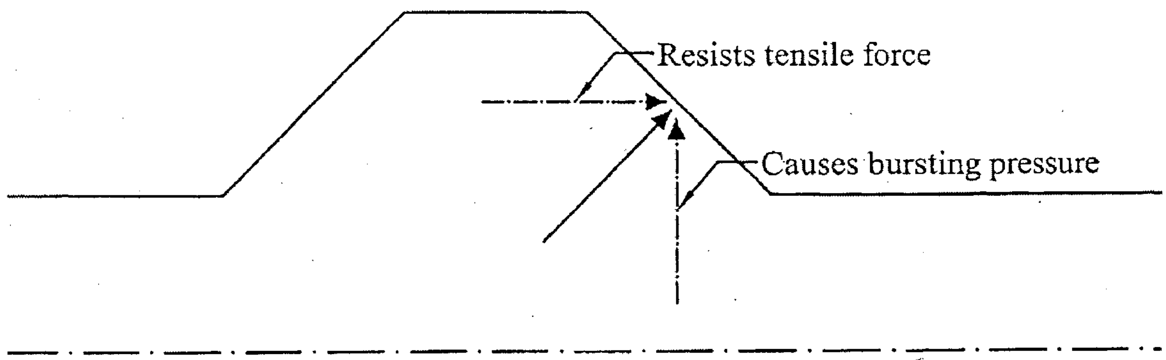

Fig. 4.5: Actions at the lug bore

4.4 Measurement of Bond

Many different types of tests have been used to investigate the bond characteristics of the steel reinforcement in the concrete. These include:

- Pull-out tests (eccentric and concentric)
- Variety of bond beam tests (National Bureau of Standard Beam, University of Texas, McGill University)
- Semibeam specimen test
- Standard tension specimen test

Broms and Raab (1961), Houde and Mirza (1972) and others have undertaken many experimental research programs using the tension specimens to measure the bond strength. Tepfers (1979) focused his research programs on prediction of bond strength for deformed steel bars. He proposed an analytical model in which the concrete surrounding a single reinforcing bar is characterized as a thick-walled cylinder subjected to internal shear and pressure. He proposed that bond strength is determined by the capacity of the concrete surrounding the reinforcing bars to carry the hoop stresses. Three modes of system failure were proposed: elastic, partially cracked-elastic, and plastic. The elastic mode of failure describes a system in which the concrete surrounding the reinforcing bar exhibits a linearly elastic material response and bond strength corresponds to the concrete carrying a peak tensile stress equal to the concrete tensile strength. The partially cracked-elastic mode of failure defines a system in which radial cracks initiate in the concrete at the steel rebar-concrete interface at the lugs, but do not propagate to the surface of the specimen. The cracked concrete is assumed to have no tensile strength and bond strength corresponds to the uncracked concrete carrying a maximum stress equal to the tensile strength. The plastic failure mode describes a system in which all of the concrete surrounding the anchored bar is assumed to carry a tensile hoop stress equal to the concrete tensile strength.

The relevant tests are briefly described as follows:

Pullout test

In a pull out test, the concrete stress at the unloaded end is zero, and the concrete is in compression at the loaded end, while the steel is in tension, which eliminates the transverse tension cracking. This method is not intended for establishing bond strength values for structural design purposes, because these tests do not directly represent the stress state in the concrete beams. However, this method is adequate enough to study the effect of different parameters on the bond strength such as comparing the slip resistance of the various concrete mixes, some with supplementary cementing materials, and the various corrosion levels.

Tension test

In case of tension tests, both the concrete and the reinforcing steel are in tension, and thus the tension specimen represents a simplified model of the tension zone of a reinforced concrete beam.

Chapter 5

Deterioration of Bond at the Steel-Concrete Interface

5.1 Introduction

Corrosion products occupy a considerably larger volume than the original uncorroded iron in the steel, thereby causing large internal pressures, leading to cracking and spalling of the concrete cover. This cover loss causes decrease in the concrete confinement and in addition, the surface of the bar becomes covered with corrosion products, leading to a considerable decrease in bond at the steel-concrete interface. This loss of bond is more dangerous to the safety of the structural element than the strength loss caused by the loss of the rebar cross-sectional area. This chapter summarizes the influence of significant factors affecting the bond behaviour of corroded steel bars such as the concrete strength, water cement ratio, bar diameter, concrete cover thickness, extent of rebar corrosion (mass loss, or cross-sectional area loss), crack width, loss of rebar lugs and cover to bar diameter (C/d_b) ratio. Finally, some critical values of these parameters affecting the bond strength of rebars are suggested from the information presently available, which could help practicing structural engineers in designing new structures for safety and durability.

5.2 Factors affecting bond strength

The main factors affecting the bond strength between the steel and the reinforced concrete are:

- Concrete composition and strength
- Steel bar type
- Corrosion
- Bar profile, rib geometry
- Concrete cover thickness and bar diameter ratio
- Water/cement ratio

5.2.1 Concrete strength and composition

Concrete strength has considerable influence on bond behaviour. Based on the tests performed on eccentric pullout specimens using higher strength concretes, Perry and Thompson (1966) found that the location of the maximum bond stress for the same force in the bars moved closer to the loaded end indicating lower slip values. Tepfers (1973) showed that with higher compressive strength concrete, the slope of the bond stress distribution varies considerably over the splice length when compared to that with lower concrete strengths. Martin (1982) studied the influence of concrete composition, cement content, water/cement ratio and the concrete consistencies on bond behaviour. Based on the pullout test results with concrete strengths ranging from 16 to 50 MPa, for a slip value ranging from 0.01 mm to 1 mm, he observed that the bond stress was proportional to the compressive strength. However, for the slip values smaller than 0.01 mm and greater than 1 mm, the bond stress was proportional to (the concrete strength) $^{2/3}$. He observed the influence of grading of aggregates and consistency of fresh concrete mix on bond properties. He found that the bond capacity of the reinforcing bar increased with the size of the aggregate.

The use of supplementary cementitious materials, such as fly ash, silica fume, ground granulated blast furnace slag, and natural pozzolans, in concrete structures has become a widely accepted practice in many countries, primarily due to their favourable effects on concrete strength and durability. Also, a great deal of research has been performed on the effects of partial replacement of the cement with one or more supplementary cementitious materials on the concrete properties. However, this research has not provided clear conclusions concerning the optimum use of these materials and the curing procedures to support both hydration and pozzolanic reactions needed to ensure enhanced durability. Thus, there is a need to address the technical issues associated with the use of supplementary cementitious materials in concrete structures and to develop guidelines on their use. According to Hamad and Itani (1998), replacement of 5 to 20% of cement by an equal volume of silica fume resulted in an average of 8 percent reduction in bond strength. It must be emphasized that the reduction in the hydroxyl ions in the pore solution due to the pozzolanic reactions, and the resulting reduction in its pH, results in damage of the steel passivation layer besides reducing the chloride threshold level. Therefore, the use of fly ash in high volumes to replace the cement in concrete still remains an issue of great concern, related mainly to the unfavourable pore solution chemistry of the blended fly ash cements because of the removal of hydroxyl ions from the pore solution by the pozzolanic reactions, and to a lower degree to the presence of carbon in the fly ashes. It is now well recognized (Rasheeduzzafar *et al.*, 1992) that passivation of steel is a function of the relative concentrations of chloride and hydroxyl ions in the pore solution, in terms of Cl^-/OH^- ratio, rather than the chloride concentration. Based on Gouda's work, Diamond (1986), conducted tests on alkaline solutions with pH ranging from 11.8 to 13.95, and he proposed a threshold depassivation Cl^-/OH^- ratio of 0.30 (corresponding to a pH of 13.3). However, Amleh (2000) observed the superior corrosion protection performance of fly ash concretes, because of their reduced permeability, which contradicts the notion of increased susceptibility of steel to corrosion by the increased aggressivity of the pore solution. The limited research on the influence of the concrete strength and composition on bond behaviour does not provide conclusive information on the influence on bond capacity between the steel and the concrete, requiring more research.

5.2.2 Steel bar type

5.2.2.1 Plain steel bars

The principal cause of deterioration of structural concrete is corrosion of the embedded steel reinforcement. The oxides of iron, resulting from steel corrosion occupy a volume much larger than the parent metal, which creates tensile hoop stresses in the concrete surrounding the bar and eventually leads to longitudinal cracking of the concrete cover. The resulting bond deterioration at the steel rebar – concrete interface suffers significant degradation, seriously reducing the safety of the structure. Plain bars, used mostly in the first half of 20^{th} century, demonstrate small chemical adhesion and cohesion between the rebar and the concrete (0.5-1.0 MPa), and friction at the rebar surface. In plain bars, the bond depends primarily on friction. The loss of bond due to corrosion is basically due to a mechanically weak layer of corrosion products at the steel bar-concrete interface, and a reduction in the concrete confinement due to longitudinal concrete splitting cracks. Cairns *et al.* (2002) derived the following conservative empirical relationship, based on a series of accelerated tests on eccentric pull out specimens, reinforced with 16 mm diameter plain bars and a concrete cover thickness of 20 mm (C/d_b ratio=1.25):

$$f_{bres} = f_{bd}\,(1\text{-}0.4\,\sqrt{w_{cr}}) \geq 0 \qquad (5.1)$$

where f_{bres} = residual bond strength

f_{bd} = design bond strength, and

w_{cr} = width of longitudinal crack in the concrete cover

Cairns *et al.* (2000) developed a qualitative summary plot of the results from several studies on the time effects of corrosion on bond strength of plain steel rebars. Figure 5.1 shows that bond at the steel bar-concrete interface suffers the most rapid degradation as a result of corrosion, and therefore, it can significantly reduce the structural safety. Also, the reduction in bond strength presents a greater risk to the integrity of concrete structures than the loss of the reinforcement section.

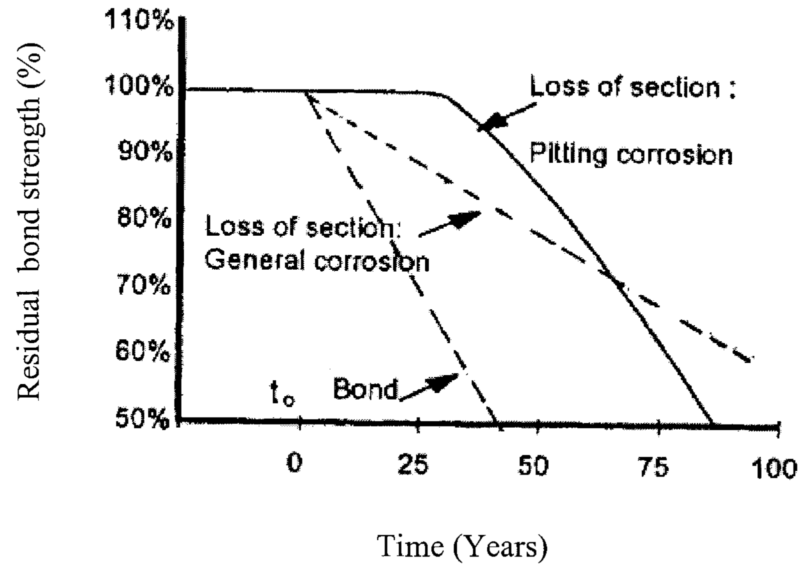

Fig. 5.1: Residual bond strength versus corrosion time (years) (Cairns *et al.*, 2002)
(t_0 stands for time of initiation of corrosion cracking)

According to Mo and Chan (1996), since plain bars have no deformations, it is expected that no bearing component of bond exists in plain bars as for the deformed bars. In plain bars, very little localized cracking can occur around the rebar and the surface of the concrete; adhesion and friction are the main contributors to the bond strength. Therefore, increasing the concrete compressive strength can improve the bond properties. The use of plain bars has been discontinued for the past few decades and will not be pursued any further in this thesis.

5.2.2.2 Deformed bars

Bond between deformed steel reinforcing bar and concrete consists of adhesion, friction and mechanical bond. Adhesion is based on capillary and adhesion forces between concrete and steel; friction bond is based on friction and shear resistance caused by the roughness at the steel rebar surface and the concrete. In case of deformed steel bars, adhesion and friction play a minor role which is limited to low load levels and small slip values. Mechanical bond is based on the geometry of the ribs of the reinforcing bars, which is quantified by the rib area and by the angle of the sloping front face of the ribs. For durability design, size and deformation geometry of the steel rebar needs to be selected carefully. Mirza and Amleh (2003) recommended that at least half of the rebar lug must remain at the end of the service life for safety over the design service life in a given environment. Amleh (2000) examined the effect of the geometric shape and size of the steel rebar on the transfer of the force from the steel to the surrounding concrete. She showed that the effect of corrosion of the ribs weakens the bond between the deformed bars and the concrete, which depends mainly on the mechanical interlocking of the ribs.

5.2.2.3 Uncorroded bars

Considerable experimental and analytical research was undertaken in the late 1960's at McGill University and elsewhere to study the basics of force transfer at the steel rebar-concrete interface, the associated bond stress-slip relationships and the other force – displacement relationships (dowel action and aggregate interlock), for nonlinear finite element analyses of structural concrete (Mirza *et al.*, 1982). Houde (1973) undertook a study to derive the bond stress-slip relationship using tension specimens by including the effect of the load level, the size of concrete restraining the bar, the quality of the concrete, thickness of the concrete cover, and the type of test-transfer or anchorage, as both were required to simulate the central and the end zone of a reinforced concrete beam. He conducted 62 concentric tension tests on concrete prism specimens 33 × 8.1 × 3.5 inch (838 × 205 × 88 mm) size, reinforced with No. 4, No. 6, and No. 8 bars; twelve of these tests were performed with internally instrumented No. 8 bars. These No. 4, No. 6, and No. 8 bars had cross sectional areas of 126 mm^2, 283 mm^2 and 506 mm^2 respectively. He derived a fourth order relationship between the bond stress (*u*) and the local slip (*d*):

$$u=1.95 \times 10^6 d - 2.35 \times 10^9 d^2 + 1.39 \times 10^{12} d^3 - 0.33 \times 10^{15} d^4 \tag{5.2}$$

where u is the bond stress in psi and d is the slip in inches.

He found that the bond stress at the steel-concrete interface reached the maximum value at an average slip value of 12 × 10^{-4} inches (3.048 × 10^{-2} mm) (Fig. 5.2).

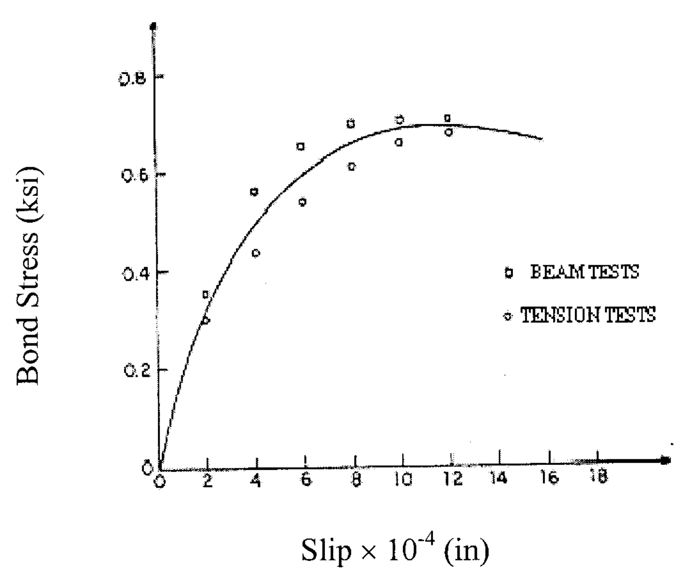

Fig. 5.2: Unit bond stress versus unit slip (Houde, 1973)

The bond stress-slip relationship proposed by Houde (1973) was applicable directly at any point along the bar, which was an attractive situation in any finite element analysis where cracks progressively appear in a random manner under increasing loads. These nonlinear bond stress-slip relationships, along with the appropriate concrete constitutive relationships and suitable failure criteria were then used to analyze the tension and the other specimens using nonlinear finite element analysis. These computer models utilized orthogonal springs to model the basic actions at the steel rebar-concrete interface, simulating the longitudinal and transverse actions, parallel and perpendicular to the bar, respectively. The longitudinal spring stiffness was assumed to be equal to the slope of the selected empirical nonlinear bond stress-slip relationship at a selected load level, while the concrete and steel were assumed to be connected rigidly by assigning a large value to the transverse spring stiffness.

These McGill and other analyses demonstrated a fair agreement with the experimental data, although the computed responses were stiffer than those observed. Goto (1971) studied the nature of cracking around a deformed reinforcing bar and found that separation does not produce complete unloading and that bond forces are transmitted solely by the rib bearing in the vicinity of a main crack. He found that the concrete around the reinforcing bar presents the appearance of a comb-like structure through formation of internal cracks (Fig. 5.3). The teeth of this comb-like concrete were deformed in the direction of the nearest primary crack by compressive forces transmitted from the bar lugs as the steel tension is increased. Since the internal cracks were inclined at about 60 degrees to the bar axis, the deformation of the teeth of the comb-like structure tightened the concrete around the reinforcing steel bar and increased the frictional resistance between the concrete and the steel rebar. The reaction of this tightening force also produced ring tension in the concrete around the bar – a principal cause of the formation of longitudinal cracks.

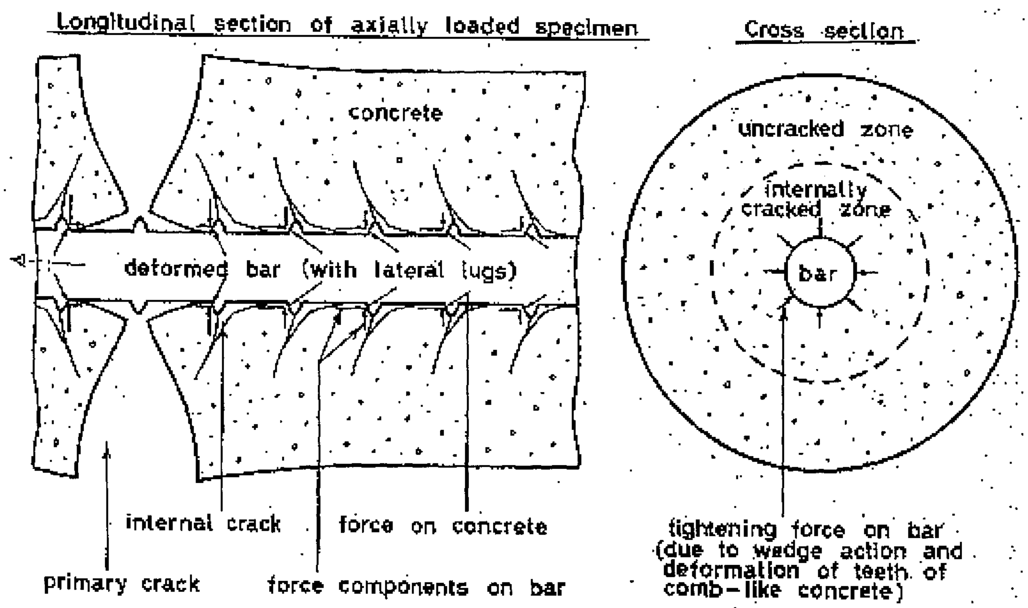

Fig. 5.3: Deformation of concrete around reinforcing steel after formation of internal cracks (Goto, 1971)

Goto suggested that a crack forms with a minimal width at the bar surface initially. An increase in loading causes loss of adhesion adjacent to the crack, transferring the load to the bar ribs and internal cracks form close to the main crack. Further loading causes more internal cracks to form at successively greater distances from the main crack. Steel stresses reach a local peak at the crack, but between the cracks, the steel stress is lower due to the concrete contribution. This transfer of forces produces bond stresses. The internal cracks observed by Goto at low load levels along with the ability of this cracked concrete near the rebar to transmit the loads to the uncracked concrete were incorporated in the model, and this gave a much better agreement with the experimental results (Mirza *et al.*, 1982). Some investigators have recently attempted to develop computer models for analysis of bond behaviour at the steel - concrete interface, using three-dimensional finite element analysis, modeling the concrete using non-linear fracture mechanics (Lungdren and Gylloft, 2000, and Lungdren *et al.*, 2002). They used nonlinear finite element analysis program DIANA for detailed studies, modeling the concrete and the steel rebar using solid elements to simulate the bond behaviour and the accompanying mechanisms of failure. They noted that the parameters influencing the basic force transfer mechanism at the steel rebar-concrete interface include friction, normal stresses accompanying the rebar slip, adhesion and an upper limit determined by the strength of the concrete ribs between the rebar lugs. In addition, they observed that when concrete splitting is prevented, the maximum capacity of the ribbed bars can be evaluated from the action of the inclined compressive struts resulting from the actions at the steel rebar-concrete interface for pullout failure, due to the concrete splitting, or yielding of the reinforcement (Fig. 5.4). Both bond stresses and splitting stresses are caused by the bond action. If the concrete surrounding the reinforcement bar is well confined and can withstand the splitting forces, a pullout failure is obtained (curve a); otherwise splitting stresses can cause a decrease in the bond capacity (curve b). They also noted the diminution of the bond capacity due to the yielding of the reinforcement. It was also demonstrated that their model could be used to deal with cycling loading in a physically reasonable way.

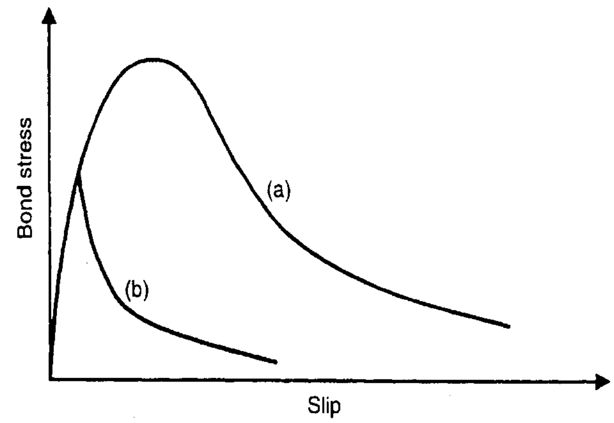

Fig. 5.4: Qualitative bond stress-slip relationships (a) Pullout failure (b) splitting failure, or loss of bond due to rebar yielding (Lungdren and Gylloft, 2000)

The 2002 International Conference on Bond in Concrete also reported the results of a few relevant research programs on the effect of corrosion on bond at the steel rebar-concrete interface.

5.2.2.4 Corroded Bars

Bond strength of corroded bars has been the object of various experimental studies; many show bond deterioration, but at different rates for each case. Other results show no bond deterioration, or even an occasional bond strength increase at low corrosion levels. The differences in these results have brought engineers and scientists to consider bond of corroded bars as a rather intriguing problem (FIB, 2000). The considerable increase in the volume of the corrosion products (oxides, hydroxides and hydrates) produced at the steel-concrete interface from the iron in the steel results in an increase in the radial pressure, which increases the tendency for tensile splitting and cracking, followed by the spalling of the concrete cover. Therefore, the basic actions involved in the bond at the steel-concrete interface without corrosion and with the occurrence of corrosion on bond at the steel-concrete interface are similar, excepting that the corrosion products can significantly influence the friction and splitting tendency at the interface, leading to a strong interaction between the corrosion products and the bond phenomenon. There is virtually very little information in the literature on the mechanical behaviour of the corrosion products. Molina *et al.* (1993) assumed the corrosion products to behave elastically. Using the assumption that rust behaves like a granular material with its stiffness increasing with the stress level, Lungdren (2002) incorporated the layer of corrosion products in her previously developed computer model of bond at the steel-concrete interface. She studied the corrosion cracking tests to investigate the mechanical behaviour of rust. The volume increase of the corrosion products compared to the virgin steel was modelled in a corrosion layer. The volume of rust relative to the uncorroded steel, and the corrosion penetration 'x' as a function of time were provided as input. The corrosion extent was modelled in finite time steps. She developed an equation to calculate the "free" increase of the radius (i.e. the increase in the radius if normal stresses were zero):

$$a = -r + \sqrt{(r^2+(v-1).(2rx-x^2))} \tag{5.3}$$

where a is the "free" increase in radius and v is the volume of the rust relative to the volume of the uncorroded steel (Fig. 5.5). Here, x is the depth of corrosion penetration. The "real" increase of the radius, corresponding to a strain in the rust in the corroded layer is u_{ncor}. The strain ε_{cor} in the rust *is* given as:

$$\varepsilon_{cor} = u_{ncor} - a/(x+a) \tag{5.4}$$

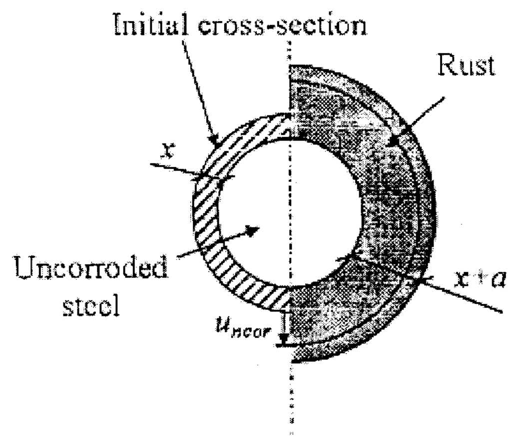

Fig. 5.5: Physical interpretation of the variables in the corrosion model (Lungdren, 2002)

From this strain in the rust, the normal stress in the layer was determined. The various types of concrete specimens used by several researchers (Ghandehari *et al.* 2000, Al-Sulaimani *et al.* 1990, Cabrera and Ghouddoussi 1992, Andrade *et al.* 1993) to calculate the corrosion penetration that caused cracking of the concrete cover, were analyzed using finite element modeling and non-linear fracture mechanics of concrete. Ghandehari *et al.* (2000) undertook pullout tests on corroded reinforcing steel bars embedded in concrete cylinders, Al-Sulaimani *et al.* (1990), Cabrera and Ghouddoussi (1992) performed their experiments on corroded reinforcement bars concentrically placed in the concrete blocks, while Andrade *et al.* (1993) carried out the tests where corroded reinforcing bars were placed eccentrically in concrete blocks. Only the concrete of the specimens was modelled, with a hole where the reinforcement was situated. A normal stress was applied at the hole in the center of the cylinder, providing results in terms of the applied normal stress versus the deformation at the hole of the concrete cylinder typical for the specimens. They concluded that the deformation of the concrete cylinder approximately equalled the deformation in the corrosion layer, u_{ncor}. The value of the strain in the rust was calculated using equations (5.3) and (5.4) by combining the measured value of u_{ncor} with the experimental corrosion penetration at cracking. The normal stress and deformation at the hole that caused cracking of the cover in each analysis, in combination with the experimentally measured corrosion penetration that caused cracking, resulted in a single point in a stress -strain plot (Fig. 5.6). This led to an assumption that stiffness of rust increases with the stress level and that it behaves like a granular material.

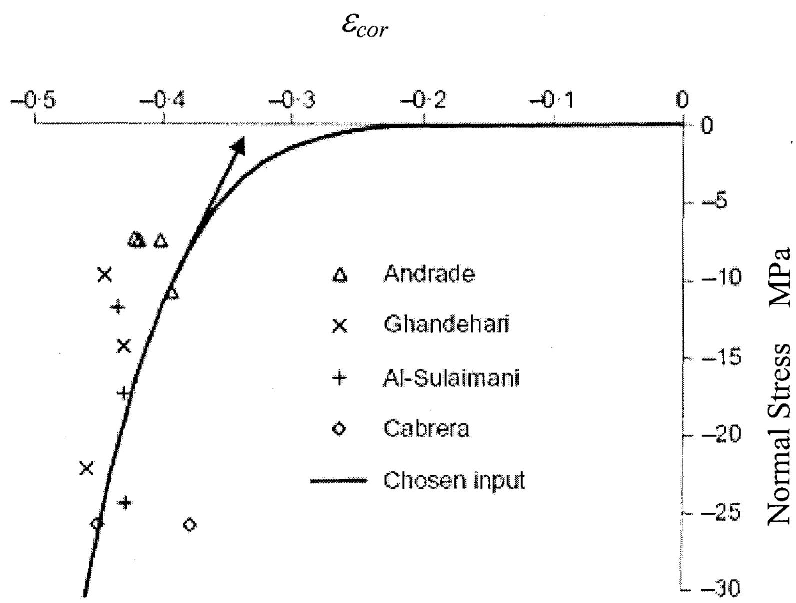

Fig. 5.6: Normal stress versus strain in the rust evaluated from a combination of experimental results and analyses together with the chosen input (Lungdren, 2002)

Lungdren (2002) also studied the effect of the considerably increased volumes of corrosion products on the bond strength to examine the influence of the concrete cover thickness and the stirrups confining the concrete. Good correlation was obtained between the test data from the pull out and beam specimens with corroded steel reinforcement tested by other investigators; the model was able to predict the loss of bond at the steel-concrete interface when concrete splitting occurred due to corrosion and mechanical forces. Shima (2002) investigated experimentally the local bond stress-slip relationships of corroded steel bars. These relationships were obtained from a measurement of strain distributions of the steel bar under a pullout force. He normalized the local bond stress and slip by dividing them by $(f_c')^{2/3}$, where f_c' is the concrete compressive strength and the bar diameter, respectively, to eliminate the effect of concrete strength and the bar diameter (Fig. 5.7).

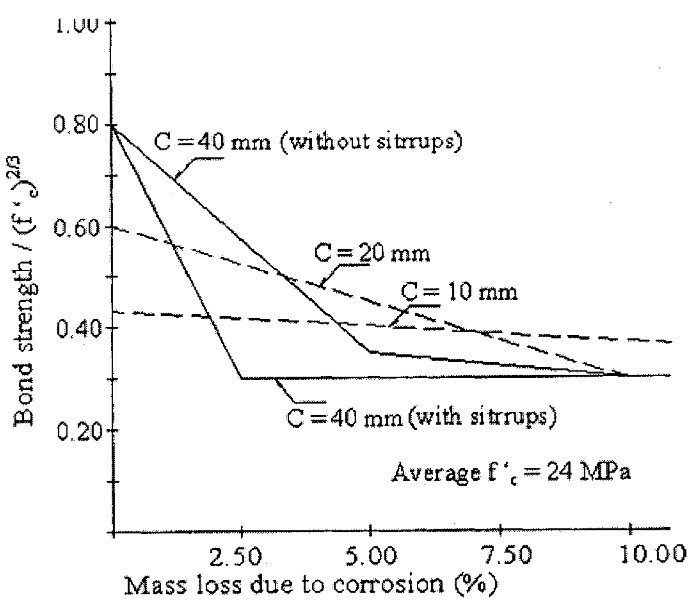

Fig. 5.7: Variation of bond strength / $(f'_c)^{2/3}$ ratio with mass loss due to corrosion (Shima, 2002)

He found a decrease in maximum local bond stress with an increase in the degree of corrosion. He indicated that the absolute values of maximum local bond stress at high corrosion levels were almost the same regardless of the concrete cover. Also, the initial values of bond strength were higher in the case of thicker concrete cover. The degree of bond stress decrement was small when the cover was small and large for large concrete cover thickness.

5.2.3 Corrosion

Bond between reinforcing steel rebars and concrete is necessary to ensure composite action between the two materials. According to Cairns *et al.* (2000), bond strength initially results from weak chemical bonds between steel and hardened cement, but this resistance is broken at a very low stress. Once slip occurs, friction contributes to bond. In plain bars, this is the major component of the strength. In deformed bars, under increasing slip, bond depends principally on the bearing, or mechanical interlock between ribs rolled on the surface of the bar and the surrounding concrete. At this stage, the reinforcing bar generates bursting forces which tend to split the surrounding concrete. The resistance provided to these bursting forces by the concrete cover and the confining reinforcement can limit the failure load.

Cairns *et al.* (2000) noted that corrosion affects the bond strength between the steel and the reinforced concrete in many ways (Fig. 5.8)

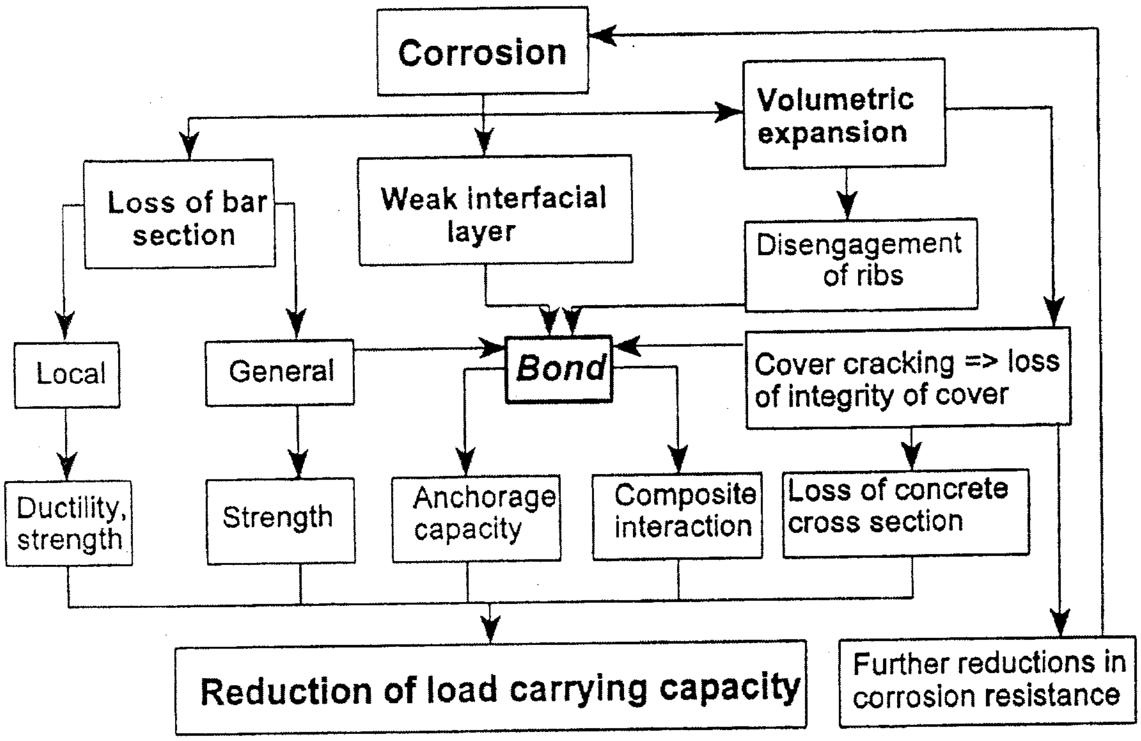

Fig. 5.8: Effect of corrosion on bond strength (Cairns *et al.,* 2000)

- An increase in the diameter of a corroding bar at first increases radial stresses between bar and concrete and therefore, it increases the frictional component of the bond. However, further corrosion leads to development of longitudinal cracking and a reduction in the resistance to the bursting forces generated by bond action.
- Corrosion products at the steel rebar-concrete interface influence friction at the interface. Al-Sulaimani *et al.* (1990) suggest that a firmly adherent layer of rust may contribute to an enhancement in the bond strength at early stages of corrosion. According to Cabrera and Ghouddoussi (1992), at more advance stages of corrosion, weak and friable material between the bar and

the concrete will certainly be at least partially responsible for the reduction in bond strength.

- Corrosion may reduce the height of the ribs of a deformed bar above the bar core. This is unlikely to be significant except at advance stages of corrosion.
- Disengagement of ribs and concrete- the layer of corrosion products may reduce the effective bearing area of the ribs (Fig. 5.9)

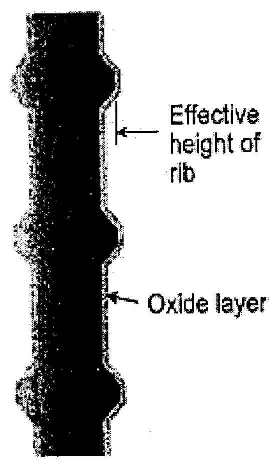

Fig. 5.9: Disengagement of ribs

Almusallam *et al.* (1996) investigated the effect of reinforcement corrosion on the bond strength between the steel rebar and the concrete, and studied the bond behaviour of steel rebars in reinforced concrete elements, including the ultimate bond strength, free-end slip, and the modes of failure in precracking, cracking and postcracking stages. They used the cantilever beam bond tests on 30 MPa concrete specimens 152 × 254 × 279 mm in size, reinforced with a 12 mm diameter deformed bars. Inverted open stirrups and compression reinforcement were used to avoid any possible shear and compression failures, respectively. This shear and compression reinforcement was isolated from the bond test bar to avoid any corrosion. Figure 5.10 shows the design details of cantilever bond test specimen (all dimensions are in mm).

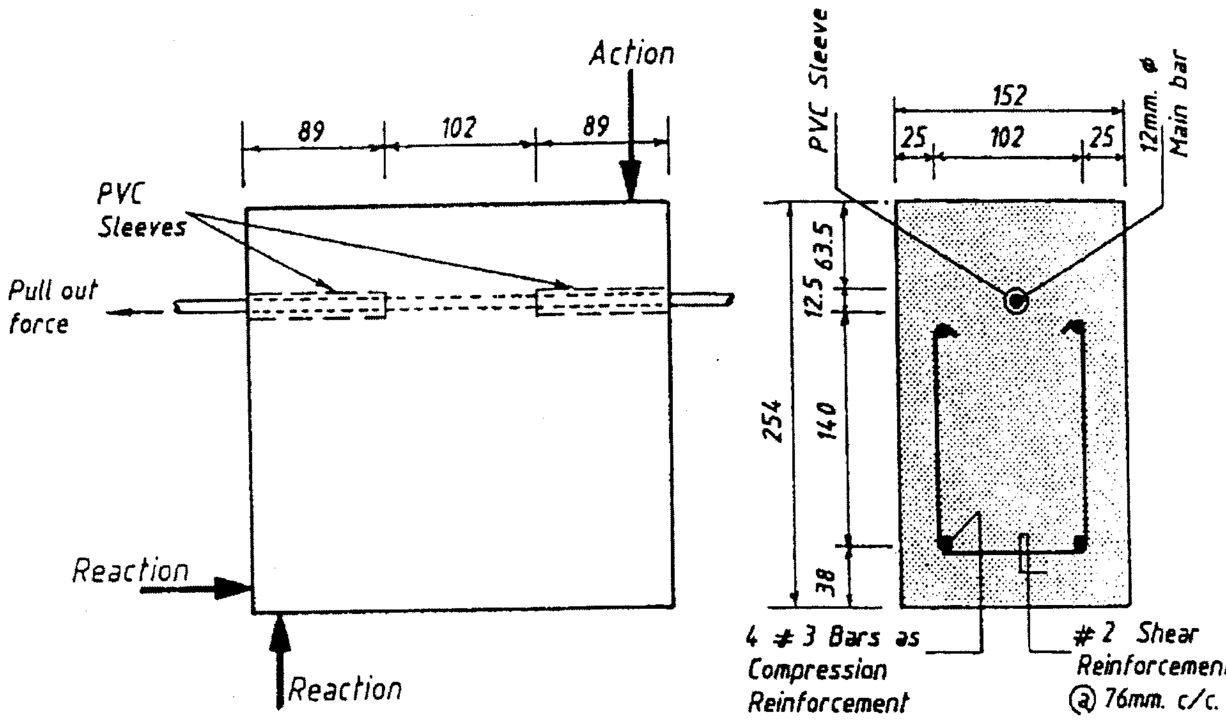

Fig. 5.10: Design details of cantilever bond test specimen (Almusallam *et al.*, 1996)

For accelerated corrosion, direct current of 0.4 A was impressed on the bar embedded in the pullout specimen using an integrated system incorporating a small rectifier with a built-in ammeter to monitor the current and a potentiometer to control the current intensity. The specimens were partially immersed in water in a glass fibre tank in such a manner that the reinforcement was totally above water resulting in the formation of products due to reinforcement corrosion. The direction of current was adjusted so that the reinforcing steel act as the anode while a stainless steel plate counter electrode was positioned in the tank to act as a cathode (Fig. 5.11). A calibration curve establishing a relationship between the duration of the impressed current and the corresponding degree of corrosion was developed; the degree of corrosion was measured as the gravimetric loss in the weight of the reinforcing bars.

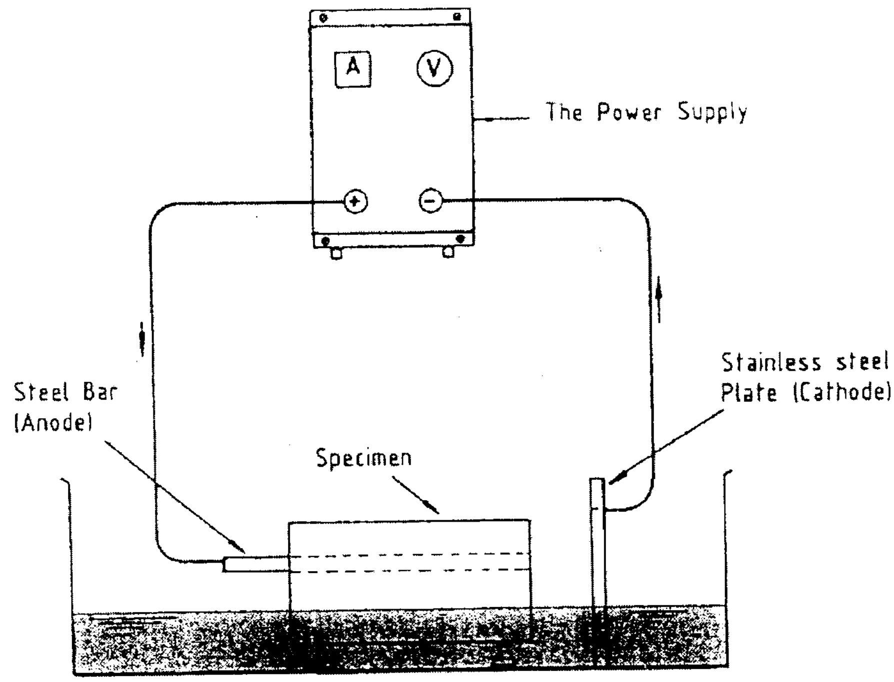

Fig. 5.11: Schematic representation of impressed current setup (Almusallam *et al.*, 1996)

The results indicated that in the precracking stage (0–4% rebar mass loss), the ultimate bond strength increased by about 17% due to the corrosion products at the steel bar surface, whereas the slip at the ultimate bond strength decreased with an increase in the degree of corrosion. After the appearance of the first crack at a corrosion level of 5%, the bond strength decreased slightly for another 1% rebar mass loss, and then it decreased rapidly to about 30% at 8% corrosion (Fig. 5.12).

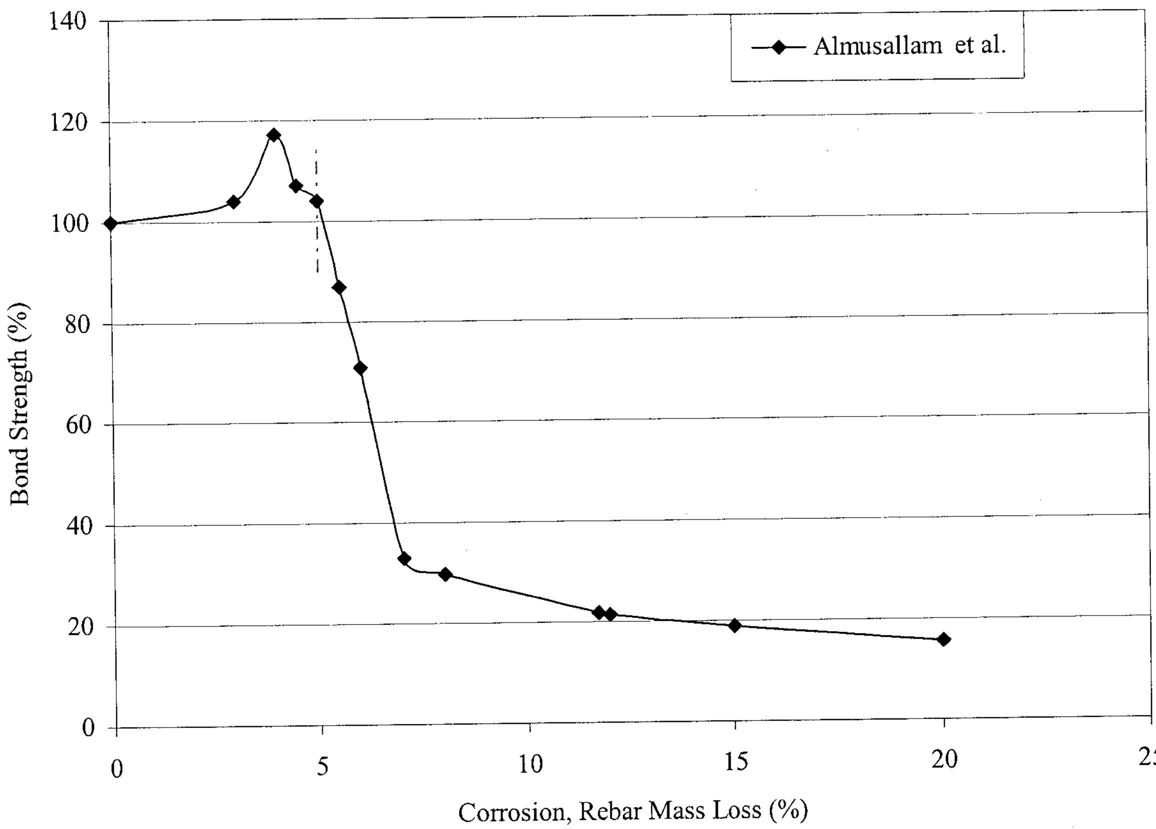

Fig. 5.12: Relationship between the bond strength and the rebar mass loss (Almusallam *et al.*, 1996)

When reinforcement mass loss was in the range of 4 to 6%, the bond failure occurred due to the splitting of the specimens along the corrosion cracks. The reason for this failure was due to the already weak concrete resulting from the presence of cracks from corrosion. Beyond 6% rebar corrosion (rebar mass loss), bond failure resulted from a continuous slippage of the rebars. The ultimate bond strength initially increased with an increase in the degree of corrosion, until it attained a maximum value of 4% rebar corrosion after which there was a sharp reduction in the ultimate bond strength up to 6%

rebar mass loss. Beyond 8% rebar corrosion level, the ultimate bond strength did not vary much even with increased corrosion level. They noted that very little corrosion after cracking was needed to reduce bond strength to an unacceptable level.

Cabrera and Ghouddoussi (1992) performed pullout tests on 150 mm cubic concrete specimens made with Ordinary Portland Cement (OPC) using 12 mm diameter reinforcing deformed bar centrally embedded in the cube. Figure 5.13 shows the schematic setup of the electrochemical system used.

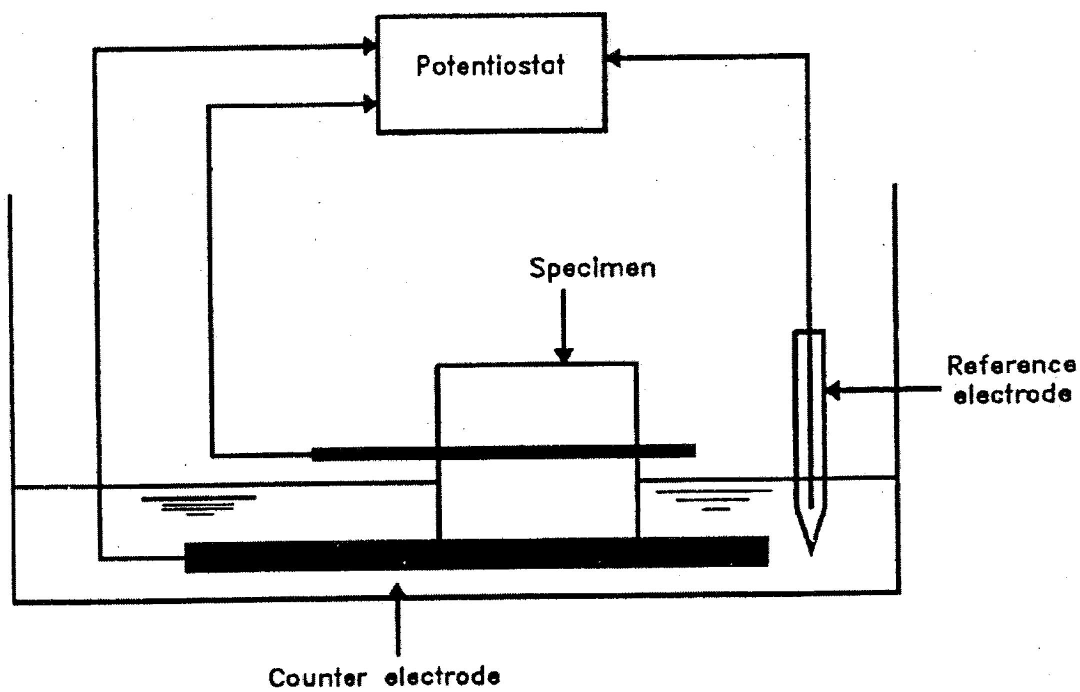

Fig. 5.13: Schematic representation of the electrochemical system (Cabrera and Ghouddoussi, 1992)

The stainless steel plate immersed in the solution was used as the counter electrode and a potentiostat was set up in such a way that the reinforcing steel bar acted as an anode and the counter electrode as cathode. To accelerate corrosion, a constant voltage of 3 Volts versus saturated calomel electrode was impressed through the system. Pullout tests were carried out using an Instron testing machine under monotonic static load. Dial gauges were used to measure the slip at both ends (Fig. 5.14).

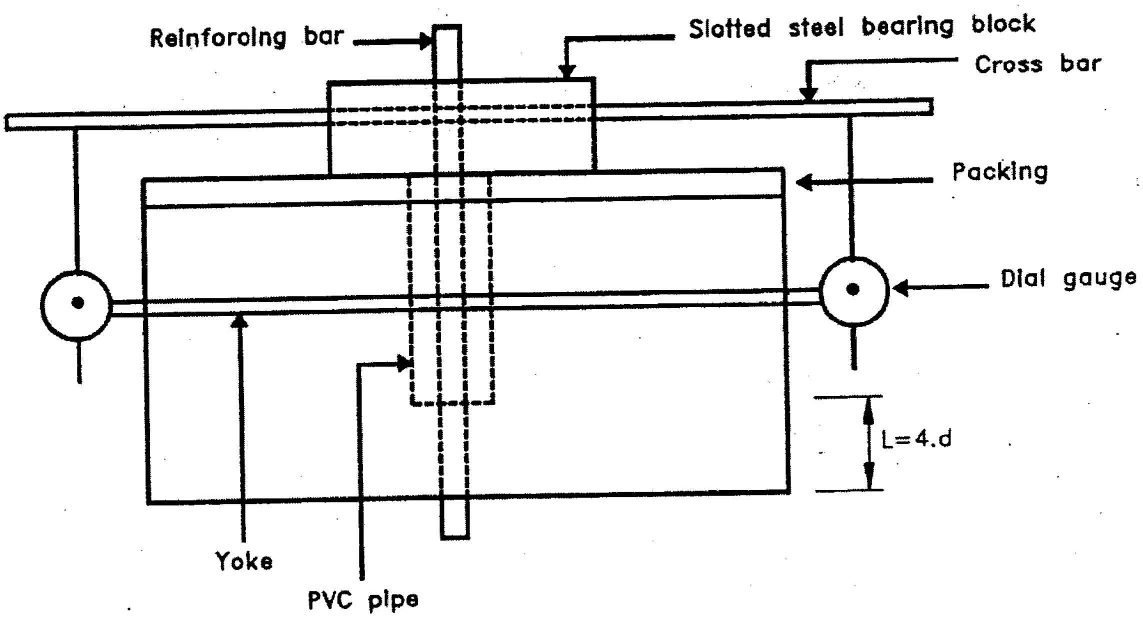

Fig. 5.14: Arrangement for the pullout test (Cabrera and Ghouddoussi, 1992)

Cabrera and Ghoudoussi (1992) found that the bond strength increased initially up to a rebar mass loss of about 1%, after which there was significant decrease in bond strength (Fig. 5.15). They noted about 27 % loss of bond strength at 6.5 % rebar mass loss. They attributed the initial increase in bond strength to the expansion resulting from the formation of corrosion products at the bar surface, occupying larger volume than the original components.

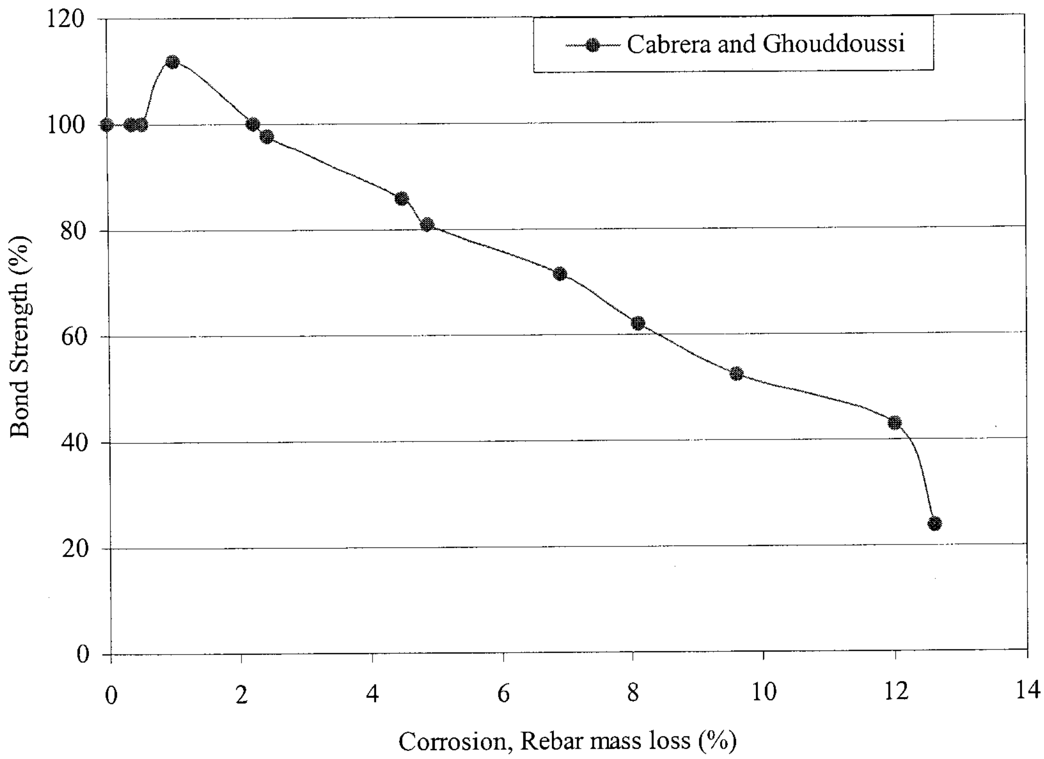

Fig. 5.15: Relationship between the bond strength and the rebar mass loss (Cabrera and Ghouddoussi, 1992)

Auyeung *et al.* (2000) used prismatic concrete specimens in which two 19 mm mild steel deformed bars of different lengths separated by 2 in. (50 mm) were embedded (Fig. 5.16). When the two bars were pulled out in opposite directions, the shorter bar pulled out of the concrete. A current was passed from the reinforcement to four copper plates attached to the sides to induce corrosion. These 5 × 7 in. (127 × 178 mm) copper plates acted as the cathodic site, which consumed the electrons given out by the reinforcing bar. A power supply with an output of 24 Volts DC and 12 amps was used to induce corrosion (Fig. 5.17). The amount of corrosion was expressed as the percentage of mass loss.

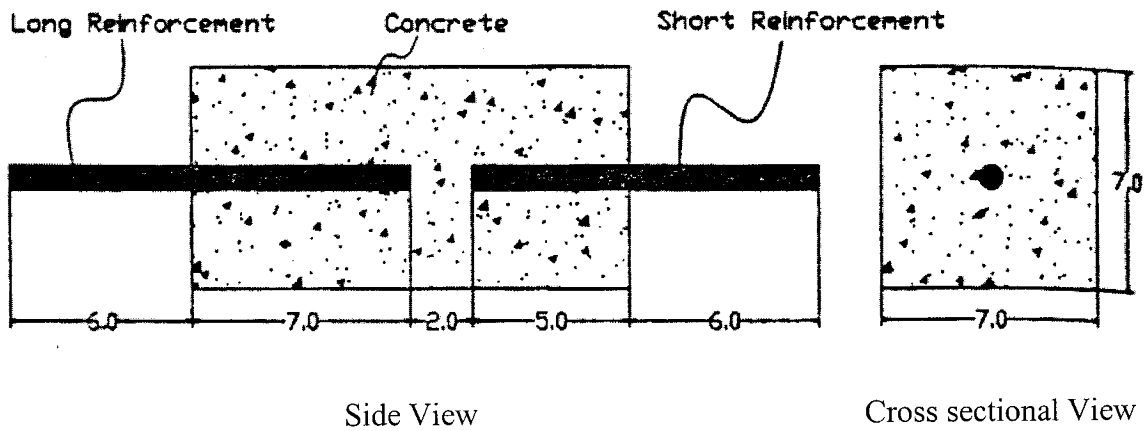

Fig. 5.16: Details of concrete prism specimen (Auyeung *et al.*, 2000)

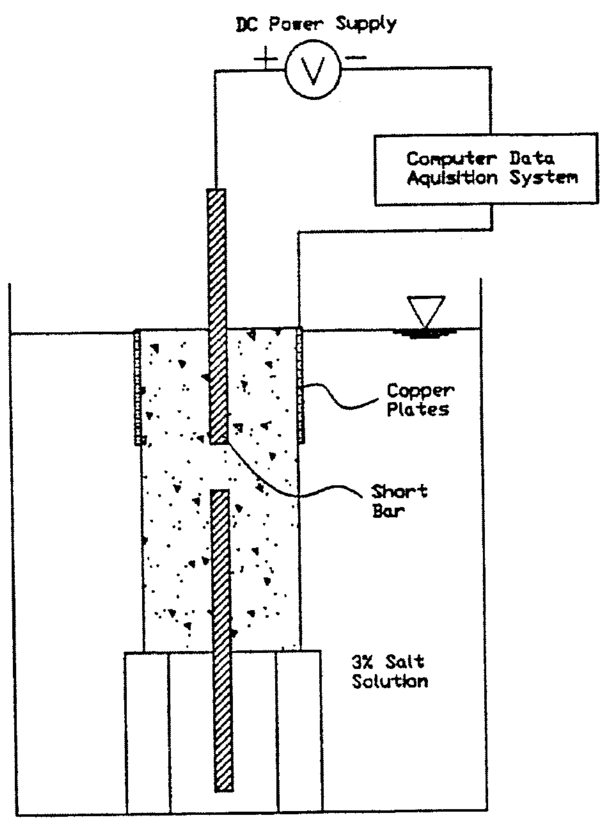

Fig. 5.17: Setup for inducing accelerated corrosion (Auyeung *et al.*, 2000)

They found that there was an increase in the bond strength at low levels of corrosion (mass loss less than 1%), but when the mass loss of the reinforcement reached approximately 2%, the concrete cracked along the bar (Fig. 5.18). There was considerable decrease (about 57%) in bond strength when the mass loss exceeds 2%, or after the appearance of cracks. They also found that even after extensive corrosion with considerable cracking of the concrete, the bond was not completely destroyed. Measurable residual bond strength, about 26 % of the maximum value, existed even when the mass loss reached 6 %.

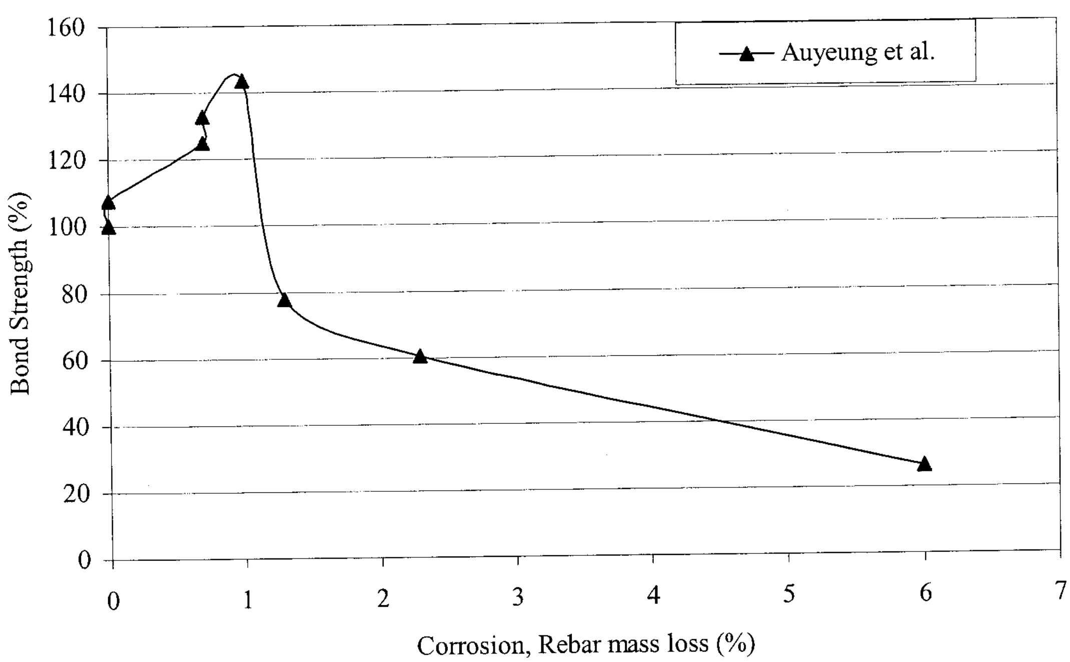

Fig. 5.18: Relationship between the bond strength and the rebar mass loss (Auyeung *et al.*, 2000)

Al-Sulaimani *et al.* (1990) conducted pullout tests on 150 mm (5.9 in.) cubic concrete specimens with 10,14 and 20 mm diameter deformed bars, respectively, embedded in the cube centrally (Fig. 5.19). They studied the bond behaviour at different stages of reinforcing bar corrosion: no corrosion, precracking, cracking, and postcracking levels. These stages of corrosion were achieved by impressing a direct current for increasing time periods on the reinforcing bar embedded in the pullout, or beam specimen subjected to accelerated corrosion by immersion in a NaCl solution and the current was arranged so that the bar served as the anode while a stainless steel plate located in the water acted as the cathode.

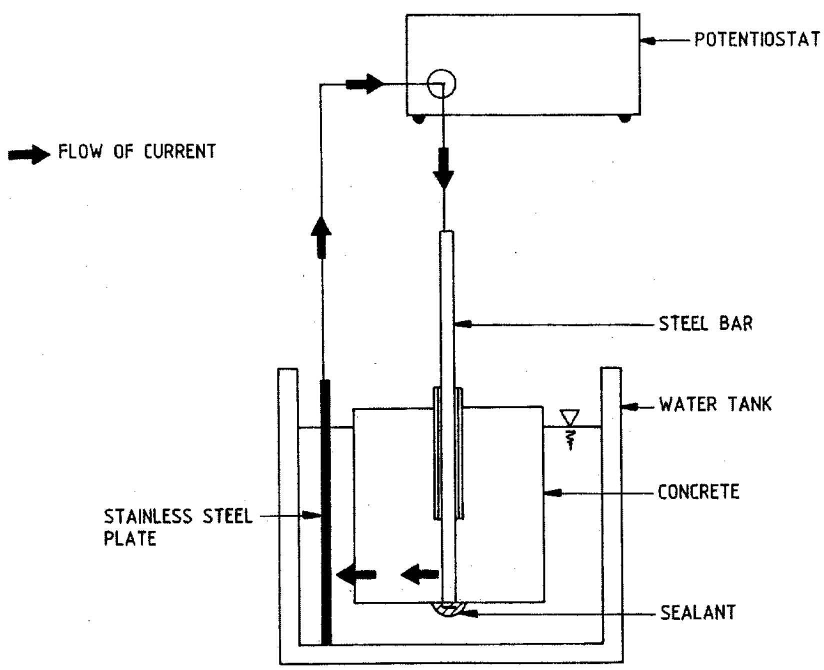

Fig. 5.19: Schematic drawing for corrosion setup (Al-Sulaimani *et al.*, 1990)

A constant current density of 2 mA/cm^2 was transmitted over the reinforcement surface and the total impressed current was adjusted for each specimen to maintain this current density for bars of different diameters. They found that up to about 1 percent corrosion (rebar mass loss), the bond strength increased slightly (Fig. 5.20). However, with further corrosion, the bond stress declined consistently until it became negligible for about 7.5 percent postcracking corrosion (rebar mass loss). With increased corrosion in the postcracking stage, the mechanical interlocking between the ribs and the concrete deteriorated significantly, and the bond failure mechanism of these specimens was increasingly influenced by the lubricating effect of the flaky corroded metal products between the concrete and the base steel.

Fig. 5.20: Relationship between the bond strength and the rebar mass loss (Al-Sulaimani *et al.*, 1990)

Amleh (2000) tested pullout specimens consisted of a pre-weighed single No. 20 bar embedded in a 300 mm long, cylindrical concrete specimen, with the bar protruding at one end only (Fig. 5.21). She used four different specimen diameters giving cover thicknesses of 100 mm, 75mm, 50 mm and 25 mm. About 50 mm of the extension parts of the bars along with another length of 25 mm within the specimen end, was epoxy-coated to protect the interface between the protruding steel rebar and the surface of the concrete specimen from corrosion.

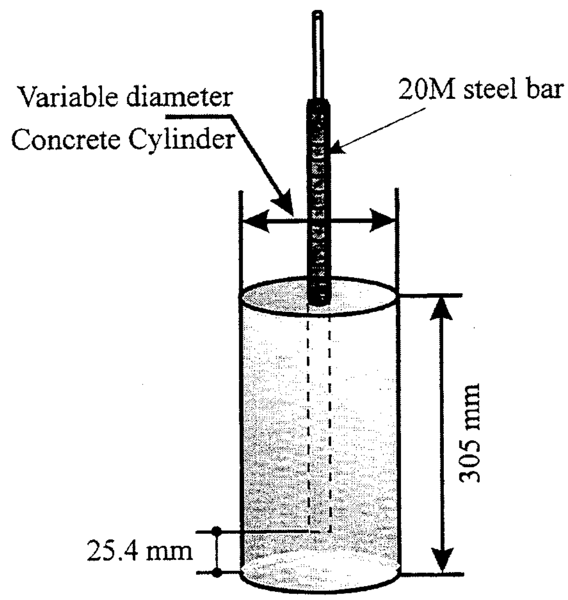

Fig. 5.21: Typical pullout test specimen (Amleh, 2000)

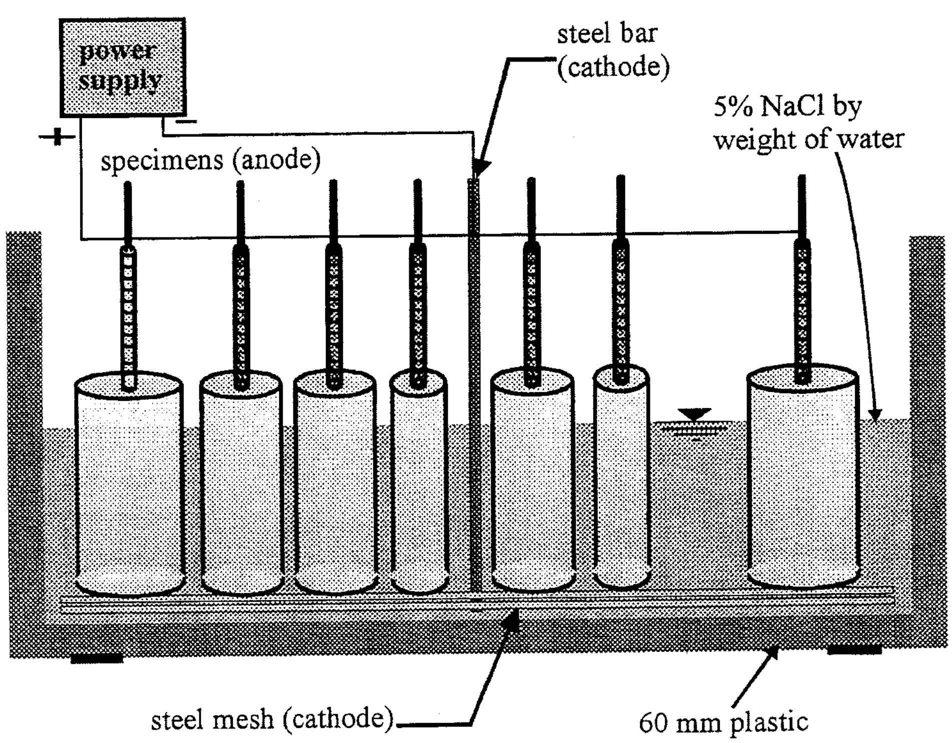

Fig. 5.22: Accelerated corrosion test set-up for pullout specimens (Amleh, 2000)

After casting and curing, the specimens were subjected to accelerated corrosion by placing them in the accelerated corrosion tanks (Fig. 5.22). The tanks were filled with an electrolytic solution (5 % NaCl sodium chloride by weight of water). A constant voltage of 5 Volts was applied to stimulate rebar corrosion. The mass loss of the steel reinforcing bar was obtained as the difference between the mass of the corroded bar (after the removal of loose corrosion products) from its mass before corrosion. She found that the value of the bond strength increased initially to a mass loss value of 2.5 percent, beyond which the bond strength deteriorated gradually with an increase in the level of corrosion as shown in Fig. 5.23.

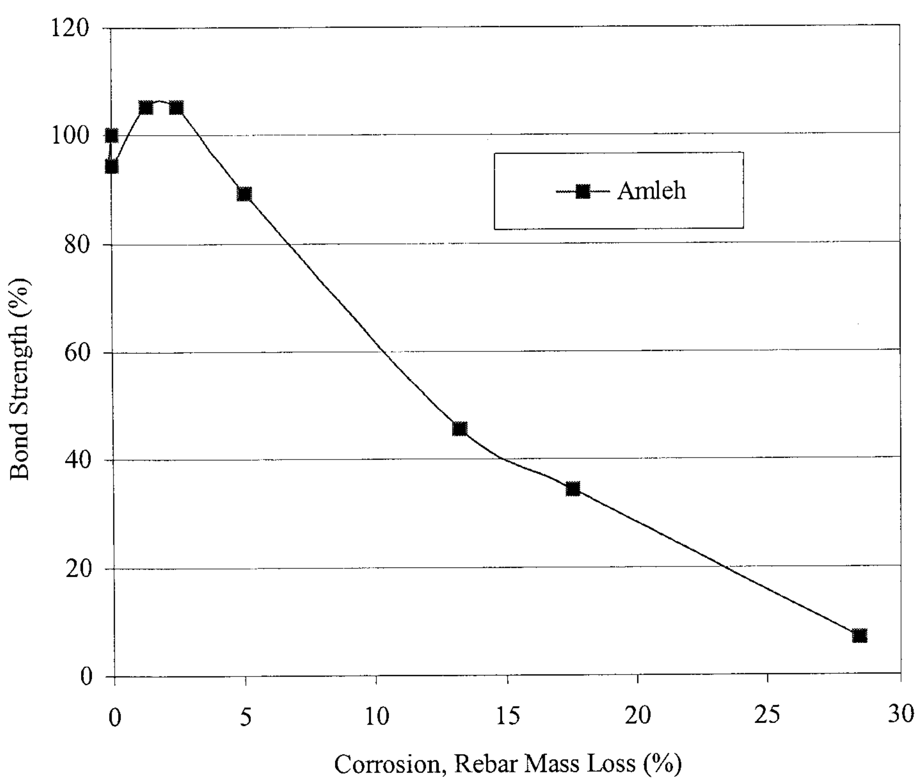

Fig. 5.23: Relationship between the bond strength and the rebar mass loss (Amleh, 2000)

Amleh also found the behaviour of 0.32 w/c ratio concrete to be close to that of concrete made with w/c ratio of 0.42. Figure 5.24 shows a plot between the normalized bond strength ratio (bond strength of the corroded specimen /bond strength of the uncorroded specimen) and the rebar mass loss (percentage corrosion). It can be seen that as the corrosion level is increased, there is a gradual decrease in the bond strength.

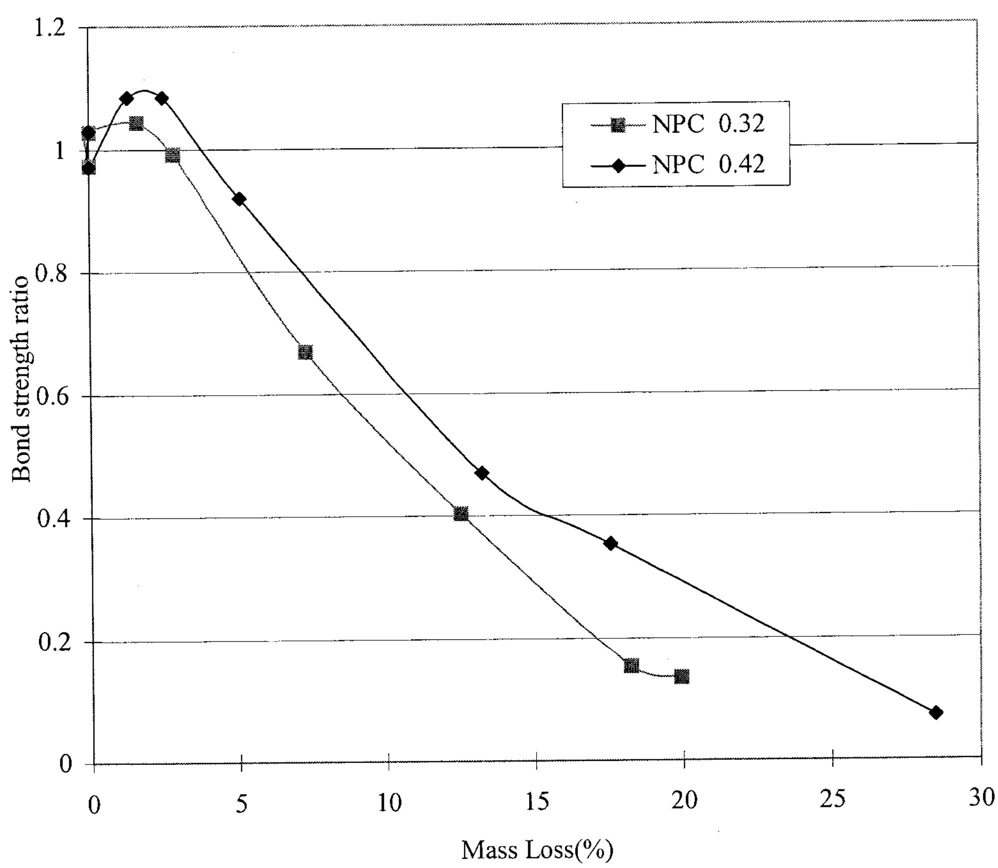

Fig. 5.24: Bond strength ratio versus mass loss of rebar (Amleh, 2000)

Amleh's Bond Strength Equations

Based on her experimental results, Amleh (2000) developed bond strength equations for pullout tests as a function of the mass loss. She showed that the bond strength at the steel-concrete interface behaved linearly with the mass loss of the steel bar. She recommended against using 25 mm thick concrete cover with any type of concrete. Bond strength equations for different types of concrete are listed in Table 5.1, which also include the values of correlation coefficient indicating the level of confidence obtained in the derived equations. Here ML is the percentage mass loss of the steel rebar, C is the concrete cover thickness, d_b is the bar diameter and f_c' is the concrete compressive strength.

Table 5.1: Bond strength equations as a function of the mass loss (After Amleh, 2000)

Concrete mixture	**Bond strength equation** (u)	**Correlation coefficient**
Point Tupper fly ash concrete	$u = (0.4 + 0.16\frac{C}{d_b})\sqrt{f_c'} - 0.34(ML)$	0.95
Thunder Bay fly ash concrete	$u = (0.4 + 0.21\frac{C}{d_b})\sqrt{f_c'} - 0.45(ML)$	0.93
Sundance fly ash concrete	$u = (0.4 + 0.25\frac{C}{d_b})\sqrt{f_c'} - 0.62(ML)$	0.91
NPC (w/c ratio = 0.32)	$u = (0.35 + 0.3\frac{C}{d_b})\sqrt{f_c'} - 0.42(ML)$	0.97
NPC (w/c ratio = 0.42)	$u = (0.35 + 0.3\frac{C}{d_b})\sqrt{f_c'} - 0.34(ML)$	0.90
HAC (w/c ratio = 0.37)	$u = (0.56 + 0.135\frac{C}{d_b})\sqrt{f_c'} - 0.31(ML)$	0.90

Table 5.2 shows the summary of pull out tests performed by different investigators:

Table 5.2: Summary of pullout results

Investigator	Bar Dia. (mm)	Specimen size	Impressed current mA/cm^2	Type of Test
Almusallam *et al.* (1996)	12	152×254×279 mm	10	Pullout
Cabrera & Ghouddoussi (1992)	12	150 mm cubic concrete	3 Volts	Pullout
Auyeung *et al.* (2000)	19	175×175×350 mm	2	Pullout
Al-Sulaimani *et al.* (1990)	20	150 mm cubic concrete	2	Pullout
	14		2	Pullout
	10		2	Pullout
Amleh (2000)	20	300 mm long cylindrical	5 Volts	Pullout

Figure 5.25 show a combined plot of rebars mass loss (percentage mass loss due to corrosion) and bond strength from the available data along with the proposed bond strength – corrosion mass loss curve. The results show that as the corrosion level increases slightly, there is an increase in bond strength, which is due to the increased rebar roughness and confinement of the small quantity of corrosion products developed at the surface. But with the first appearance of cracks, there is a considerable decrease in bond strength with increasing levels of corrosion. An approximate bond strength-corrosion mass loss curve is obtained to provide the percentage loss of bond strength with the increasing levels of corrosion.

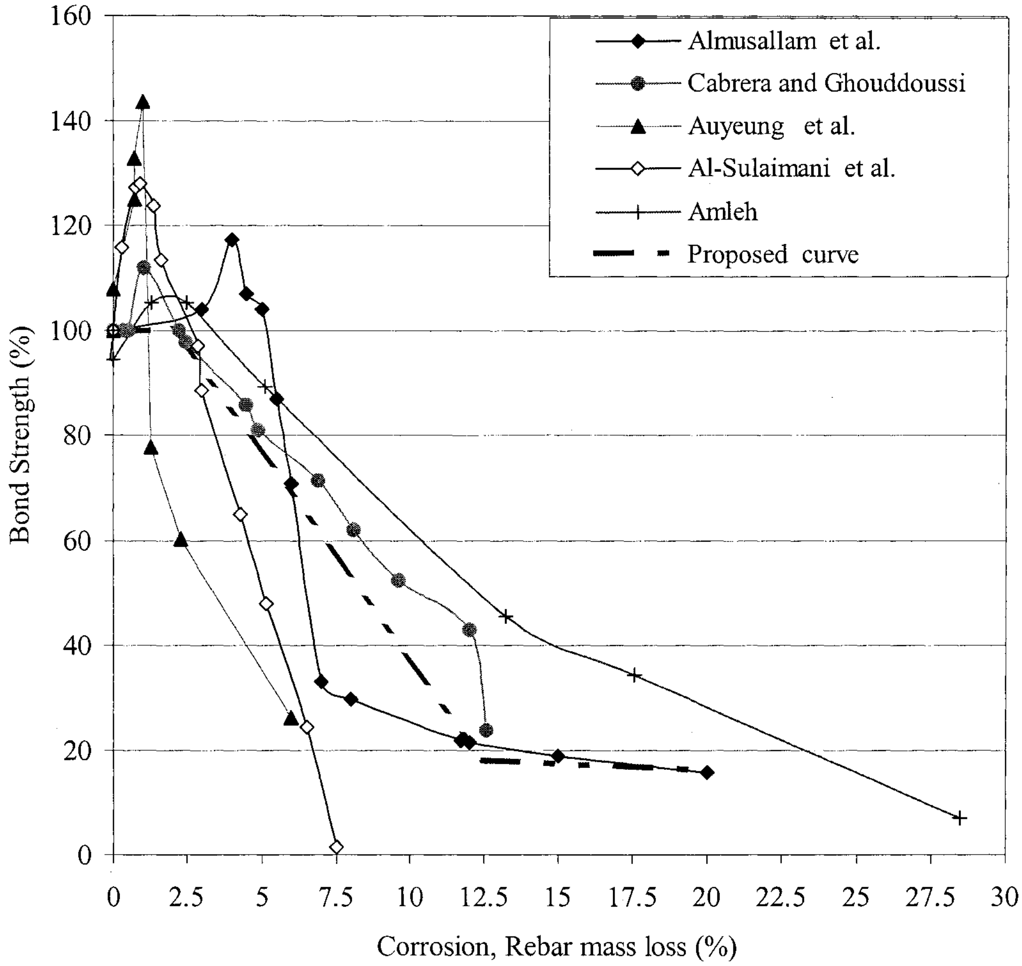

Fig 5.25: Effect of corrosion rebar mass loss on bond strength

Variations in the loss of bond as a result of a given amount of corrosion reported by different researchers are due to the following factors:

- Specimen conditioning (testing environment): In a majority of pullout tests, the corrosion process has been activated by salts (chloride) and accelerated by electric polarization of reinforcement. Conditioning has been carried out with the test specimens wholly or partly submerged in some instances, and with ponding of salt solutions. The current density applied by some authors is very high in comparison to the values used by others. Therefore, the considerably high loss of bond strength can be due to the disruptive effect from the application of such high current densities, and not due to corrosion. As in the cases of Al-Sulaimani *et al.* (1990) and Auyeung *et al.* (2000), the specimens were subjected to a constant current density of $2mA/cm^2$ (20 A/m^2) – a very high value of current density in comparison to the value used by the other authors. In both cases, the rate of deterioration of bond was much faster, and the value of bond strength was almost negligible at about 7.5 % rebar mass loss. It is clear that a considerable high value of impressed voltage or current results in a significant reduction of bond strength because of the associated large corrosion deterioration at the steel rebar surface.

- Bar diameter: Most of the authors used reinforcing bars of different diameters in their testing specimens.
- Specimen size and geometry: The testing specimens used by the authors were of different sizes. Also, their geometries (cubic, prismatic, cylindrical) were different.

Almost all the authors used different types of specimens and current intensities to ensure completion of their investigations in a given time frame. However, the results of the relative bond strength versus the rebar mass loss show similar trends despite the variations in the various parameters.

Proposed bond strength – corrosion mass loss equation

On the basis of this study, bond strength –corrosion mass loss equation is proposed by making the following assumptions:

- It is assumed that the bond strength remains constant at low levels of corrosion (up to 2 % rebar mass loss). This means that there is no loss of bond strength at low levels of corrosion.
- After 2 % rebar mass loss or corrosion, the bond strength decreases linearly with increase in corrosion and attains a value of about 18 % at 12.5 % corrosion (rebar mass loss). The value of bond strength corresponding to a given rebar mass loss is given by:

$$u_p = -7.8095\,(\mathrm{ML}) + 115.62 \quad (\text{for } 2\,\% < \mathrm{ML} < 12.5\,\%) \tag{5.5}$$

  where u_p is the percent bond strength and ML is level of corrosion or rebar mass loss expressed as a percentage.
- It is assumed that bond strength decreases linearly between 12.5 % and 20 % rebar mass loss, and then it remains constant at 16 % residual bond strength beyond 20 % rebar mass loss.

$$u_p = -0.2667\,(\mathrm{ML}) + 21.333 \qquad (\text{for } 12.5\% \leq \mathrm{ML} \leq 20\%) \tag{5.6}$$

Also,

$$u_p = 16\,\% \qquad (\text{for } \mathrm{ML} > 20\%) \tag{5.7}$$

Illustrative Example:

Assume that a No.20 bar in NPC (w/c ratio = 0.32, f_c'=60.2MPa) with a cover thickness of 100 mm has a mass loss of 3.80 % over a given service life of the structure. For a mass loss (ML) of 3.80 %, the bond strength can be calculated from equation (5.5) as:

$$u_p = -7.8095\mathrm{ML} + 115.62 = -7.8095*3.80 + 115.62 = 85.5\,\%$$

The bond strength, u, between the corroded bar and the concrete will be (Amleh, 2000):

$$u = (0.35 + 0.3\frac{C}{d_b})\sqrt{f_c'} - 0.31(ML) = (0.35 + 0.3\frac{100}{19.5})\sqrt{60.2} - 0.42(3.80) = 13.05MPa$$

The experimental value of the bond strength for a specimen (NPC with 0.32 w/c ratio, corrosion stage 2, ML=3.80%, cover thickness = 100 mm, d_b = 19.5mm) was 12.89 MPa, which is in excellent agreement with the calculated value of u (+1.22 %). Amleh (2000) also suggested an under capacity factor of 0.65 to be used while calculating the design bond strength. She noted the experimental value of the bond strength at rebar mass loss of 3.80 % as 86 % of the maximum bond strength, which is almost the same as calculated above from the predicted bond strength-mass loss equation.

5.2.4 Water-Cement ratio

Rasheeduzzafar *et al.* (1992) studied the corrosion-initiation time for 12.7 mm (1/2-in.) reinforcing steel bar embedded centrally in prismatic concrete specimens of size 4 × 2.5 × 12 in. (102 × 62.5 × 300 mm) with a minimum concrete cover thickness of 1 in. (25mm) on both sides as well as the bottom, made with w/c ratios of 0.40, 0.45, 0.50, and 0.65 and exposed to a chloride environment (5% NaCl solution). They monitored the corrosion by obtaining half-cell potentials, using a saturated calomel electrode. The values of the half-cell potentials reaching the threshold value, assumed to be – 270mV, were taken as the corrosion initiation time for the reinforcing steel. The time to initiation of corrosion was found to be about 235 days in case of concrete made with w/c ratio of 0.40, whereas it was about 100 days for the concrete with a w/c ratio of 0.65 (Fig. 5.26). This showed that concretes made with w/c ratios of 0.40 and 0.45 performed 2.35 and

1.78 times better in terms of corrosion-initiation time than concrete made with a w/c ratio of 0.65.

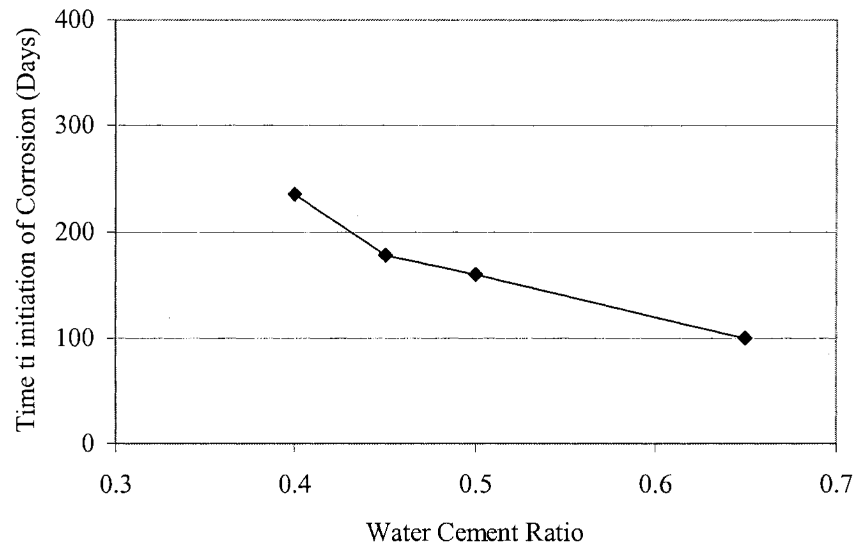

Fig. 5.26: Effect of water-cement ratio on corrosion initiation time of reinforcing steel (Rasheeduzzafar *et al.,* 1992)

They also demonstrated the beneficial effect of using richer mixes in conjunction with low w/c ratios (Fig. 5.27). Concrete made with a cement content of 750 lb/yd^3 (450 kg/m^3) and a w/c ratio of 0.40 performed 1.8 and 4.2 times better than the concretes made with cement contents of 550 lb/yd^3 (450 kg/m^3), 450 lb/yd^3 (270 kg/m^3) and w/c ratios of 0.50 and 0.575 respectively. The time to initiation of corrosion was found to be about 235 days in case of concrete made with w/c ratio of 0.40 and cement content of 650 lb/yd^3 (390 kg/m^3), which increased to about 288 days in case of concrete made with same w/c ratio of 0.40 but a cement content of 750 lb/yd^3 (450 kg/m^3). Thus, increasing the cement content from 650 to 750 lb/yd^3 (390-450 kg/m^3), while keeping the same w/c ratio of 0.40 increased corrosion – initiation times by 22 %.

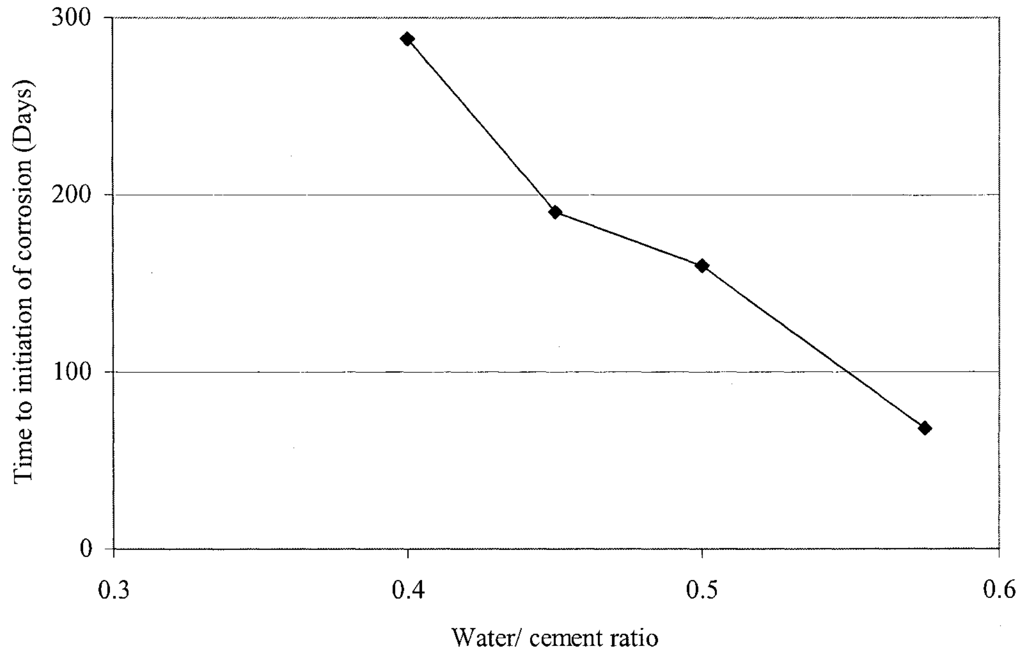

Fig. 5.27: Effect of increase in cement content with the associated decrease in w/c ratio on corrosion of reinforcing steel in concrete (Rasheeduzzafar *et al.,* 1992)

Based on tests using concrete cylindrical specimens, 1000 mm long by 25 mm diameter, each reinforced symmetrically with a pre-weighed single 20M deformed reinforcing bar, made with two NPC concretes (w/c ratios of 0.32 and 0.52), Amleh (2000) found that for 0.32 w/c ratio concrete specimens, a 1.5 percent rebar mass loss due to corrosion resulted in a 2 percent loss of the bond strength, while 14.5 percent rebar mass loss due to corrosion resulted in an 85 percent loss of the bond strength. She also noted that as expected, the performance of the NPC concrete specimens with w/c ratio of 0.32 in terms of cracking, crack width and deterioration of bond was superior to that of concrete specimens with w/c ratio of 0.52. (Fig. 5.28)

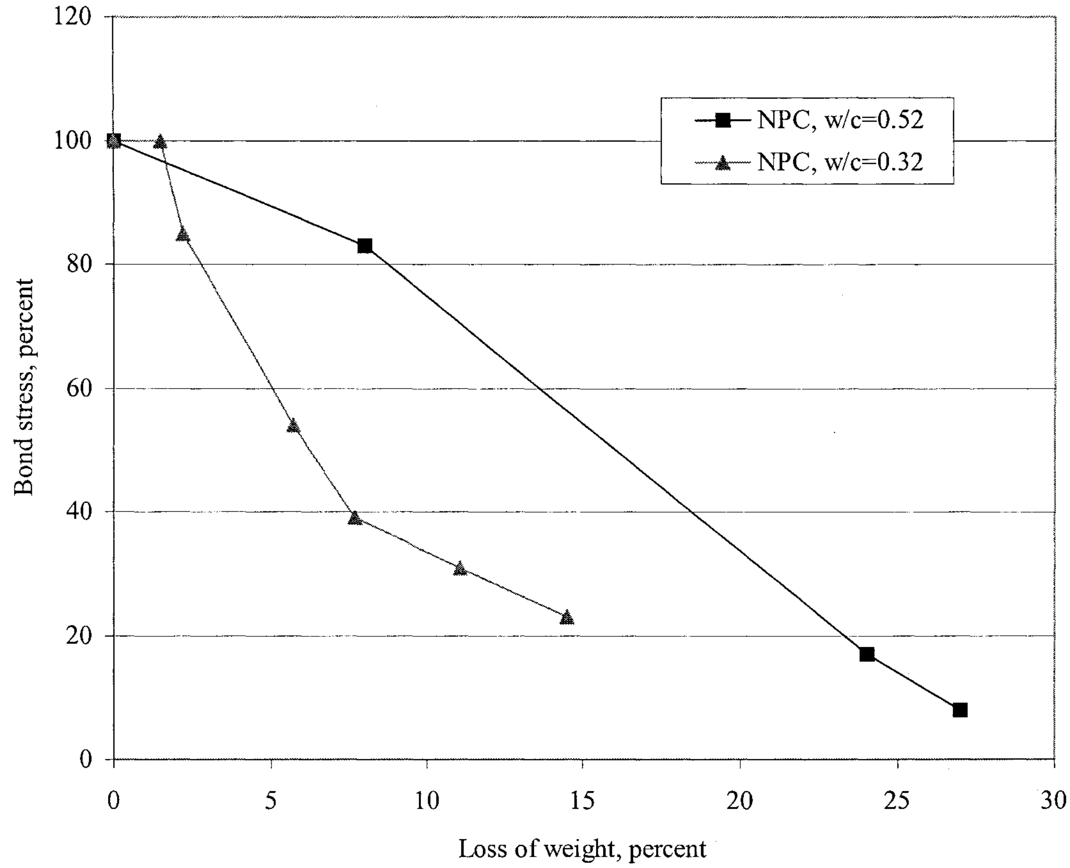

Fig. 5.28: Relative bond stress versus level of corrosion (Amleh, 2000)

Richardson (2002) recommended a water/cement ratio between 0.4 and 0.5 as an important requirement for durability design. He suggested that water/cement ratio must be low enough to minimize the initial volume of capillary pore network created by the mix water and high enough to supply a water-filled capillary pore structure with an early volume at least twice that of the unhydrated cement.

5.2.5 Cover – to - bar diameter (C/d_b) ratio

According to Al-Sulaimani *et al.* (1990), increasing the bar diameter signified the higher bursting forces resulting from the corrosion process cause cracking of the concrete, whereas the thickness and quality of concrete cover over the reinforcement characterize the resistance to the splitting corrosion forces. Therefore, cover thickness/ bar diameter C/d_b ratio is a significant corrosion protection parameter. They conducted pullout tests on 150 mm cubic concrete specimens reinforced with a single 10,14 and 20mm diameter deformed bars, embedded centrally to give C/d_b ratios of 7.50, 5.36 and 3.75 respectively. To simulate the corrosion process, direct current was impressed on the bar embedded in the specimens using an integrated system incorporating a small rectifier supply with an in-built ammeter to monitor the current, and a potentiometer to control the current intensity. The specimens were subjected to accelerated corrosion by immersion in a NaCl solution and the current was arranged so that the bars served as the anode while a stainless steel plate located in the water acted as the cathode. A constant current density of 2 mA/cm^2 was passed over the reinforcement surface and the total impressed current was adjusted for each specimen to maintain this current density constant for bars of different diameters. Cracking level was defined as the appearance of first visible crack. The results showed that about 4% rebar mass loss due to corrosion was needed to initiate cracking for a C/d_b ratio of 7, while only about 1% mass loss was found to be sufficient to crack the reinforced concrete components with a C/d_b ratio of 3.

Amleh (2000) tested 192 pullout specimens, made with two NPC concretes (w/c ratios of 0.32 and 0.42), three fly ash concretes (Point Tupper, Thunder Bay and Sundance fly ash), and a high alumina cement concrete (w/c ratio of 0.37). All cylindrical specimens, 305 mm long, were axially reinforced with one No. 20 (19.5mm diameter) rebar, and the cylinder size was varied to accommodate four different concrete cover thicknesses (25, 50, 75 and 100mm). Corrosion of the embedded steel bar was delayed due to the increase in the concrete cover thickness. Also, the results showed the largest concrete resistivity and the associated lowest values of corrosion current and corrosion activity for Sundance and Thunder Bay fly ash concrete mixtures. The results further demonstrated the corrosion protection superiority of NPC concrete with a w/c ratio of 0.32 compared with the NPC concrete with a w/c ratio of 0.42, showing the importance of the quality of the concrete cover in addition to its thickness. With Sundance fly ash concrete, the time to cracking for a 100mm, 75mm, 50mm and 25mm thick cover was found to be 240, 185, 150 and 51 days respectively, which shows the time to cracking for a 100mm thick cover is 1.3, 1.6 and 4.7 times the cracking times those for cover thicknesses of 75, 50 and 25mm, respectively. Whereas, for NPC concrete with a w/c ratio of 0.32, the time to cracking for a 100mm, 75mm, 50mm and 25mm thick cover was found to be 192, 160, 100 and 40 days, respectively. Therefore, for NPC concrete with a w/c ratio of 0.32, a 100mm thick cover provided 1.2, 1.9 and 4.74 times the protection against the concrete cover cracking than for thicknesses of 75, 50 and 25 mm, respectively. She found that for NPC concrete with w/c ratios of 0.32, about 4 percent rebar mass loss was needed to initiate cracking for a C/d_b ratio of 5.13 (100 mm cover thickness). By contrast, only about 1% loss of mass was found sufficient to crack reinforced concrete components with a C/d_b ratio of 1.3 (25 mm cover thickness).

Rasheeduzzafar *et al.* (1992) provided data showing the significant role of the C/d_b ratio as a corrosion-protection factor. They performed tests on 3.4 × 4 × 30 in. (86.4 × 102 × 762 mm) concrete beams containing mild steel bars of six different diameters– 0.32, 0.375, 0.50, 0.75, 1 and 1.5 in. (8, 9.5, 12.7, 19, 25.4 and 38.1 mm). Concrete cover thicknesses of 0.95 in. (24.1 mm) and 1.45 in. (36.8 mm) were used respectively, with 1.5

in. (38.1 mm) and 0.32 in. (8 mm) diameter bars, whereas concrete cover thickness of 1.25 in. (31.75 mm) was used for the remaining bars to give six different cover to bar diameter ratios of 0.63, 1.25, 1.70, 2.50, 3.33 and 4.53. Reinforcing bar from each of the beams tested was retrieved immediately after the appearance of the longitudinal crack along the bar. Corrosion products were removed and the extent of rebar corrosion was measured as the loss in the rebar weight. They determined the effect of the C/d_b ratio on the amount of corrosion required to cause cracking. About 3.2% rebar mass loss was needed to initiate cracking for a C/d_b ratio of 5; only about 0.67% rebar mass loss was found to be sufficient to crack reinforced concrete components with a C/d_b ratio of 2. Rebar mass loss that could be tolerated without cracking for a C/d_b ratio of 4 was 15 and 3.5 times as much for a C/d_b ratio of 1 and 2, respectively.

They examined that even a cover of 2 inches (51 mm) may not provide adequate corrosion protection in some cases, if the C/d_b ratio was low. They suggested that clear cover specifications without an interactive consideration of the bar diameter leads to inadequate detailing for corrosion protection. They noted from examinations of several chloride-laden structures in Saudi-Arabia, that even with adequate cover thicknesses, premature corrosion occurred in several of these structures because the C/d_b ratios were too small. They noted an example of large diameter mild steel sleeve-anchor bolt assembly cast into the four corners of a concrete foundation block with a normally adequate cover of 51mm (2 in.). The average value of the C/d_b ratio was about 0.97 in comparison to the typical C/d_b ratio value of 4.0, recommended for foundations cast against earth. In this case, corrosion cracking occurred in the chloride-contaminated concrete foundations within only 1.5 years after construction.

They also determined the time to initiation of corrosion of reinforcing steel for concrete cover thicknesses of 6.4, 12.7, 19, 38.1 and 50.8mm (0.25, 0.50, 0.75, 1.50 and 2.0 inches) made with two concretes with w/c ratios of 0.45 and 0.65 (Fig. 5.29).

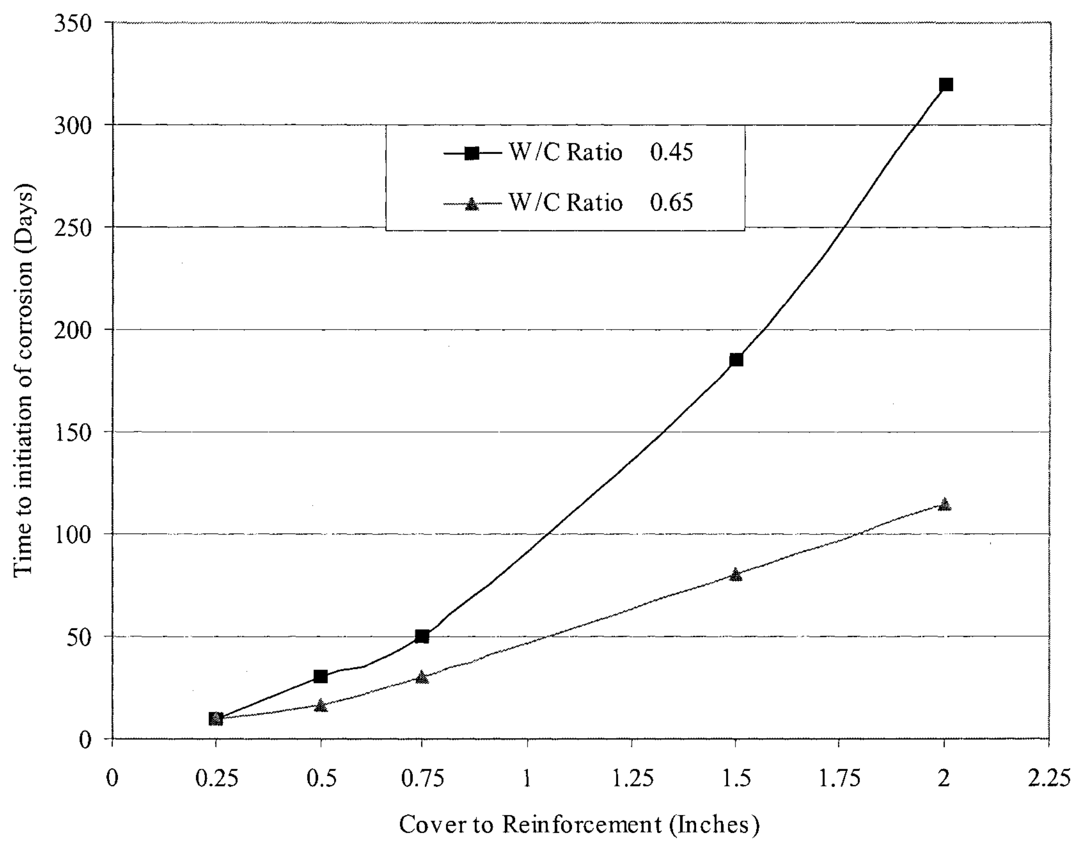

Fig. 5.29: Effect of concrete cover thickness over the steel bar on time to initiation of corrosion (Rasheeduzzafar *et al.,* 1992)

In the case of concrete made with w/c ratio of 0.45, the time to initiation of corrosion was found to be about 310 days with a 2-inch (50.8 mm) thick cover, whereas it was about 51 days and 25 days with ¾-inch (19mm) and ½-inch (12.7mm) cover thicknesses, respectively. Therefore, a 2-inch (50.8 mm) cover of 0.45 w/c ratio concrete was 6 and 12 times as protective against corrosion initiation as ¾-inch (19mm) and ½-inch (12.7mm) cover thicknesses. However, a similar increase in the concrete cover thickness for a low quality 0.65 w/c ratio concrete was only half as effective for corrosion protection as the high-quality 0.45 w/c ratio concrete cover.

Table 5.3 summarizes the information available from three different researchers about the bar size, cover to bar diameter ratio, specimen geometry and the environment in which the specimens were tested. Figure 5.30 shows the relationship between the cover to bar diameter ratio (C/d_b) and percentage rebar corrosion (rebar mass loss) to cause cracking.

Table 5.3: Summary of test results

Investigator	**Bar Dia. (mm)**	**C/d_b Ratio**	**Specimen size**	**Impressed current mA/cm^2**
Al-Sulaimani *et al.* (1990)	20	3.75	150 mm cubic concrete	2
	14	5.36		2
	10	7.5		2
Amleh (2000)	20	5.13	305 mm long cylindrical	5 Volts
		3.85		
		2.56		
		1.3		
Rasheeduzzafar *et al.* (1992)	8	4.53	86.4×102×762 mm	3
	9.5	3.33		
	12.7	2.5		
	19	1.70		
	25.4	1.25		
	38.1	0.63		

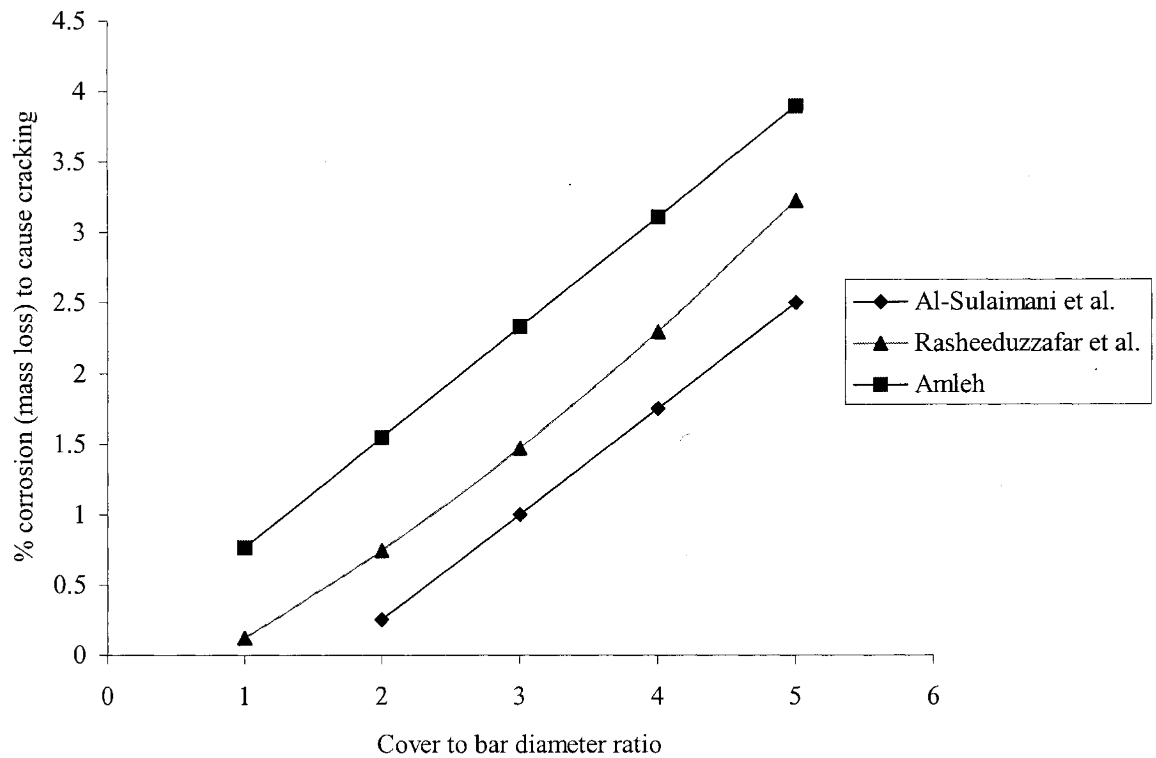

Fig. 5.30: Relationship between cover to bar diameter ratio and percentage corrosion (mass loss) to cause cracking

The curves show a linear behaviour between the two parameters. The difference between the percentage rebar mass loss (corrosion) required to cause cracking with respect to C/d_b ratio can be due to the size and geometry of the specimens, and the environment in which they were tested. The figure clearly shows the effectiveness of C/d_b as a corrosion protection parameter. Al-Sulaimani *et al.* (1990) and Rasheeduzzafar *et al.* (1992) used current densities of 2 mA/cm^2 and 3 mA/cm^2 respectively, for accelerating corrosion, which were very high as compared to the impressed current of 5 Volts used by Amleh (2000). Therefore, the rate of corrosion to cause cracking was faster in both the cases with respect to different cover to bar diameter ratios.

The effect of cover to bar diameter (C/d_b) ratio on the percentage increase in time to initiation of corrosion is shown in Fig. 5.31. It is clear that about 6.7 times more time is required for initiation of corrosion if the value of C/d_b ratio is increased from 1 to 4.

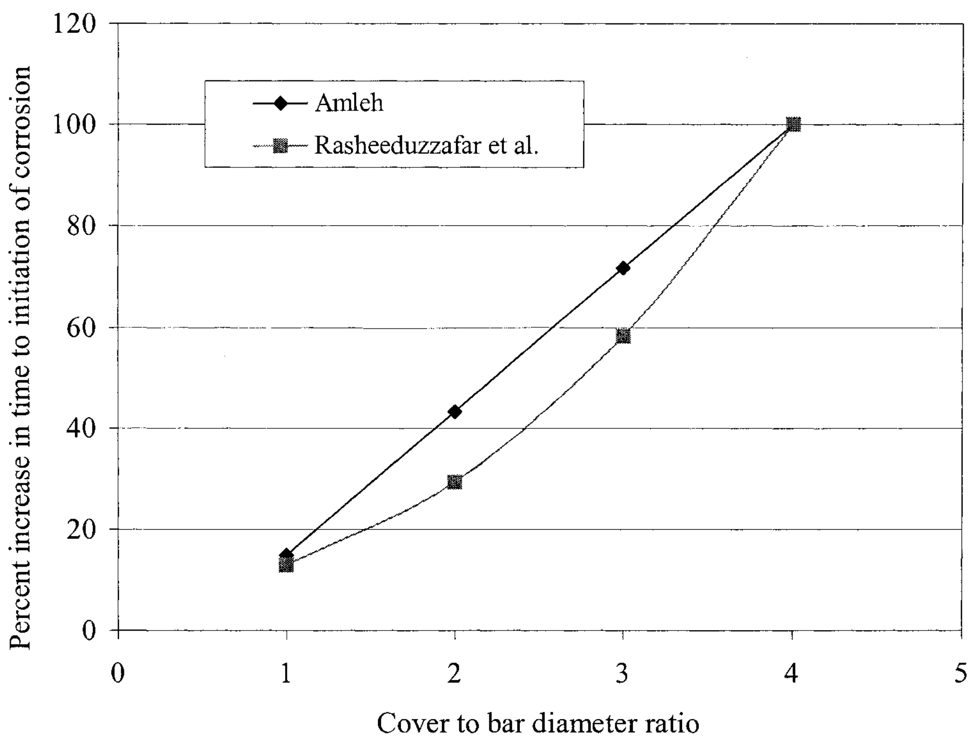

Fig. 5.31: Effect of cover to bar diameter ratio on percent increase in time to initiation of corrosion

This presentation shows quantitatively the vital importance of the concrete cover thickness to bar diameter (C/d_b) ratio in providing protection to steel and underlines the fact that in terms of design practices, cover to reinforcement has the most significant effect on the extent of reinforcement corrosion deterioration. These results clearly point to the need for careful detailing of C/d_b ratio for protection against corrosion in structural concrete. The results show that initiation of corrosion is delayed significantly for C/d_b ratios between 3 and 4.

5.2.6 Crack width

The effect of the crack width due to corrosion on the ultimate bond strength and the effect of the degree of corrosion (rebar mass loss percentage) on the surface crack width are shown in Figures 5.32 and 5.33. Almusallam *et al.* (1996) evaluated the effect of different crack widths and the rib profile degradation for various degrees of corrosion on the bond strength. They used the cantilever beam bond tests on 30 MPa concrete specimens 152 × 254 × 279 mm in size, reinforced with a 12 mm diameter deformed bars. They studied the effect of the crack width due to corrosion on the ultimate bond strength, in addition to the effect of the degree of corrosion (rebar mass loss percentage) on the surface crack width. The ultimate bond strength decreased abruptly from 100% to 64% at the initial stages of the formation of cracks and the associated resulting reduction in the confinement. They noted the deteriorating effect of the crack width on the bond strength after a certain degree of corrosion, whereas, there was no significant change in the bond strength beyond a certain level. A significant increase in the crack width was noted at corrosion levels between 5% and 7%, resulting in a significant decrease in the bond strength, ranging from 30% to 70% of the ultimate strength. They noted that after 0.3 mm crack width, there was a considerable decrease in the bond strength. Amleh (2000) also studied the effect of crack width on bond strength. She also found that after 0.3 mm crack width, there was a considerable decrease in bond strength. It is generally accepted that the cracks less than 0.3 mm in width usually self heal by the dust and other particles from the environment.

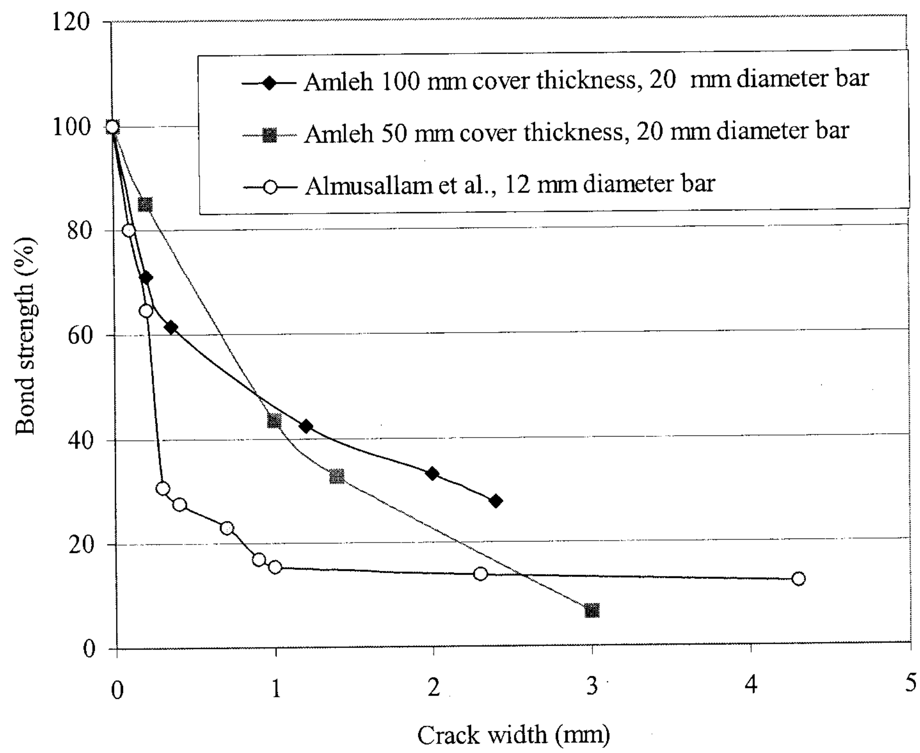

Fig. 5.32: Relationship between effect of crack width due to corrosion on the bond strength

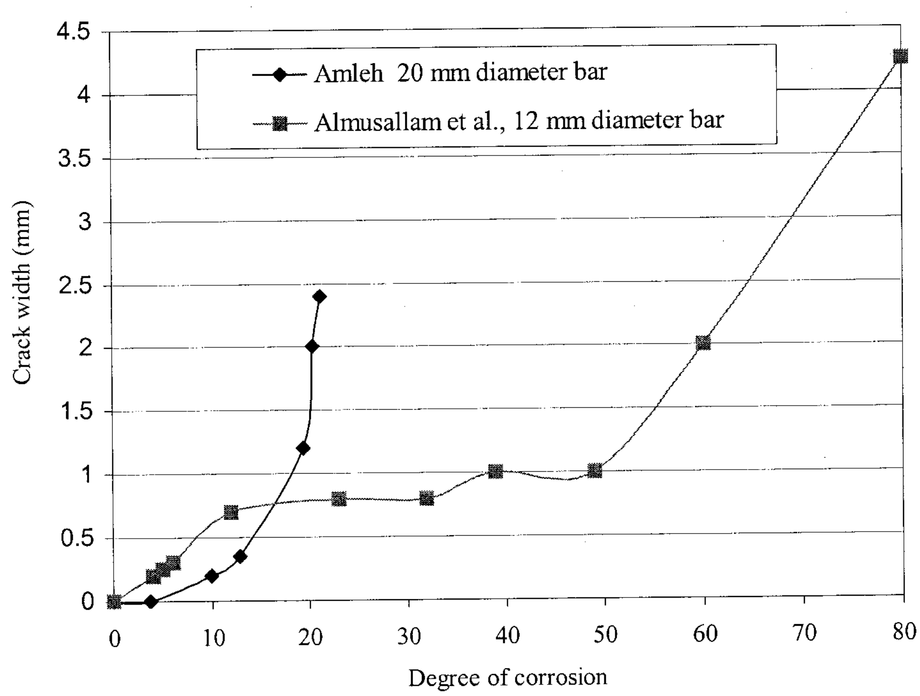

Fig. 5.33: Relationship between effect of degree of corrosion on surface crack width

From the results of their investigation, using 20 tension specimens, Amleh and Mirza (2002) showed that as the corrosion level (rebar mass loss) increases, the crack spacing increases, showing increasing loss of bond at the steel-concrete interface (Table 5.4).

Table 5.4: Test results for tension specimens

Specimen	Corrosion stage	First cracking load (kN)	Yield load (kN)	Ultimate load (kN)	Rebar mass loss due to corrosion (%)	Average transverse crack spacing (mm)	Maximum transverse crack spacing (mm)	Nominal bond stress (%)
CONCRETE WATER-CEMENT RATIO = 0.32								
C3-1C	0	19	127	200	0	77	95	100
C3-5C	1	34	125	202	1.5	77	100	100
C3-8C	2	48	124	199	2.2	91	180	85
C3-10C	3	35	121	193	4.5	111	220	69
C3-9C	4	30	122	193	5.7	143	250	54
C3-6C	5	31	115	189	7.7	200	220	39
C3-3C	6	48	93	147	11.1	250	270	31
C3-4C	7	37	83	127	14.5	333	350	23
CONCRETE WATER-CEMENT RATIO = 0.52								
C7-1C	0	18	127	200	0	83	110	100
C7-4C	1	23	116	190	18.0	100	160	83
C7-5C	2	24	103	169	11	125	200	67
C7-8C	3	23	96	154	16	143	200	58
C7-3C	4	17	87.5	128	15	200	220	42
C7-7C	5	28	83	125	20	250	300	33
C7-10C	6	59	81.5	121	22	333	350	25
C7-6C	7	63	70	104	24	500	500	17
C7-9C	8	-	45	76	27	1000	150	8

The levels of corrosion attained in the various specimens varied from no corrosion to extensive corrosion. The width of the longitudinal cracks was used as the basis for ascertaining the level of corrosion attained. The number of transverse cracks and the maximum average spacing with respect to different levels of corrosion were also studied.

Figures 5.34 and 5.35 show the steel stress at the crack versus the crack width for the two NPC concretes with w/c ratios of 0.32 and 0.52, showing that as the crack width increases with the level of corrosion, the bond at the steel-concrete interface deteriorates.

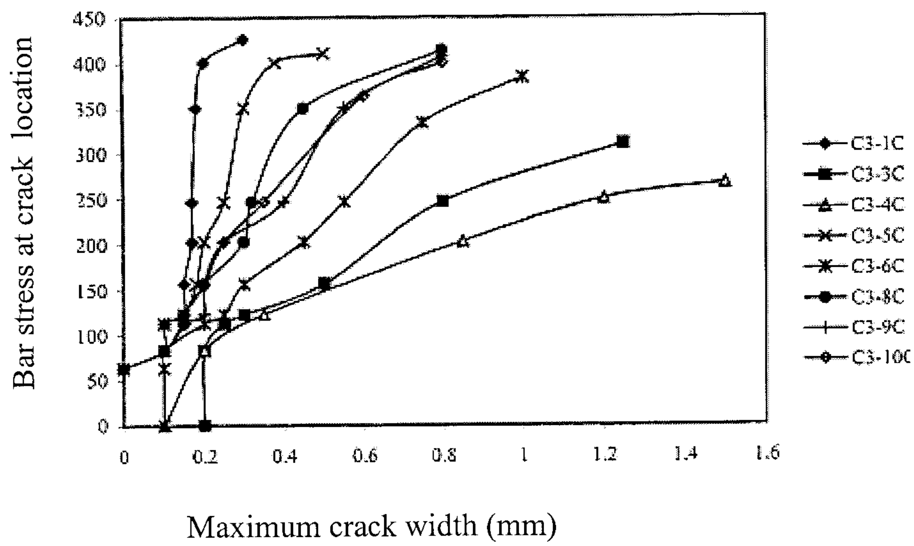

Fig. 5.34: Variation of steel bar stress at crack location with the maximum crack width (w/c ratio 0.32) (Amleh and Mirza, 2002)

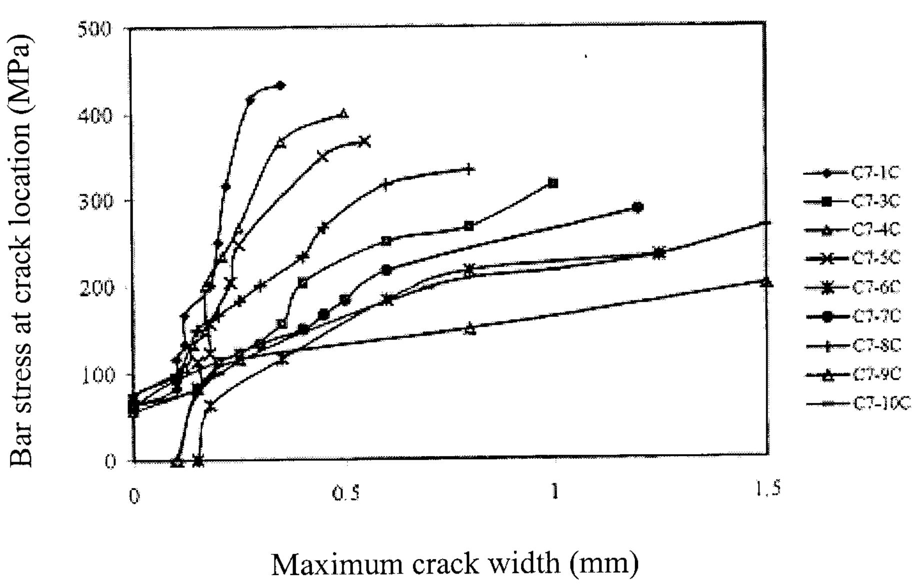

Fig. 5.35: Variation of steel bar stress at crack location with the maximum crack width (w/c ratio 0.52) (Amleh and Mirza, 2002)

Comparisons of Figures 5.34 and 5.35 also show better performances of the 0.32 w/c ratio concrete specimens with smaller crack widths at the same steel stress level as compared with the 0.52 w/c ratio concrete specimens, demonstrating improved bond characteristics.

5.2.7 Bar profile and rib geometry

Lutz and Gergely (1967) stated that the bond in case of deformed bars is developed mainly by the bearing pressure of the bar ribs against the concrete. It has been established through tests on arrangements of different bar patterns that bond strength of ribbed bars increases with an increase in relative rib area, at least where the bars are confined by links or a larger concrete cover (Cairns and Jones 1995, Darwin and Graham 1993). The area of bar ribs bearing on concrete can be reduced by corrosion in two ways:

- As the corrosion products occupy larger volume than that of the material oxidized, the corrosion products will tend to "raise apart" the bar and concrete, which leads to the spalling of concrete cover. The interlock between the bar rib and the concrete will be reduced by an amount equal to the thickness of the corrosion layer (Fig. 5.36). The reduction in the rib bearing height will be roughly equal to half the width of the longitudinal crack generated by corrosion.

- Ribs of deformed bars eventually lost due to corrosion

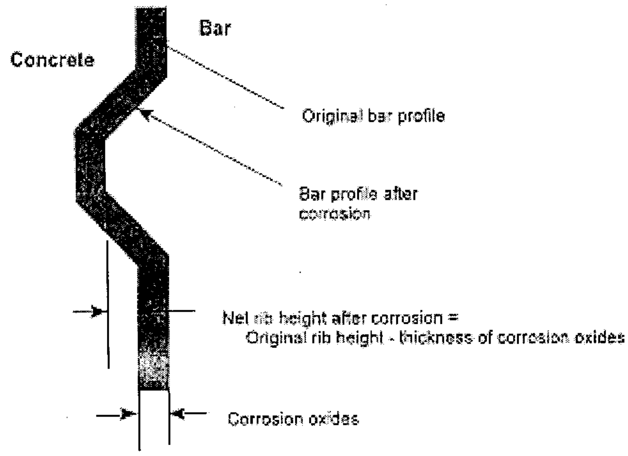

Fig. 5.36: Reduction in rib/concrete interlock as a result of corrosion (Cairns *et al.,* 2000)

Park and Paulay (1975) have shown that the best performance of a bar embedded in concrete over a short length *'c'* which is the rib spacing, occurs for a value of the ratio of the bearing area to the shearing area, *a/c* where *a* is the rib height, equal to 0.065 (Fig. 5.37)

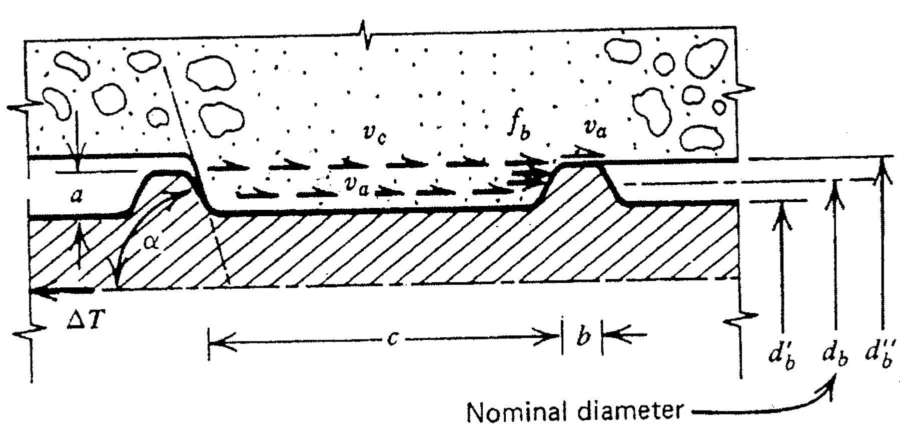

Fig. 5.37: Stresses between two ribs of a deformed bar

Almusallam et al. (1996) showed the variation of the ultimate applied force, or the maximum bond resistance or force with the percentage loss in the lug profile along with degree of corrosion (Figures 5.38, 5.39 and 5.40).

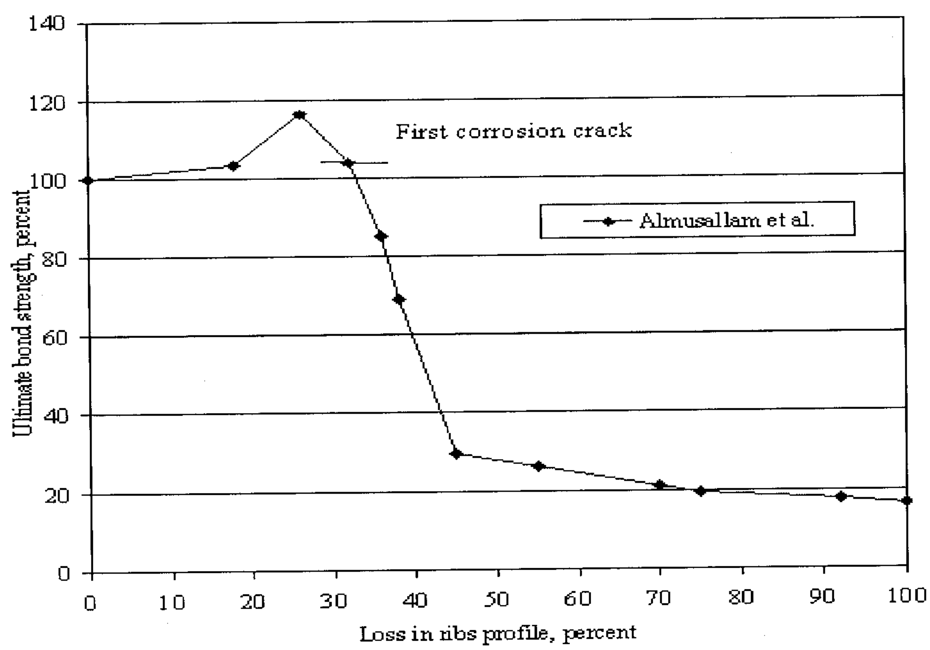

Fig. 5.38: Effect of the percentage loss of rib profile on the ultimate bond strength (Almusallam *et al.,* 1996)

They noted an initial increase in the bond strength up to 26% loss in the rib profile. However, there was a sharp reduction in the ultimate bond strength for rib degradation in the range of 26 to 45%, which might be attributed to the formation of small cracks around the reinforcing bars and a significant reduction in the rib profile with the resulting reduction in the interlocking action between the ribs and the concrete. They recorded no significant change in the bond strength from 45% to 100% rib degradation.

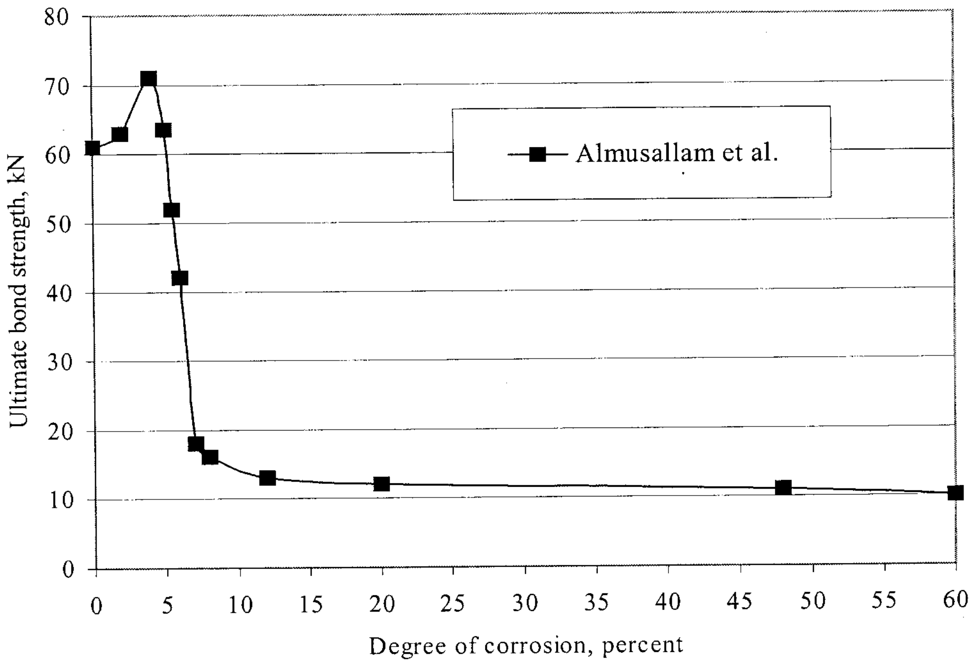

Fig. 5.39: Relationship between ultimate bond strength and different degrees of corrosion (Almusallam *et al.*, 1996)

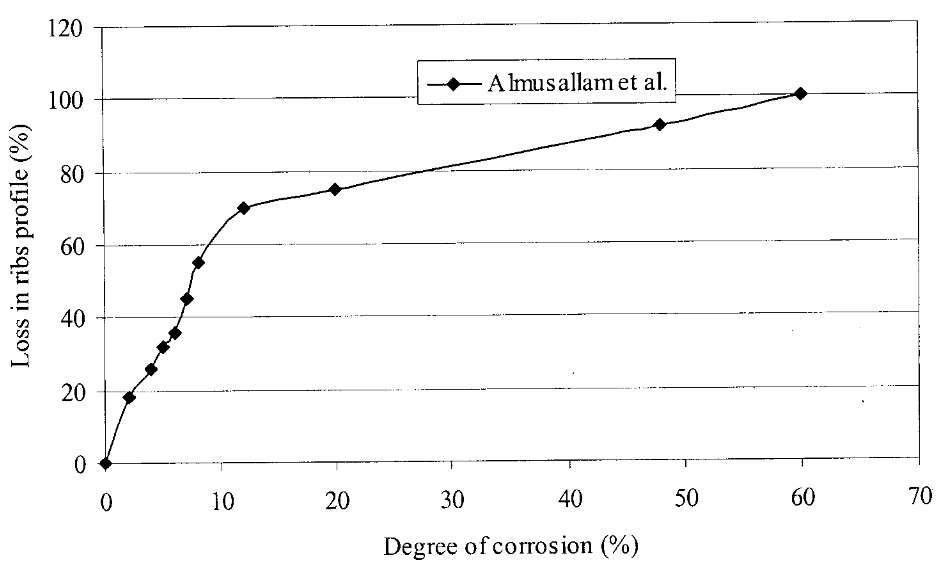

Fig. 5.40: Effect of degree of corrosion on loss in ribs profile

At ultimate bond strength of about 18 kN, which corresponded to a corrosion mass loss of about 7%, the lug profile loss was 45%, while at a maximum ultimate bond force of about 13 kN (a mass loss of about 12%), this loss was about 70%. At this stage, the failure mode changed from splitting to continuous slippage of the bar with the ribs being mostly lost. The higher bond resistance in the early corrosion stages was due to the action of the lugs bearing against the concrete and confined corrosion products. The insignificant change in the bond strength in later stages was the indication of rib degradation that their interlocking action within the concrete became negligible.

Almusallam's data shows that a rib profile loss of 26 % represents the critical value beyond which a sharp reduction in bond strength occurs.

5.3 Comparison of testing methods

Amleh (2000) investigated the influence of corrosion on the bond behaviour between the reinforcing steel and the concrete using two series of tests, pullout and direct tension tests. Pullout and tension specimens, reinforced with a single bar, were subjected to eight different stages of corrosion, and then subjected to axial tensile forces to determine the deterioration of bond at the steel rebar-concrete interface. Figure 5.41 shows the relationship between percentage corrosion (rebar mass loss) and the corresponding bond strength values as calculated by Amleh from both series of tests. It is clear that the bond strength decreases linearly after initial mass loss due to corrosion (when mass loss exceeds 1.5 %). Also, the deterioration of bond is almost same in both the tests.

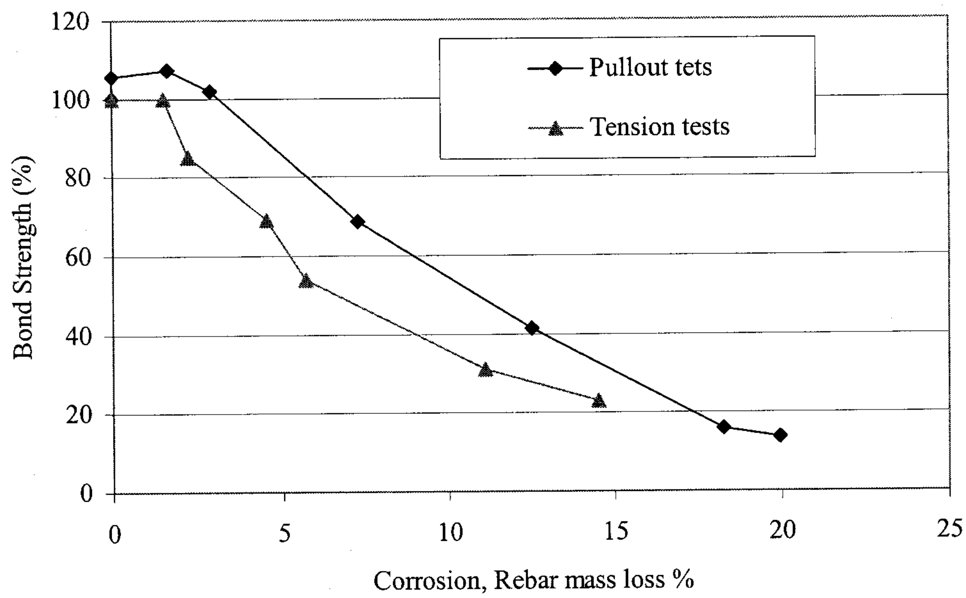

Fig. 5.41: Comparison between pullout tests and tension tests (Amleh, 2000)

5.4 Summary

The present research has considered the various parameters, which influence the deterioration of bond at the steel-concrete interface. It is found that initially bond strength increases with corrosion and starts decreasing as cracks form. The majority of information available shows that the tests were conducted under accelerated corrosion conditions using an impressed current, therefore, the quantitative results from these studies should be applied with considerable care to structures in the field. There are also considerable variations in the loss of bond as a result of a given amount of corrosion reported by different researchers, which are related to the environment (the environment in which the specimens are tested), bar diameter, cover thickness, concrete quality, etc. A bond strength-corrosion mass loss equation is proposed to determine the percentage loss of bond strength with increasing levels of corrosion. It is assumed that the bond strength remains constant at low levels of corrosion (up to 2% rebar mass loss), then decreases linearly attaining a value of about 18% at 12.5 % corrosion and it remains constant at 16% residual bond strength beyond 20% rebar mass loss. From the information available, the critical values of crack width and loss in the rib profile are found to be 0.3 mm and 26 %, respectively. The concrete cover thickness -to- bar diameter ratio (C/d_b) along with the water/cement ratio is found to be most significant parameters in evaluating the residual bond strength. It is recommended that concrete cover thickness -to- bar diameter (C/d_b) ratio between 3 and 4 be adopted for designing and detailing new reinforced concrete structures to delay the initiation of concrete cracking due to corrosion. However, more research is needed in this area.

Chapter 6

Framework for durability design

6.1 Information

The present design approach with respect to durability of concrete structures is largely empirical. It is based on deemed-to-satisfy rules (for example minimum cover thickness, maximum water/cement ratio, minimum cement content) and the assumption that if these rules are met, the structure will achieve an acceptably long (but unspecified) life. Improved durability results in increased building costs, but the current design methods do not have the tools to demonstrate that future maintenance and repair costs will decrease. The concrete industry is, therefore, unable to compete on the basis of durability. The current design codes do not include working or service life as a design parameter. A performance-based design and assessment provides the option of an objective competition between the various alternatives on the basis of durability. It uses realistic environmental and material models capable of predicting the future behaviour of a concrete structure and hence quantifying the performance with respect to time. In this context, performance means that with relatively accurate mathematical models, it can be shown that the essential functions of the structures are fulfilled. This is achieved by defining a performance limit and it is then shown that the probability of falling below this limit is acceptably low, demonstrating that the structure is reliable. The performance, the performance limits, the service life and the reliability level (or the accepted failure probability) need to be specified by the codes, or by the owner of the structure, or they can be derived from an economic optimization. The codes basically emphasize prescriptive qualitative provisions related to the various materials and they do not recognize that durability can be attained only by successful performance of the entire structure and its components in a given environment. Moreover, the environmental loads - the microclimate near the segment of the structural element under consideration also needs to be defined quantitatively. The levels of performance in terms of the various modes of deterioration and their combination(s) also have not been defined in the various codes. Durability of engineering structures introduces novel concepts in design for service life, maintenance strategies, and repair techniques. It provides the technical knowledge for assessing the service life of structures and for taking measures to safeguard the functioning of a structure during its service life. A good understanding of durability can help the engineer to assess a structure over its entire design service life, including the service phase.

6.2 Classification of the environment

A long service life is considered synonymous with durability. As durability under one set of conditions does not necessarily mean durability under another, it is customary to classify the environment when defining durability. Defining, or classifying, the aggressivity in which the structure is to be placed becomes an essential part of design.

Unfortunately, to classify environmental aggressivity is the weakest link in the chain of decisions needed to provide long-term durable structures.

6.2.1 Identification of microclimate and macroclimate

Microclimate is the climate near the surface of the structure, which includes temperature, moisture, and chloride conditions or other aggressive substances, while macroclimate is the general climate around the location of the structure, including the air temperature, humidity, flow etc. – information which can be obtained from meteorological offices.

6.2.2 Identification of aggressive substances

According to the location of structure, the engineer must identify and quantify the aggressive substances in the soils and in the sea by different chemical methods, such as free chlorides, sulphates, acids, and alkalies.

After defining and classifying the aggressivity of the environment in which the structure might be built, special design is needed for these areas for the material chosen and the protection strategy required.

6.2.3 Determination of transport and deterioration mechanisms

The important deterioration mechanisms of concrete structures should be examined. These include:

- Physical causes of concrete deterioration

Mehta and Gerwick (1982) grouped the physical causes of concrete deterioration into two categories: (i) surface wear or loss of mass, (ii) cracking (Figure 6.1)

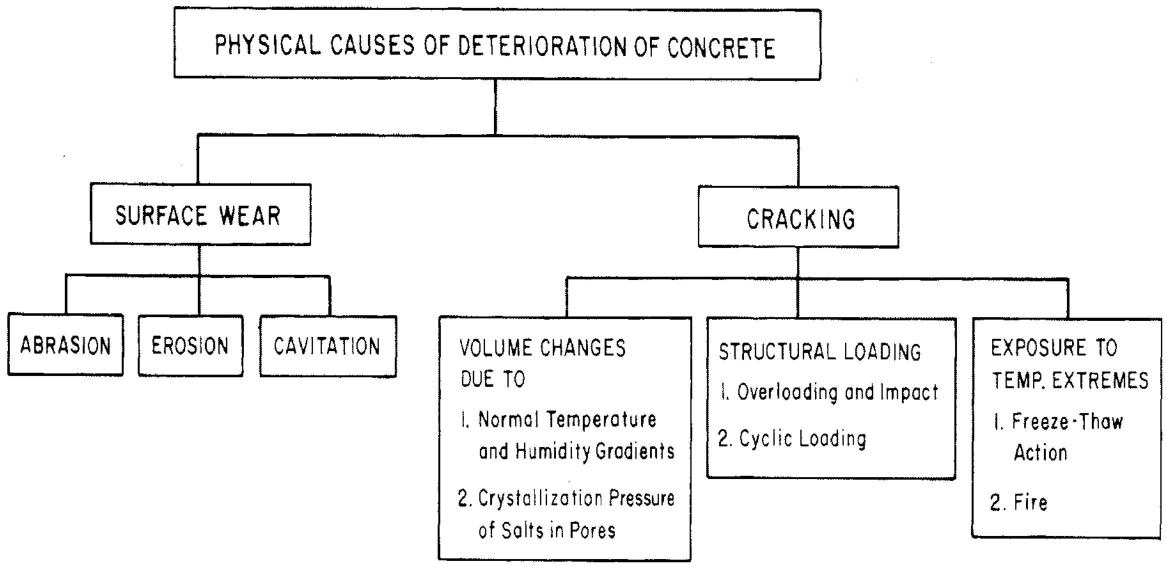

Fig. 6.1: Physical causes of concrete deterioration (Mehta and Gerwick, 1982)

- Chemical attack

  The deterioration processes triggered by chemical reactions involves generally, but not necessarily, chemical interactions between the aggressive agents in the environment and the constituents of the cement paste. The exceptions include alkali-aggregate reactions, which occur between the alkalies present in the cement paste and certain reactive materials in the aggregate.

- Reinforcement corrosion initiated by chlorides ingress, or carbonation

  The damage to the concrete resulting from the corrosion of embedded steel results in expansion, cracking and eventually spalling of the concrete cover. In addition to the loss of the cover, a reinforced concrete member may suffer structural damage due to loss of bond between steel and concrete and loss of rebar cross-sectional area.

Possible transport mechanisms at different areas of the structure should be determined. The rate of transport of different aggressive substances into the concrete should be established once the materials are chosen.

6.3 Structural design

Design, construction, operation and maintenance of a typical concrete structure or system is initially dependent on the input from the following (Mirza and Amleh, 1995):

a) The owner, or the client through a clear definition of the needs over the service life of the system.

b) The designers (architects and engineers) by preparing designs, details and specifications and other requisite conditions through the service life of the facility, such as regular and irregular maintenance during its operation. The structure must be designed for both functional and environmental loadings to be sustained during an expected service life with a minimum requirement of maintenance.

c) The contractors and the subcontractors who are responsible for implementing the design output from item (b) above.

d) The user who is very often either responsible directly for the maintenance of the facility, or indirectly by ensuring that the owner attends to the required maintenance as it arises.

6.3.1 Design strategies

Structural design, comprising architectural concepts of layout together with engineering selection of structural form, determines the overall geometry of the structure, including the exposed parts. It is generally accepted that improved durability performance cannot be achieved by only improving the basic qualities of the concrete and the reinforcing steel, but it also requires specific considerations in several areas, including architectural and structural design for functional and environmental loadings, construction practices and inspection and maintenance procedures. Often, small and simple details related to the design, execution and maintenance may tip the scale in deciding whether or not the structure will attain longevity.

Strategies:

- Avoid complexity in structural form:
- Minimize exposed concrete surface area
- Drainage over concrete: "no water-no trouble"

6.3.2 Choice of concrete

Durability performance of new structures can be enhanced by using one or more of the following potential approaches:

- High quality reinforced concrete
- Protective surface coatings
- Special concrete admixtures

- Ensuring execution procedures which enhance quality, specifically in the outer concrete layer which is the cover of the member:
- Provide adequate concrete cover thickness along with low permeability to suit the environment conditions

6.3.3 Choice of steel

- Provide corrosion-resistant reinforcement in the design of new structures.
- Use adequate bar diameter and concrete cover thickness: Ensure that the C/d_b ratio is at least between 3 and 4.
- Use cathodic protection (for protecting existing structures, or as a preparatory measure for new structures
- Use corrosion inhibitors in the concrete mixture
- Limitation of crack widths
- Structural detailing: The practicality of appropriate concreting and compaction should be followed while detailing the reinforcement. Gaps for the insertion of a vibrator should be provided in case of crossing layers of reinforcing bars. Add extra reinforcement in areas, which have stress concentration at some locations to avoid the formation of large cracks.

6.4 Quality control

The site engineer must check the following in an appropriate manner:

- Bar spacings, gaps for inserting a vibrator
- Concrete cover, suitability and spacing of spacers

- Concrete mix design and quality assurance system for concrete quality
- Measures for curing

6.5 Maintenance/ Inspection plan

Regular and systematic inspections should be performed to identify and quantify possible ongoing deterioration. Inspection constitutes an integral part of structural safety and serviceability by providing a link between the environmental conditions to which the structure is subjected and the manner in which it performs over time. While deciding the final layout plan, it is necessary to foresee which requirements must be fulfilled at the design stage to ensure reasonable conditions for inspection and maintenance. Some critical zones can be equipped with advanced corrosion monitoring equipments, through which one could obtain early warning of oncoming risks of corrosion in the various components.

6.6 Provisions for durability in National codes

The various national building codes do not deal directly with the rational design of concrete structures for durability over a specified service life. Most of the practising engineers use the code provisions without understanding the microstructures of the concrete and the reinforcing steel and the reasons why they deteriorate in aggressive environments. It is necessary that the national codes provide durability provisions, which will enable the practising engineers to analyse the various mechanical, physical, chemical and biological deterioration mechanisms, and to thoroughly know and investigate the causes of any deterioration problem, either in designing a new structure, or in rehabilitation of an existing deteriorated structure.

6.7 Preliminary design method for durability

There is a need to develop durability design strategies throughout the design, construction and maintenance phases to guarantee that the structure will attain its required service life. The structure shall be of high quality and high performance through excellence of concept, design, construction, maintenance and operation. The structure shall be designed to provide the required strength, durability, overall stability, safety and serviceability with appropriate safeguards against excessive cracking, fatigue, deterioration of concrete and corrosion of reinforcement during the design service life. The developer shall perform and complete all of the work in an effective, competent, skillful and careful manner to build the structure and to ensure that the structure during a design service life would not lose its strength, functionality and aesthetic performance. The durability design method for new concrete structures should include the following steps:

1. Establish the environmental loads (microclimate) for the various segments of all structural members, e.g., bridge piers in sea (atmospheric zone, tidal zone, zone below low tide, etc.).
   (a) Design the various measures, such as providing multiple barriers to enable the member to perform satisfactorily over the design service life. This would involve choice of materials, such as the concrete strength and impermeability, corrosion

inhibitors, type of steel and protective coatings, and other protective measures, including regular maintenance of the structure.

(b) Design the member for the various mechanical loads. Carefully detail the member geometry and all details to ensure that inspection and maintenance can be easily handled. Several researchers are working in this area and their findings will be useful to the practicing engineers.

2. (a) Select the steel type carefully to ensure the survival of at least half of the bar lug over the design service life in the most aggressive environment.

   (b) Determine the effect of the microclimate on the cover concrete and evaluate the probable crack widths on the surface. Establish the rate of deterioration of the concrete and the reinforcing steel due to any possible corrosion of the steel rebar. The corrosion initiation phase should be made as long as possible to ensure that the design life will be achieved with an appropriate maintenance program. The details selected earlier may need to be modified to ensure that the width of any crack is less than about 0.5mm. Provide stirrups or lateral ties which will help confine the concrete and considerably reduce the tendency of the concrete cover to crack. With appropriate confinement, the loss of bond due to corrosion of the steel reinforcement can be reduced to about 20 – 30%. More research is needed in this area.

   (c) In selecting the concrete cover to the steel rebars, ensure that the C/d_b ratio is at least between 3 and 4. For larger concrete covers, it may be necessary to use a wire mesh halfway in the concrete cover.

(d) Consider the use of formwork lined with a permeable liner to ensure at least the same water/cement ratio in the cover concrete as in the concrete within the member. Ensure very high quality control on placing of steel and concrete, along with its consolidation and curing.

(e) From the above parameters, evaluate the bond strength available near the end of the service life and ensure safety of the member and the structure at that stage. The information needed for the preliminary design is summarized in Figures 6.2 through 6.5.

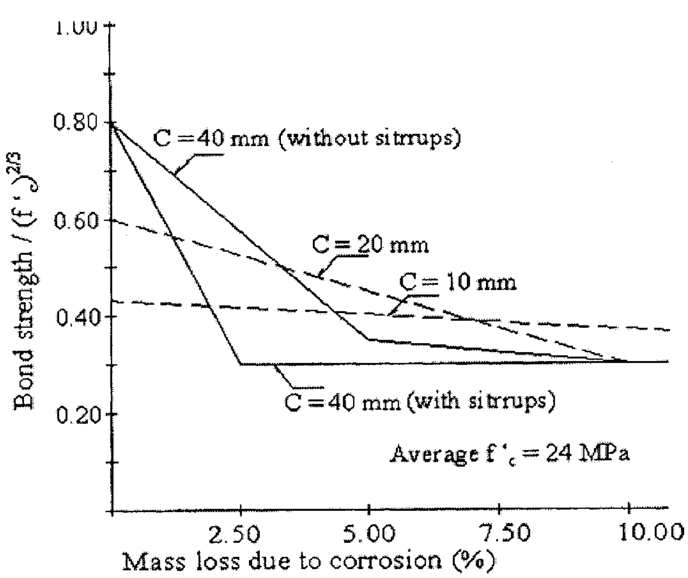

Fig. 6.2: Variation of bond strength / $(f'_c)^{2/3}$ ratio with mass loss due to corrosion (Adapted from Shima, 2002)

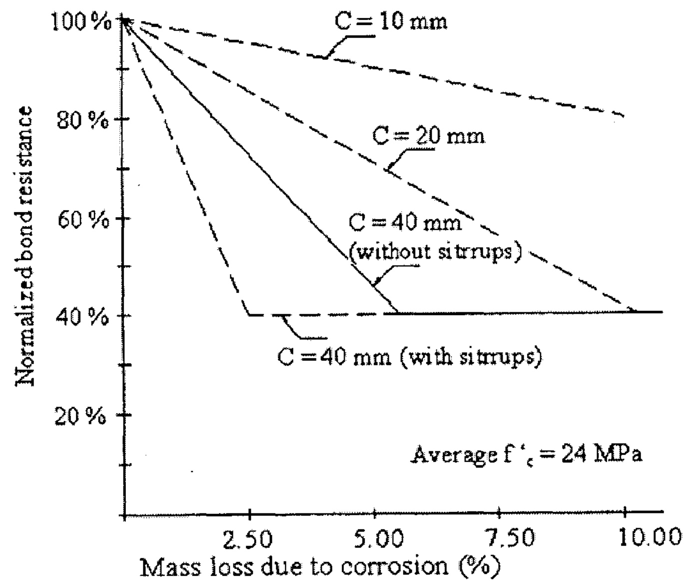

Fig. 6.3: Variation of normalized bond resistance with mass loss due to corrosion (Adapted from Shima, 2002)

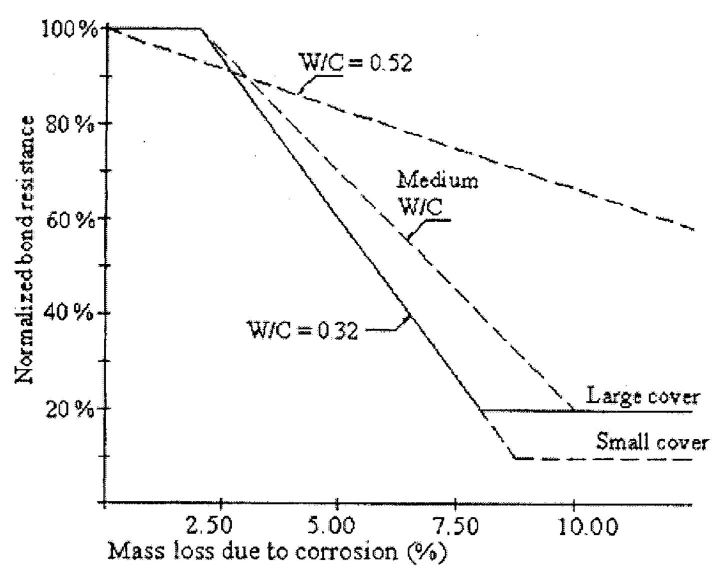

Fig. 6.4: Variation of normalized bond resistance with mass loss due to corrosion (Adapted from Amleh, 2000)

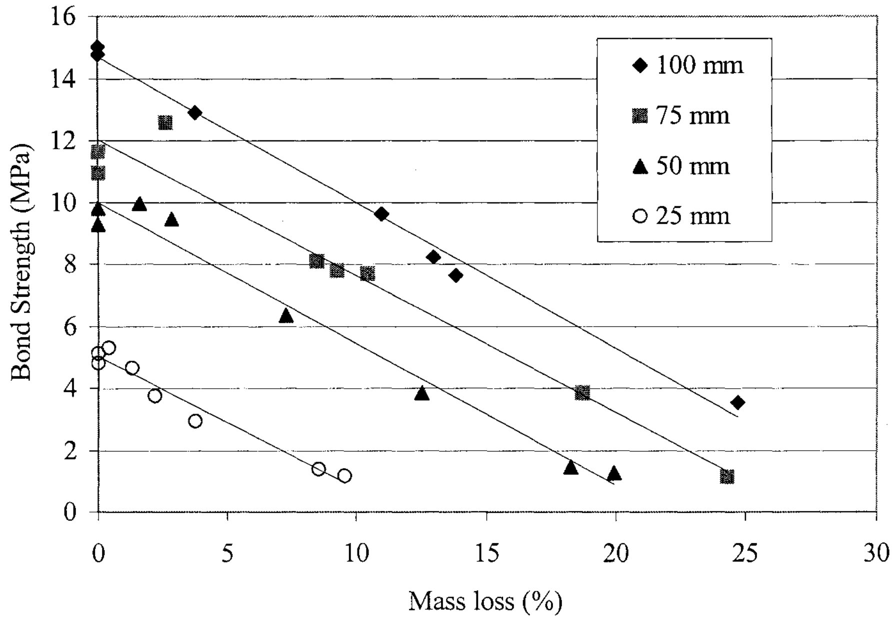

Fig. 6.5: Variation of bond strength with mass loss for the normal Portland cement concrete mixture with 0.32 w/c ratio and different concrete cover thickness (Adapted from Amleh, 2000)

Figure 6.2 leads to the following observations:

- Bond strength decreases with increase in the level of corrosion.
- Values of bond strength at high levels of corrosion (about 10 % rebar mass loss) are almost the same irrespective of the concrete cover.
- Initial values of bond strength are higher in the case of thicker concrete cover.

The following deductions can be made from Fig. 6.3:

- Bond resistance decreases almost linearly with the level of corrosion.
- Degree of bond stress decrement is small when the cover is small and is large when the cover is large. (However, the concrete cover thicknesses of 20 mm and 10 mm are not practical in structures in the field),

- Bond resistance attains a constant value of 40% after certain level of corrosion (2.5% for 40mm thick cover with stirrups and about 6% for same cover but without stirrups).

An examination of Amleh's Figures 6.4 and 6.5 results in following recommendations:

- While deciding for the water/cement ratio, the concrete cover thickness must be selected appropriately.
- Large concrete cover thickness shows better performance than small concrete covers. However, it may be necessary to use a wire mesh half way around the larger concrete covers.
- Avoid using 25 mm thick or smaller concrete covers.
- Bond strength is higher in case of thick concrete covers.

A step-by-step preliminary design method for durability for new concrete structures is proposed. It is noted that the bond strength decreases almost linearly with the level of corrosion. Concrete cover thickness along with the rebar diameter and water-cement ratio are important parameters influencing the deterioration of bond at the steel-concrete interface. An increase in cover to rebar diameter ratio helps in decreasing the mass loss of the rebar with concrete, thus increasing the service life of the structure. More research is needed to evaluate the influence of the various parameters on deterioration of bond at the steel-concrete interface, before a reliable design procedure can be developed based on semi-probabilistic considerations, as for the other phenomena in structural concrete design.

Chapter 7

Summary and Conclusions

7.1 Summary

This research was aimed at formulating a framework for durability design of concrete elements against corrosion due to deterioration of bond at the steel rebar- concrete interface. The importance of concrete with a low water-cement (w/c) ratio and an appropriate concrete cover thickness to rebar diameter (C/d_b) ratio is emphasized. The findings can be summarized and conclusions drawn as follows:

1. Mass loss of the reinforcement is an important parameter, for a given situation; it can help define the corrosion level, and this information can be used to develop a correlation between corrosion, cracking, bond strength at the steel-concrete interface, and the ultimate strength of the reinforced concrete element. Results show that the mass loss of the reinforcing bar in the concrete depends on many factors, such as the concrete cover thickness and concrete permeability, reinforcing bar size, crack width, water/cement ratio and ratio of the concrete cover thickness and rebar diameter. Increased concrete cover and lower concrete permeability can help decrease the mass loss of the rebars in the concrete. The increase in the C/d_b ratio also helps to decrease the mass loss of the rebar in the concrete, thus increasing the service life of the structure.

2. The influence of the various parameters, such as the concrete w/c ratio, cover thickness and bar diameter (C/d_b) ratio, which influence the deterioration of bond at the steel-concrete interface due to corrosion of the reinforcing steel, is reviewed. A preliminary design equation for prediction of bond strength at different corrosion levels (mass loss) is presented. The equation shows favorable results with the experimental values obtained by other authors.
3. It is found that initially bond strength increases slightly for small levels of corrosion, which lead to the formation of a firm layer of corrosion products on the steel rebar-concrete interface, thereby improving the bond strength characteristics slightly. However, at higher levels of corrosion, a firm layer of corrosion products transforms into a flaky layer resulting in the deterioration of bond. Following this stage, the bond strength decreases almost linearly with the increase in mass loss.
4. The research results from various authors, involving the various parameters influencing the deterioration of bond at the steel-concrete interface due to corrosion of the reinforcing steel are reviewed summarily. Although more research is needed to define the environmental loads and some parameters, such as the confinement of the concrete due to the lateral reinforcement, a preliminary durability design procedure is proposed to minimize the bond loss over the design service life and it will help the practicing engineers in designing new structures for durability.
5. The critical values of crack width and loss in the rib profile are found to be 0.3 mm and 26 %, respectively. The concrete cover thickness -to- bar diameter ratio (C/d_b) along with the water/cement ratio is found to be most significant parameters in evaluating the residual bond strength. It is recommended that concrete cover

thickness -to- bar diameter (C/d_b) ratio between 3 and 4 be adopted for designing and detailing new reinforced concrete structures to delay the initiation of concrete cracking due to corrosion.

7.2 Future research

It is recommended that the future research focus on the following:

1. Presently, there is not much information available on the deterioration of bond between the concrete and the reinforcing steel with the levels of corrosion using different water/cement ratios, cover-to-bar diameter ratios, crack width, using new materials and technologies such as high performance concrete and steel.
2. Because very few experimental investigations have been undertaken on the behaviour of reinforced concrete elements subjected to corrosion, more experimental work is necessary to monitor and assess the structural behavior of corroded concrete elements. The influence of the different parameters, such as the reinforcing bar diameter, type of loading, concrete cover thickness, concrete strength and the steel yield strength on the behaviour of reinforced concrete elements subjected to corrosion need to be studied both in the laboratory and in the field.
3. It would be extremely useful for the engineering practice to develop reliability-based design methods for new and deteriorated concrete infrastructure.
4. Correlation of the results from the equations and recommendations, developed in this research program, with the data obtained from performance of structures in the field will help in increasing the reliability of the process. More research is needed in this area.

References

ACI Committee 201 (1982), *"Guide to Durable Concrete"*. American Concrete Institute, ACI 201.2R-77, Detroit, 37 pp.

ACI Committee 222R (1989), *"Corrosion of Metals in Concrete"*. Report of the ACI Committee 222, ACI Manual of Concrete Practice 1994, Part I, Materials and General Properties of Concrete, pp. 222R-1 to 222R-30.

ACI Committee 318 (1990), *"Building Code Requirements for Reinforced Concrete (ACI 318M-89) and Commentary (ACI 318RM-89)"*. American Concrete Institute, June 1990.

ACI Committee 408 (1991), *"Bond under cyclic loading – State of the Art"*. ACI Material Journal, Vol. 88, No. 6, pp. 669-673.

Almusallam, A.A., Al-Gahtani, A.S., Aziz, A.R., and Rasheeduzzafar (1996), *"Effect of reinforcement corrosion on bond strength"*. Construction and Building Materials, Vol. 10, No. 2, pp. 123-129.

Al-Sulaimani, G.J., Kaleemullah M., Basunbul, I.A., and Rasheeduzzafar (1990), *"Influence of corrosion and cracking on bond behaviour and strength of reinforced concrete members"*. ACI Structural Journal, Vol. 87, No. 2, pp. 220-231.

Amleh, L. (2000). *"Bond deterioration of reinforcing steel in concrete due to corrosion"*. Ph.D Thesis, Department of Civil Engineering and Applied Mechanics, McGill University, Montreal, Canada.

Amleh, L. and Mirza, M.S. (2002). *"Effect of Concrete W/C Ratio & Corrosion in Concrete Mix on Bond between Steel and Concrete"*. Proceedings of International Conference on Bond in Concrete – From Research to Standards, Budapest, Hungary, pp. 285-292.

Andrade, C., Alonso, C., and Molina, F. J. (1993), *"Cover cracking as a function of bar corrosion.1. Experimental test"*. Materials and Structures, Vol. 26, No. 162, pp. 453-464.

Auyeung Y., Balaguru, P. and Chung L. (2000), *"Bond Behaviour of Corroded Reinforcement Bars"*. ACI Materials Journal, Vol. 97, No. 2, March-April 2000, pp. 214-220.

Baltay, P. and Gjelsvik, A. (1990), *"Coefficient of friction for steel on concrete at high normal stress"*. Journal of Materials in Civil Engg., Vol. 2, No.1, February 1990, pp. 46-49.

Basheer, P.A.M. (1991), *"Clam Permeability Tests for Assessing the Durability of concrete"*. Ph.D. Thesis. The Queen's University of Belfast.

Basheer, P.A.M., Long, A.E. and Montgomery, F.R. (1994), *"An Interaction Model for Causes of Deterioration and Permeability of Concrete"*. Malhotra Symposium on Concrete Technology, San Francisco, CA, 21-25 March 1994, SP 144, ACI, Detroit, pp. 213-33.

Bob, C. (1996), *"Probabilistic assessment of reinforcement corrosion in existing structures"*. Concrete Repair, Rehabilitation and Protection.

Broms, B., and Raab, A. (1961), *"The Fundamental Concepts of the Cracking Phenomenon in Reinforced Concrete Beams"*. Report No. 310, School of Civil Engineering, Cornell University, Ithaca, pp. 1095-1108

Broomfield, J.P. (1997), *"Corrosion of Steel in Concrete – Understanding, Investigation and Repair"*. E & FN Spon, London.

BS 8110 (1989), *"British Standards Institution. Structure use of Concrete"*. Part I: Code of Practice for Design and Construction, London.

Cabrera, J. G. and Ghouddoussi, P. (1992), *"The Effect of Reinforcement Corrosion on the Strength of the Steel/Concrete Bond"*. International Conference Bond in concrete from Research to Practice Proceedings, pp. 11-24.

Cairns, J. and Jones, K. (1995), *" Influence of rib geometry on strength of lapped joints: an experimental and analytical study"*. Magazine of Concrete Research, Vol. 47, No. 172.

Cairns, J., Pantazopoulou, V., Noghabai, K. and Rodriguez, J. (2000), *"Bond of corroded reinforcement"*. Chapter 4, *fib Bulletin 10*, pp. 187-212, Lausanne 2000.

Cairns, J., Du, Y., and Johnston, M. (2002), *"Residual bond capacity of corroded plain surface reinforcement"*. Proceedings of the International Conference on Bond in Concrete. From Research to Standards, Budapest, Hungary, pp. 129-136.

CEB Bulletin d'information No. 182 (1989), "*Durable Concrete Structures*". CEB Design Guide, CEB.

Comite Euro-International du Beton, *"CEB Durable Concrete Structures"*. Thomas Telford Ltd., London, 1992.

"High Performance Concrete: Improving Canada's Infrastructure and International Competitiveness", *Concrete Canada.,* Vol. 1, October 1993.

CSA Standards A23.1-94. *"Concrete Materials and Methods of Concrete Construction"*. Canadian Standard Association, June 1994.

CSA S-6: 2000. *"Canadian Highway Bridge Design Code"*. Canadian Standard Association, Toronto.

Darwin, D. and Graham, E.K. (1993), *" Effect of deformation height and spacing on bond strength of reinforcing bars"*. ACI Structural Journal, Vol. 90, No.6, pp. 646-657.

Diamond, S. (1986), *"Chloride Concentrations in Concrete Pore Solutions Resulting from Calcium and Sodium Admixture"*. Cement Concrete Aggregates, Vol. 8, No. 2.

FIB (2000): *"Bond of corroded reinforcement"*. Chapter 4, *fib Bulletin 10*, pp. 187-212, Lausanne 2000.

Fontana, M.G. (1986), *"Corrosion Engineering"*. McGraw-Hill, Toronto, Canada.

Ghandehari, M., Zulli, M. and Shah, S.P. (2000), *"Influence of corrosion on bond degradation in reinforced concrete"*. Proceedings EM2000, Fourteenth Engineering Mechanics Conference, ASCE, Austin, Texas.

Goto, Y. (1971), *"Cracks Formed in Concrete Around Deformed Tension Bars"*. ACI Journal, Proc. Vol. 68, No. 4, pp. 244-251.

Grigg, N.S. (1988), *"Infrastructure Engineering and Management"*. John Wiley and Sons, New York.

Hamad, B. S. and Itani, M. S. (1998), *"Bond of Reinforcement in High Performance Concrete: Role of Silica Fume, Casting Position, and Superplasticizer Dosage".* ACI Materials Journal, Vol. 95, Issue 5, pp. 499-511.

Houde, J. (1973), *"Study of Force Displacement Relations for the Finite-Element Analysis of Reinforced Concrete".* Ph.D Thesis, Department of Civil Engineering and Applied Mechanics. McGill University, Montreal, Canada.

Houde, J., and Mirza, M.S. (1972), *"A study of bond stress-slip relationships in reinforced concrete".* Structural Concrete Series No. 72-8, McGill University.

Jacob. F., and Carper, K.L. (1997), *"Construction failures".* John Wiley and Sons.

Lounis. Z., and Mirza, M.S. (1996), *"A probabilistic approach for predicting the service life of the structure".* Notes for the Course 303-624B. Durability of Structures, McGill University.

Lungdren, K., and Gylloft, K. (2000), *"A model for bond between concrete and reinforcement".* Magazine of Concrete Research, Vol. 52, No. 1, February 2000, pp. 53-63.

Lungdren, K., Gustavson, R., and Magnusson, J. (2002), *"Finite Element modeling as a tool to understand the bond mechanisms"*. Proceedings of the International Conference on Bond in Concrete. From Research to Standards, Budapest, Hungary, pp. 27-34.

Lungdren, K. (2002), *"Modelling the effect of corrosion on bond in reinforced concrete"*. Magazine of Concrete Research, Vol. 54, No. 3, June, pp. 165-173.

Lutz, L.A., and Gergely, P. (1967), *"Mechanics of bond and slip of deformed bars in concrete"*. ACI Journal, pp. 711-721.

Mehta, P.K. and Gerwick, B.C. (1982), *"Cracking-Corrosion Interaction in Concrete exposed to Marine Environment"*. Journal Concrete International, Vol. 4, No.10, pp. 45-51

Mehta, P.K. and Montiero, P.J.M. (1993), *"Concrete: Structure, Properties, and Materials"*. Prentice Hall, New Jersey.

Mirza, M.S., Gerstle, K., Ingraffea, A.R., Murray, D., and Nilson, A.H. (1982), *"Modeling of reinforcement and representation of bond"*. Finite Element Analysis of Reinforce Concrete. A state-of-the-art Report, ASCE, New York, U.S.A.

Mirza, M.S. and Amleh, L. (1995), *"Recent Developments in Diagnosis and Rehabilitation of Concrete Structures"*. Proceedings of the Special ACI Conference, Montreal, Quebec, November 7, pp. 193-235.

Mirza, M.S. (1998), *"Key-Note Presentation, Public Works and Government Services Workshop on Infrastructure Management"*. Ottawa, Canada.

Mirza, M.S., Shao, Y., and Collinge, J.P. (1998), *"Post-Mortem of the Abandoned Dickson Bridge"*. CSCE Annual Conference-Structural Speciality, Halifax, Canada, June 1998

Mirza, M.S. and Amleh, L. (2003). *"A framework for durability design of bond deterioration due to corrosion"*. Celebrating Concrete: People and Practice, *University of Dundee.*

Mo, Y.L. and Chan, J. (1996), *"Bond and Slip of Plain Rebars in Concrete"*. Journal of Materials in Civil Engineering, Vol. 8, No.4, pp. 208-211.

Molina, F.J., Alonso, C., and Andrade, C. (1993), *"Cover cracking as a function of rebar corrosion, Part II – Numerical Model"*. Materials and Structures, Vol. 26, pp. 532-548.

Page, C.L. (1988), 'Basic Principles of Corrosion', in Schiessl, P., *"Corrosion of Steel in Concrete"*- RILEM Report. Chapman and Hall, London, pp. 3-21.

Park, R. and Paulay, T. (1975), *"Reinforced Concrete Structures"*. John Wiley & Sons, Inc. New York.

Perry, E.S. and Thompson, J.N. (1966), *"Bond Stress Distribution on Reinforcing Steel in Beams and Pullout Specimens"*. ACI Journal, Proc. Vol. 63, No. 8, pp. 865-875.

Rasheeduzzafar, Al-Sadoun, S.S., and Gahtani, A.S. (1992), *"Corrosion cracking in relation to bar diameter and cover thickness"*. Journal of Materials in Civil Engineering, Vol. 4, No. 4, pp. 327-342.

Richardson, Mark G. (1991), *"Carbonation of Reinforced Concrete: Its causes and Management"*. Citis Ltd., Dublin.

Richardson, Mark G. (2002), *"Fundamentals of Durable Reinforced Concrete"*. Spon Press, London and New York.

RILEM Report of TC-60 CSC (1988), *"Corrosion of steel in concrete"*. Chapman and Hall, London, pp.3-21.

Rostam, S. (1994), *"Design for durability: The Great Belt Link"*. Concrete Technology: New trends, Industrial applications, Edited by Aguado *et al.,* Pubilished by E&FN Spon, 2-6 Boundary Row, London SE1 8IIN, UK.

Sarja, A and Vesikari, E. (1996), *"Durability Design of Concrete Structures".* Report of RILEM Technical Committee 130-CSL.

Schiessl, P. (1987), *"Influence of the Composition of Concrete on the Corrosion Protection of the Reinforcement"*, Concrete Durability Katharine and Bryant Mather International Conference. American Concrete Institute, ACI SP-100, Vol. 2, Detroit, pp. 1633-50.

Shima, H. (2002), *"Local bond stress-slip relationship of corroded bars embedded in concrete".* Proceedings of the International Conference on Bond in Concrete. From Research to Standards, Budapest, Hungary, pp. 153-158.

Somerville, G. (1984), *"The Interdependence of Research, Durability and Structural Design".* Institution of Civil Engineers, Proceedings of Symposium on design Life of Buildings. Thomas Telford Ltd., London, pp. 233-50.

Tepfers, R. (1973), *"A Theory of Bond Applied to Overlapped Tensile Reinforcement Splices for Deformed Bars".* Division of Concrete Structures, Chalmers University of Technology, Goteborg, Sweden, Publication 73 No. 2, 328p.

Tepfers, R.A. (1979), *"Cracking of Concrete Cover Along Anchored Deformed Reinforcing Bars".* Magazines of Concrete Research, Vol. 31, No. 106, pp. 3-12.

Treece, R.A. and Jirsa, J.O. (1989), *"Bond Strength of Epoxy-Coated Reinforcing Bars"*. ACI Materials Journal, Vol. 86, No. 2, pp. 167-174.

Tuutti, K. (1982), *"Corrosion of steel in concrete"*. Swedish cement and concrete research institute, Stockholm.

Woodward, R.J. and Williams, F.W. (1989), *"Collapse of Ynes-y-Gwas Bridge, West Glamorgan"*. Proceedings of the Institution of Civil Engineers Part I, Vol. 84, pp. 635-69.

www.confederationbridge.com

www.lafargenorthamerica.com